

Fiber-Reinforced Concrete for Pavement Overlays: Technical Overview

Final Report
April 2019



Sponsored by

Federal Highway Administration
Technology Transfer Concrete Consortium (TTCC) Pooled Fund TPF-5(313)
(Part of Intrans Project 15-532)

IOWA STATE UNIVERSITY
Institute for Transportation

**National Concrete Pavement
Technology Center**



About the National CP Tech Center

The mission of the National Concrete Pavement Technology (CP Tech) Center at Iowa State University is to unite key transportation stakeholders around the central goal of advancing concrete pavement technology through research, tech transfer, and technology implementation.

Notice

This document is disseminated under the sponsorship of the U.S. Department of Transportation in the interest of information exchange. The U.S. Government assumes no liability for the use of the information contained in this document. This report does not constitute a standard, specification, or regulation.

The U.S. Government does not endorse products or manufacturers. Trademarks or manufacturers' names appear in this report only because they are considered essential to the objective of the document.

Quality Assurance Statement

The Federal Highway Administration (FHWA) provides high-quality information to serve Government, industry, and the public in a manner that promotes public understanding. Standards and policies are used to ensure and maximize the quality, objectivity, utility, and integrity of its information. FHWA periodically reviews quality issues and adjusts its programs and processes to ensure continuous quality improvement.

Iowa State University Non-Discrimination Statement

Iowa State University does not discriminate on the basis of race, color, age, religion, national origin, pregnancy, sexual orientation, gender identity, genetic information, sex, marital status, disability, or status as a U.S. veteran. Inquiries regarding non-discrimination policies may be directed to Office of Equal Opportunity, 3410 Beardshear Hall, 515 Morrill Road, Ames, Iowa 50011, Tel. 515-294-7612, Hotline: 515-294-1222, email eooffice@iastate.edu.

Additional Iowa Department of Transportation Statements

Federal and state laws prohibit employment and/or public accommodation discrimination on the basis of age, color, creed, disability, gender identity, national origin, pregnancy, race, religion, sex, sexual orientation or veteran's status. If you believe you have been discriminated against, please contact the Iowa Civil Rights Commission at 800-457-4416 or the Iowa Department of Transportation affirmative action officer. If you need accommodations because of a disability to access the Iowa Department of Transportation's services, contact the agency's affirmative action officer at 800-262-0003.

The preparation of this report was financed in part through funds provided by the Iowa Department of Transportation through its "Second Revised Agreement for the Management of Research Conducted by Iowa State University for the Iowa Department of Transportation" and its amendments.

Front Cover Image Credits

Armen Amirkhanian (FRC overlay) and Dan King, Iowa Concrete Paving Association (slipform paver)

Technical Report Documentation Page

1. Report No. InTrans Project 15-532	2. Government Accession No.	3. Recipient's Catalog No.	
4. Title and Subtitle Fiber-Reinforced Concrete for Pavement Overlays: Technical Overview		5. Report Date April 2019	
		6. Performing Organization Code	
7. Author(s) Jeffery Roesler, Amanda Bordelon, Alexander S. Brand, and Armen Amirkhanian		8. Performing Organization Report No. InTrans Project 15-532	
9. Performing Organization Name and Address National Concrete Pavement Technology Center Iowa State University 2711 South Loop Drive, Suite 4700 Ames, IA 50010-8664		10. Work Unit No. (TRAIS)	
		11. Contract or Grant No.	
12. Sponsoring Organization Name and Address Technology Transfer Concrete Consortium Iowa Department of Transportation (TTCC) Transportation Pooled Fund (lead state) 800 Lincoln Way 800 Lincoln Way Ames, IA 50010 Ames, IA 50010		13. Type of Report and Period Covered Final Report	
		14. Sponsoring Agency Code Part of TPF-5(313)	
15. Supplementary Notes Visit www.intrans.iastate.edu for color pdfs of this and other research reports.			
16. Abstract <p>This report summarizes the state of the art regarding different fiber types, test methods, structural design, and the construction modifications required to accommodate fiber-reinforced concrete (FRC) materials in concrete overlays.</p> <p>This document is a companion report to <i>Overview of Fiber-Reinforced Concrete Bridge Decks</i>, which summarizes the experience from existing bridge deck and bridge deck overlay construction projects that have employed FRC materials.</p>			
17. Key Words concrete overlays—fiber-reinforced concrete—macrofibers		18. Distribution Statement No restrictions.	
19. Security Classification (of this report) Unclassified.	20. Security Classification (of this page) Unclassified.	21. No. of Pages 96	22. Price NA

FIBER-REINFORCED CONCRETE FOR PAVEMENT OVERLAYS: TECHNICAL OVERVIEW

**Final Report
April 2019**

Principal Investigator

Steve Tritsch, Associate Director
National Concrete Pavement Technology Center, Iowa State University

Authors

Jeffery Roesler, Professor
Civil and Environmental Engineering, University of Illinois, Urbana-Champaign

Amanda Bordelon, Assistant Professor
Civil Engineering, Utah Valley University

Alexander S. Brand, Assistant Professor
Civil and Environmental Engineering, Virginia Polytechnic Institute and State University

Armen Amirkhanian, Assistant Professor
Civil, Construction, and Environmental Engineering, The University of Alabama

Sponsored through
Technology Transfer Concrete Consortium (TTCC)
Transportation Pooled Fund
TPF-5(313)

Preparation of this report was financed in part
through funds provided by the Iowa Department of Transportation
through its Research Management Agreement with the
Institute for Transportation
(InTrans Project 15-532)

A report from
National Concrete Pavement Technology Center
Iowa State University
2711 South Loop Drive, Suite 4700
Ames, IA 50010-8664
Phone: 515-294-8103 / Fax: 515-294-0467
www.cptechcenter.org

TABLE OF CONTENTS

ACKNOWLEDGMENTS	xi
1 INTRODUCTION	1
1.1 Background	1
1.2 Report Objective	2
2 BACKGROUND ON FRC PAVEMENTS	3
2.1 Historical Overview of Fibers in Concrete Pavements	4
2.2 Field Applications and Performance	4
2.3 Laboratory Studies of FRC Slabs and Pavements	6
3 TYPES AND CHARACTERISTICS OF FIBERS	12
3.1 Characteristics of Fibers	12
3.2 Fiber Material Types	15
3.3 Deflection Hardening versus Softening Behavior	19
4 BEHAVIOR OF FRC MATERIALS FOR CONCRETE PAVEMENTS	22
4.1 Fresh Concrete Properties	22
4.2 Hardened Concrete Properties	23
4.3 Selection of Fiber Type for Pavement Design	32
5 CONCRETE PAVEMENT DESIGN METHODOLOGY WITH FRC MATERIALS	33
5.1 Residual Strength Estimation Software for FRC Overlay Design	36
5.2 Concrete Overlay Thickness and FRC Material Design Process	38
5.3 Common FRC Overlay Questions and Answers	40
6 CONSTRUCTION MODIFICATIONS WITH FRC PAVEMENT OVERLAYS	47
6.1 Existing Pavement Surface Preparation	47
6.2 FRC Mixture Proportioning	47
6.3 FRC Batching and Mixing	48
6.4 Placement and Consolidation	49
6.5 Finishing	49
6.6 Joints	54
6.7 Maintenance	54
7 FRC TEST METHODS	56
7.1 Fresh Property Testing	56
7.2 Hardened Property Testing	57
8 EXAMPLE FRC OVERLAY SPECIFICATION	70
9 RESEARCH NEEDS FOR FRC OVERLAYS	71
10 SUMMARY OF FRC OVERLAYS FOR PAVEMENTS	72
REFERENCES	73

APPENDIX A: DESCRIPTION OF RESIDUAL STRENGTH ESTIMATOR
SOFTWARE FOR FRC CONCRETE OVERLAYS81

LIST OF FIGURES

Figure 2.1. Examples of FRC overlays: (a) bus pad with 4 in. thick inlay, (b) minor arterial roadway (11,700 ADT) with 4 in. thick overlay, (c) local quarry road (30 to 120 ADT) with 4.5 in. thick overlay, (d) county road with 5 in. thick overlay	3
Figure 2.2. Two-lift concrete slab with a 2 in. plain concrete top lift and a 4 in. bottom lift containing reclaimed asphalt pavement aggregates and 0.43% synthetic macrofibers by volume.....	7
Figure 3.1. Examples of different macrofiber types, top to bottom: crimped, embossed, bi-tapered, and twisted synthetic; straight fibrillated synthetic (two images); hooked-end and crimped steel; and twisted basalt.....	13
Figure 3.2. Synthetic macrofibers packaged in (a) a discrete bundle or (b) loose.....	14
Figure 3.3. Example of fiber balling in a hardened BCOA application in a parking lot, shown with a lens cap 60 mm in diameter	17
Figure 3.4. Schematic of deflection hardening and softening response under flexural loading for plain concrete and FRC	20
Figure 4.1. Example of the post-cracking behavior of notched FRC beam specimen with synthetic macrofiber volume of 0.43%	24
Figure 4.2. Low-cycle fatigue of concretes containing different macrofibers at different volume fractions.....	29
Figure 5.1. Fatigue-based design examples for FRC ($R_{150} = 20\%$ or $f_{150D} = 150$ psi) and plain concrete with two slab sizes: 6 ft (1.8 m) and 4 ft (1.2 m).....	34
Figure 5.2. Screenshot of the Residual Strength Estimator software tool for local road/street design	37
Figure 5.3. Flow chart showing the steps involved in (a) designing an FRC overlay and comparing its thickness to that of plain concrete and (b) determining the amount of fibers necessary to meet the design specification	39
Figure 5.4. Benefits of using macrofibers in concrete overlays	40
Figure 5.5. Example of slab migration in BCOA without macrofibers	41
Figure 5.6. Example ASTM C1609 load-deflection results for several fiber types and amounts with the same concrete mixture design.....	43
Figure 6.1. Construction of an FRC overlay in Iowa.....	49
Figure 6.2. Examples of the surface appearance of FRC with a slipform pavement edge (upper left), with the use of transverse tining and curing compound (upper right), and for a hand-finished troweled surface (bottom)	50
Figure 6.3. FRC overlay with 4 lb/yd ³ of synthetic macrofiber showing excellent finishability	52
Figure 6.4. FRC overlays with synthetic macrofibers and longitudinal tining.....	53
Figure 7.1. Geometry of the ASTM C1609 beam specimen and test configuration setup	58
Figure 7.2. ASTM C1609 test setup showing the LVDT measuring the deflection at the top of the beam at midspan and the ASTM C1812 roller assembly	59
Figure 7.3. Load-deflection response curve from an ASTM C1609 test for a concrete specimen with 0.27% by volume synthetic macrofibers tested at an age of 56 days	60
Figure 7.4. Geometry of the ASTM C1399 beam setup, where $L = 300$ mm, $d = b = 100$ mm, and the thickness of the steel plate is 12 mm.....	62

Figure 7.5. Schematic example of load-deflection response for the ASTM C1399 test	63
Figure 7.6. Geometry of the EN 14651 notched beam setup, where $L = 500$ mm, beam depth and width is 150 mm, and notch depth is ≤ 5 mm	64
Figure 7.7. EN 14651 setup, with an LVDT measuring deflection at the beam mid-span (left) and a clip-on gauge measuring CMOD (right)	64
Figure 7.8. ASTM C1550 round panel test setup and failure mode	65
Figure 7.9. Barcelona test (double-punch test) setup with a circumferential extensometer attached at the mid-height of the FRC cylinder to measure TCOD	66
Figure 7.10. Notched beam fracture testing of FRC showing (a) the clip-on gauge attached to knife edges on the bottom of the beam across the notch, (a, b) the string potentiometer attached to the exterior of the beam, and (b) the fractured specimen.....	67
Figure 7.11. (a) Schematic showing the dimensions of a 150 mm wedge split test specimen, with the wedge vertically thrust between the roller bearings to induce a horizontal tensile splitting force, and (b) test specimen being loaded with the wedge split tension apparatus and LVDTs mounted on either side of the specimen.....	68
Figure 7.12. Fracture geometry of the DCT test for FRC (a) during and (b) after testing	69
Figure A.1. Screenshot of the Residual Strength Estimator software.....	81

LIST OF TABLES

Table 2.1. Load levels and reduction in slab load capacity after cracking	8
Table 2.2. University of Illinois APT test results for FRC and plain concrete	10
Table 3.1. Typical macrofiber or microfiber properties	16
Table 3.2. Fiber characteristics and volumes resulting in deflection hardening or deflection softening behavior for concrete overlay mixtures.....	21
Table 4.1. Recommended aggregate gradations for FRC	23
Table 4.2. ASTM C1609 results for two macro-synthetic fibers at two fiber volumes.....	25
Table 4.3. ASTM C1609 residual strength values for FRCs with different fiber types, fiber volumes, and concrete ages.....	25
Table 4.4. Average 7-day strength and fracture properties of FRC.....	26
Table 4.5. Effect of fiber type, fiber volume, and concrete age on the wedge splitting total fracture energy	27
Table 4.6. Beam fatigue testing for FRC with steel fibers.....	28
Table 4.7. Flexural strength and toughness of FRC exposed to freeze/thaw and fatigue.....	30
Table 5.1. Summary of existing concrete overlay design procedures	35
Table 5.2. Examples of criteria for selecting the condition of the pre-existing asphalt	42
Table 5.3. Example residual strength values for different fiber types and amounts.....	43
Table 5.4. Recommended limits for and corrosion durability of steel fibers in concrete.....	46
Table 6.1. Concrete constituents and mixture proportions for a pavement overlay with synthetic macrofibers at two dosage levels.....	48
Table A.1. Input choices and index values in the FRC Residual Strength Estimator software	82
Table A.2. Maximum and minimum f_{150} values in the FRC Residual Strength Estimator software	83
Table A.3. Design suggestions and warnings in the FRC Residual Strength Estimator software	84

ACKNOWLEDGMENTS

This work was supported by the Technology Transfer Concrete Consortium (TTCC) Pooled Fund Study TPF-5(313).

1 INTRODUCTION

1.1 Background

Fiber reinforcement technology for pavements has been in use for decades, with most of the early research and applications using steel macrofibers to improve the fatigue life of newly constructed concrete pavements. Despite its demonstrated benefits to concrete pavement performance, the use of steel macrofibers made fiber-reinforced concrete (FRC) an unattractive option because of the high volume fractions recommended for the steel macrofibers, the requirement of mixture design modifications, constructability questions, concerns regarding corrosion, and added material costs. Additionally, there was little technical guidance as to how fibers impact the structural design of concrete pavements, which prevented information on fibers from being incorporated significantly into concrete pavement design methods and standards.

Synthetic microfibers were introduced in the 1980s with the objective of minimizing the appearance of early-age plastic shrinkage cracks due to surface moisture loss in concrete. However, these early synthetic microfibers did not improve the load-deflection response of concrete and therefore could not provide enhancements to the structural design of concrete slabs and pavements. Synthetic macrofibers were specifically introduced approximately 20 years ago to improve the flexural toughness of concrete materials and slabs and thus improve concrete performance in a way similar to that of steel macrofibers. Synthetic macrofibers have since been adopted by concrete slab-on-grade (e.g., floors) designers and by multiple state departments of transportation (DOTs) to provide structural benefits for concrete overlays. Additionally, several standardized tests to assess the quality and quantity of macrofibers (both steel and synthetic) in FRC mixtures are now available, as is guidance on structural pavement design with macrofibers and field-proven guidance on FRC construction.

The main challenges in incorporating macrofibers into concrete overlay design on a national scale have involved educating engineers, agencies, contractors, and material suppliers on several frequently asked questions: What macrofiber materials and types should be used? What dosage amounts should be specified? What standard tests should be run to characterize the impact of a particular macrofiber on the flexural toughness of a concrete mixture? How does the existing condition of the road influence design? How are the macrofiber properties accounted for in the design of a structural overlay, e.g., in terms of thickness and slab size? Additionally, little guidance on best practices is available for pavement and material engineers that explains when macrofibers are necessary, how to recognize and adjust for the fresh and hardened property changes that occur with the addition of macrofibers, acceptance testing standards relevant to FRC for overlays, and the necessary adjustments to the construction and finishing processes.

Multiple transportation agencies have used FRC for bridge decks. However, a limited number of guides, documents, and procedures are available on designing concrete bridge decks and overlays with macrofibers. A separate technical report (Amirkhanian and Roesler 2019) has been published summarizing the use of FRC in bridge decks and overlays. That report summarizes the types of macrofibers employed in bridge decks and overlays, material testing methods, construction specifications, FRC performance in terms of the amount of cracking and crack

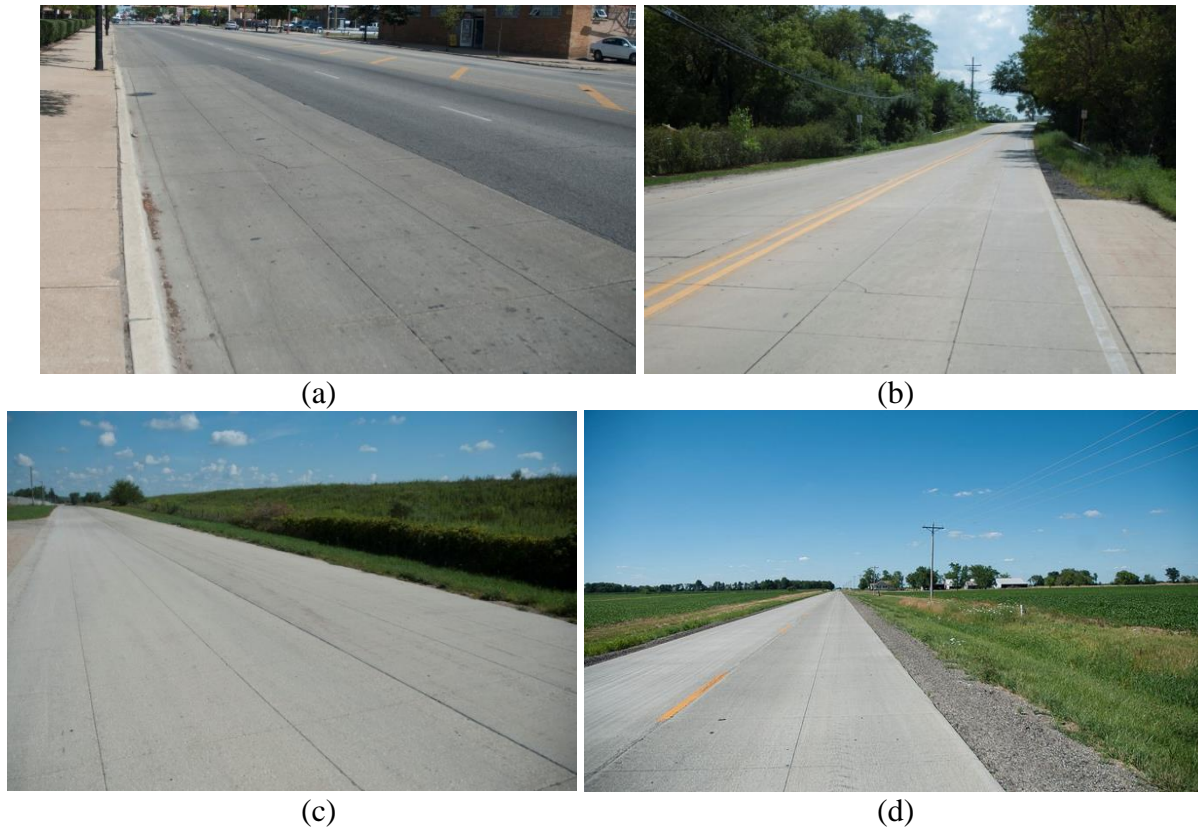
widths, and the current adjustments to the bridge deck design to account for the macrofiber dosage.

1.2 Report Objective

The overall objective of this technical report is to assist pavement engineers in determining the appropriate macrofiber reinforcement for bonded and unbonded concrete overlays. Specifically, this technical report provides an overview of the types of macrofibers used in concrete overlays, the effect of macrofibers on concrete pavement design, pertinent FRC test methods, and recommended best practices, guidance, and specifications for the use of FRC materials in pavements.

2 BACKGROUND ON FRC PAVEMENTS

A significant number of pavement applications use FRC material technology, including highways, local streets, intersections, parking lots, bus pads, sidewalks, driveways, bridge decks, pavement overlays, industrial floors, airfield pavement overlays, and patches (see Figure 2.1).



King and Roesler 2014

Figure 2.1. Examples of FRC overlays: (a) bus pad with 4 in. thick inlay, (b) minor arterial roadway (11,700 ADT) with 4 in. thick overlay, (c) local quarry road (30 to 120 ADT) with 4.5 in. thick overlay, (d) county road with 5 in. thick overlay

As of 2001, 80 million m³ (105 million yd³) of FRC were being produced annually for use in slabs on grade (60%), fiber-reinforced shotcrete (25%), precast elements (5%), and other applications (10%) (Bentur and Mindess 2007).

For pavement applications, FRC can be used for new construction as well as for maintenance (patching), rehabilitation (overlays), and reconstruction. For minor pavement rehabilitation, the use of FRC for bonded concrete overlays on asphalt or composite pavements has seen significant growth in the past 10 years. The thickness of a bonded concrete overlay of asphalt (BCOA) ranges from 3 to 6 in., and the majority of FRC overlays of this type have been for the thinner installations, as illustrated by the examples in Figure 2.1. (The synthetic macrofiber dosages for the inlay and overlays shown in Figure 2.1 were approximately 7.5 lb/yd³ for (a) and 4 lb/yd³ for

(b), (c), and (d).) Barman and Hansen (2018) recently completed a review of thin concrete overlay projects using macrofibers conducted by state DOTs. For major pavement rehabilitation, unbonded concrete overlays with macrofibers have been applied over existing concrete, asphalt, or composite pavements to provide a long-life design. Finally, for new pavement and reconstruction options, a combination of short-jointed slabs and macrofibers has been used successfully in Latin America (Covarrubias et al. 2010, Del Rio and Covarrubias 2016).

2.1 Historical Overview of Fibers in Concrete Pavements

The first commercial application of steel fiber-reinforced concrete pavement in the United States was in 1971 at a truck weigh station in Ohio (ACI Committee 544 2009). Since then, a significant number of fiber-reinforced pavements have been constructed, highlighting the versatility of FRC and its ability to be used for virtually any paved concrete surface. For instance, in Illinois BCOA pavements have been used for county highways, local roads, intersections, bus pads, and parking lots (King and Roesler 2014). While typically used for jointed plain concrete pavement (JPCP) systems, macrofibers have also been added to continuously reinforced concrete pavement (CRCP) mixtures (Folliard et al. 2006, Dahal et al. 2019a, Dahal et al. 2019b). Roller-compacted concrete (RCC) pavements with macrofibers have also been constructed recently on residential streets in Kansas and in France (Nguyen et al. 2012), and laboratory research has corroborated the benefits of macrofibers for both the fresh and hardened properties of RCC pavements (LaHucik et al. 2017).

On airfield pavements, the first applications of FRC used steel macrofibers. These sections, some of which were FRC overlays, were constructed in the 1970s and 1980s at US Navy airfields (Norfolk Naval Air Station, Fallon Naval Air Station) as well as commercial airports (Newark International Airport, John F. Kennedy International Airport, Stapleton International Airport, Tampa International Airport, Cannon International Airport, McCarran International Airport, Salt Lake City International Airport) (Rollings 1986). Some of the early airfield applications of FRC with polypropylene fibers occurred at St. Louis Lambert International Airport, Houston Intercontinental Airport, and London Heathrow Airport (Shoenberger and Tom 1992). An FRC airfield taxiway at the Chicago Rockford International Airport was constructed with steel macrofibers, shrinkage-compensating cement, and longitudinal post-tensioning (Herrin and Naughton III 2003). A 20-year survey of the post-tensioned FRC section (1,200 ft in length) and FRC-only sections with transverse joint spacing varying between 85 and 200 ft demonstrated that the taxiway is experiencing excellent performance. To facilitate the construction of isolation joints, Chicago O'Hare International Airport successfully used synthetic macrofibers as an alternative to a thickened edge joint, which is the current recommended standard by the Federal Aviation Administration (FAA) (Henschen et al. 2014).

2.2 Field Applications and Performance

The National Concrete Overlay Explorer (<http://overlays.acpa.org/>) maintained by the American Concrete Pavement Association includes data on bonded and unbonded concrete overlays, including FRC overlays, around the United States. As of April 2018, the database included 89 FRC overlay projects, two-thirds of which have been constructed since 2000. The majority

(54%) of the FRC overlays were BCOA. The states with the most FRC overlays listed in the National Concrete Overlay Explorer were Illinois (17%), Kansas (12%), Oklahoma (11%), Pennsylvania (9%), Wisconsin (9%), and Missouri (8%).

While some studies have reported no benefit to using fibers in concrete overlays, such as a study of BCOA sections constructed at a truck weigh station off of I-10 in Florida (Armaghani and Tu 1999), or have concluded that there are insufficient field data to assess the benefits of FRC overlays (Vandenbossche et al. 2011), a number of other studies have found that the addition of macrofibers can be beneficial. One report describing a survey of BCOA pavements, both with and without macrofibers, in Illinois found that

macrofibers proved very effective in providing extra structural capacity and maintaining joint load transfer efficiency in UTW [ultra-thin whitetopping] pavements as assumed in the thickness design procedure. Several projects that used macrofibers and had higher amounts of observed slab cracking [...] were still in good serviceable condition and provided smooth rides[...]. On the basis of the survey and FWD [falling weight deflectometer] observations, macrofibers should be continued in all UTW pavements less than or equal to 4 inches. With the ability of macrofibers to tie adjacent slab lanes together, provide additional slab capacity, and reduce the rate of crack deterioration, they should be considered for thicker UTW sections also up to 6 inches. Only a minimum dosage is necessary for parking lots with cars, but for roadways a design residual strength $R_{150} > 20\%$ is recommended to be continued. For projects with high distress severity in the underlying asphalt or heavy truck traffic, or where there are issues with the underlying support, higher synthetic macrofiber dosages (up to 7.5 lb/yd³) are recommended as a way to try to maintain continuity between adjacent slabs and prevent premature cracks from deteriorating rapidly. (King and Roesler 2014)

Synthetic fiber-reinforced concrete overlay test sections were constructed at the Minnesota Road Research Facility (MnROAD) in 1997, 2013, and 2017 (Vandenbossche and Rettner 1998, Burnham 2005, Barman and Hansen 2018). The sections constructed in 1997 had macrofiber contents of either 3 lb/yd³ (0.2% by volume) polypropylene or 25 lb/yd³ (1.6% by volume) polyolefin. The test section constructed in 2013 had 6.5 lb/yd³ (0.5% by volume) polypropylene. In both studies, the addition of macrofibers was not reported to provide significant benefit to the overall performance of the pavement (Burnham 2005, Snyder 2009), and the higher dosage in 1997 may have been a contributing factor to accelerated joint deterioration. Distresses and the primary failures of these test sections were concluded to be related to the high traffic volume, wheel placement relative to the slab sizes, and the bond condition between the overlay and the underlying asphalt (Burnham 2005). A closer look at the macrofibers employed in the 1997 MnROAD test sections found that these synthetic fibers had a very low elastic modulus and therefore would not be expected to significantly enhance the structural performance of the BCOA.

The test sections constructed in 2017 at MnROAD consisted of 3 in. to 5 in. thick slabs with plain or FRC mixtures. The test sections were all unbonded designs over either an aggregate base or an existing concrete pavement. The section with a 0.75% volume fraction of twisted synthetic

fiber cast with a 3 in. thickness over a weak aggregate base exhibited a significant number of shattered slabs and surface deformations. The specific fiber used in this application untwists during mixing to yield a fiber with a very small diameter and a lower elastic modulus and may have not sufficiently enhanced the performance of the ultra-thin unbonded overlay (Barman and Hansen 2018).

In South Africa, ultra-thin continuously-reinforced concrete pavements (UTCRC) have been investigated for new construction and overlay applications. These pavement structures are as thin as 2 in. (50 mm) and contain both reinforcing steel and discrete steel macrofibers (Kannemeyer et al. 2008). There has been widespread use of macrofibers in the design of concrete pavements in many Latin America countries. These designs have built on BCOA technology from the US and short-jointed slab technology from Chile (Covarrubias and Covarrubias 2008, Covarrubias et al. 2010). One of the first of these FRC overlays was applied to Route 24 in Uruguay, where an existing asphalt that was rutting was overlaid in 2012 with a 6 in. concrete overlay with synthetic macrofibers. Several unbonded overlays, reconstructions, and new concrete pavements have been constructed in Chile and Peru with macrofibers (Del Rio and Covarrubias 2016), and short-jointed concrete slabs with macrofibers have been constructed in Bolivia, Guatemala, and Nicaragua.

2.3 Laboratory Studies of FRC Slabs and Pavements

2.3.1 Large-Scale Tests on FRC Slabs

A number of studies have performed large-scale laboratory testing of FRC slabs over the past 30 years to evaluate FRC containing either steel or synthetic macrofibers (Beckett and Humphreys 1989, Beckett 1990, Falkner and Teutsch 1993, Falkner et al. 1995, Barros and Figueiras 1998, Elsaigh 2001, Roesler et al. 2004, Roesler et al. 2006, Meda et al. 2004, Roberts-Wollmann et al. 2004, Sorelli et al. 2006, Amirkhanian 2012, Brand et al. 2014). In all of these studies, the ultimate capacity of the FRC slabs was found to increase relative to plain concrete slabs, depending on the type and dosage of the macrofibers. Additionally, most of these studies found that the first flexural cracking load of the slabs with macrofibers increased. In one study, the addition of recycled coarse aggregates (reclaimed asphalt pavement and recycled concrete aggregate [RCA]) to concrete reduced its flexural strength, but the addition of synthetic macrofibers offset this reduction such that the concrete slab's capacity was comparable to that of conventional virgin aggregate concrete (Figure 2.2) (Brand et al. 2014).



Figure 2.2. Two-lift concrete slab with a 2 in. plain concrete top lift and a 4 in. bottom lift containing reclaimed asphalt pavement aggregates and 0.43% synthetic macrofibers by volume

In another study, concrete slabs were constructed with plain concrete and steel macrofiber-reinforced concrete; both concretes had similar mechanical properties and exhibited similar slab load capacities despite the steel macrofiber-reinforced concrete slabs being 16.6% thinner than the plain concrete slabs (Elsaigh 2001). Another study found that the addition of 0.32% and 0.48% by volume of one type of synthetic macrofiber to concrete slabs increased the slabs' flexural cracking load by 25% and 32%, respectively, and their ultimate load capacity by 20% and 34%, respectively (Roesler et al. 2006). Furthermore, the increase in slab capacity has been shown to be related to the fiber volume of the concrete as well as the fiber's aspect ratio (Beckett 1990, Falkner et al. 1995).

Table 2.1 shows the cracking load results for interior-loaded concrete slabs with either synthetic (polypropylene/polyethylene blend) or steel macrofibers.

Table 2.1. Load levels and reduction in slab load capacity after cracking

Macrofiber Type	Macrofiber Volume	Tensile Cracking Load (kN)	First Flexural Crack		Second Flexural Crack		Collapse Load	
			Load (kN)	Load reduction (%)	Load (kN)	Load Reduction (%)	Load (kN)	Load Reduction (%)
Plain (control)	0%	75	108	42	145	43	135	26
Synthetic	0.32%	75	135	25	148	19	174	6
Synthetic	0.48%	70	143	12	162	9	195	Stable
Steel (hooked-end)	0.35%	70	141	8	185	3	228	Stable
Steel (crimped)	0.5%	70	167	5	200	5	220	Stable

Centrally loaded concrete slabs were 2.2 m (7.2 ft) square and 127 mm (5 in.) thick.

Source: Roesler et al. 2004

The tensile cracking load refers to the load at which the concrete approximately initiates localized cracking. The first and second flexural crack loads signify the loads at which a sudden reduction in load carrying capacity is realized from bottom-up cracking. The collapse load is the ultimate load capacity attained by the slab, with almost all of the macrofiber slabs at this point still providing a stable load-deflection response. The data in Table 2.1 demonstrate that the tensile cracking load is equivalent for concretes with and without macrofibers, which is expected because low to moderate macrofiber contents do not typically influence concrete strength. However, the increased toughness and fracture energy of the concrete resulting from the added macrofibers increases the flexural and ultimate load carrying capacity of the slab, as demonstrated in Table 2.1.

Given that FRC slabs have been shown to exhibit greater flexural capacity than plain concrete slabs, Roesler et al. (2004) concluded that, in many cases, standard beam flexural strength tests (to measure modulus of rupture) are not reliable predictors of the expected capacity or performance of the concrete slab. For certain edge-loaded concrete slabs, the ratio of slab flexural strength to beam flexural strength has been found to be 3.5 for FRC and 2.7 for plain concrete (Roesler 2006). One proposed method to account for this improved flexural slab capacity with macrofibers is to define an effective beam flexural strength derived from the results of full-scale slab tests (Altoubat et al. 2008). Based on this concept, the FRC residual strength (see Section 7.2.1.1) is added to the concrete's design flexural strength to produce an effective flexural strength, which can then be used as an input for designing a BCOA (Roesler et al. 2008) (see Chapter 5).

A specialized FRC material known as engineered cementitious composite (ECC) has been proposed as an overlay material (Zhang and Li 2002, Zhang et al. 2015, Zhang et al. 2017). ECC is a strain-hardening FRC with a synthetic fiber (often polyvinyl alcohol) volume content typically around 2%. The peak flexural strength of a concrete beam overlaid with ECC was found to be more than double (1.9 to 2.0 ksi) that of a concrete beam overlaid with conventional concrete (0.9 ksi), and the concrete beam overlaid with ECC similarly yielded greater fatigue performance (Zhang and Li 2002).

To evaluate the load transfer efficiency (LTE) of FRC slabs, Barman (2014) cast FRC and plain concrete slabs and simulated wheel loads traversing a transverse crack. Two slabs with different synthetic macrofibers (one straight and one crimped) and with equivalent concrete residual strength ratios were tested and compared to a plain concrete slab. Both slabs with synthetic macrofibers exhibited improved crack LTE over time relative to the plain concrete slab. After repeated loading of the transverse crack, the LTE of the plain concrete slab decreased by 30%, while the LTE of the slab with straight synthetic macrofibers decreased by 18% and the LTE of the slab with crimped synthetic macrofibers decreased by 9%. The magnitude of this decrease in LTE for the plain concrete was attributed to crack face fatigue and an increase in crack width. At smaller crack widths (<0.025 in.), the cracks in the plain concrete and FRC slabs had similar LTE values and exhibited similar performance. However, the FRC slabs' cracks were able to maintain higher LTE values at wider crack widths, while the plain concrete slab's crack experienced a more rapid reduction in LTE as the crack width increased. After slab and beam testing, Barman (2014) concluded that LTE of cracks can be improved by 15% to 25% with FRC compared to plain concrete.

2.3.2 Accelerated Pavement Testing of FRC

A number of studies have conducted accelerated pavement testing (APT) of FRC pavements and overlays (Parker Jr. 1974, Rajan et al. 2001, Melhem et al. 2003, Newbolds and Olek 2008, Nguyen et al. 2012, Roesler et al. 2012). One of the first APT studies of FRC pavements was for the FAA. The FAA evaluated the suitability of steel macrofibers for airfield pavements and overlays under repeated loading (Parker Jr. 1974). Design methodologies based on the results of the FAA’s study suggested that a thinner concrete slab could be constructed if FRC is used instead of plain concrete.

Another study performed at the Indiana DOT/Purdue University APT facility (Newbolds and Olek 2008) investigated the effects of BCOA thickness, substrate stiffness, substrate composition, and concrete mixture (conventional concrete, high early strength concrete, and FRC with synthetic macrofibers) on the performance of four BCOA test sections. The FRC slabs performed well with regard to resistance to cracking even when the BCOA layer was debonded, but this performance may result from the higher strength of the FRC mixtures. The synthetic macrofibers employed in these test sections were only 0.75 in. long and were added at a low dosage rate of 1.8 lb/yd³. Given the higher strength concrete, shorter polypropylene fibers, and lower dosage rates, the macrofiber did not likely contribute to the performance of the test sections.

An APT study performed at the University of Illinois evaluated the effects of slab thickness, support conditions, and use of macrofibers on short-jointed slab systems (Roesler et al. 2012). Compared to plain concrete slabs of the same dimensions (1.8 m by 1.8 m) and thickness (9 cm), the FRC slabs experienced significantly less cracking (Table 2.2) and less variability in slab deflection at the same repeated load levels.

Table 2.2. University of Illinois APT test results for FRC and plain concrete

Testing Period	Concrete Type	Base Type	Composite k-value (MPa/m)	Total	Percent Slabs Cracked	Estimated Terminal Serviceability
				Equivalent Single Axle Loads (ESALs)		
Spring	Plain	Granular	41	230,000	100	1.0
	Macro-FRC	Granular	41	230,000	42.9	2.1
Spring thaw	Plain	Granular	14	2,900	85.7	1.3
	Macro-FRC	Granular	14	4,500	28.6	2.3

Concrete slabs were 1.8 m (5.9 ft) square and 9 cm (3.5 in.) thick.
Source: Roesler et al. 2012

The APT data also suggested that FRC extended the service life of the concrete pavements, with an estimated terminal serviceability of 1.0 to 1.3 for plain concrete and 2.1 to 2.3 for FRC.

Kansas State University tested a 4 in. unbonded concrete overlay with either plain or FRC material, a joint spacing of 5 ft and 10 ft, and a width of 6 ft. The existing pavement structure

was a 6 in. rubblized concrete. The authors reported no significant performance enhancement relative to plain concrete when 3 lb/yd³ of “fiber mesh” was used, which suggested that macrofibers with toughening characteristics were not employed (Melhem et al. 2003). In France, the performance of steel macrofiber-reinforced roller compacted concrete (RCC) with and without recycled aggregates was investigated using APT (Nguyen et al. 2012). Based on the results of the APT tests, the authors recommended that when RCC and steel macrofibers are used, composite pavement thicknesses should be the same or thinner than those of current French composite designs.

3 TYPES AND CHARACTERISTICS OF FIBERS

Fiber reinforcement in concrete refers to discrete fibers that are randomly distributed and oriented within the concrete matrix. Selecting the specific fiber type for use in pavements can be challenging because of the wide variety of fibers available and the fact that each fiber can produce a different laboratory performance value for a given concrete mixture. Therefore, it is useful to review the characteristics of fibers, including their material composition, size, geometry, properties, packaging, and interaction with the concrete matrix.

3.1 Characteristics of Fibers

The main aspects to consider when selecting a fiber are the fiber's geometry (length l , diameter d , and aspect ratio l/d), texture, and material type. At present, synthetic (e.g., polypropylene) and steel are the most common fiber materials used for concrete pavements, although other materials are available, as discussed in Section 3.2 of this report. The geometric and physical properties of fibers are discussed in this section.

3.1.1 Fiber Size

Fiber can be classified according to three general size categories: macro, micro, and nano. The present report deals primarily with macrofibers, which are used for structural response enhancement in concrete, primarily through toughening mechanisms. Microfibers can be used to mitigate or reduce plastic shrinkage cracking in concrete but offer no long-term structural benefit to the concrete. Nano fibers, such as carbon nanotubes and some forms of carboxymethyl cellulose (CMC), are experimental and not currently viable for concrete pavement applications.

The length, diameter, and aspect ratio of macrofibers can vary slightly depending on the fiber material. Macrofibers are longer (around 1 to 2 in.) and have larger diameters (0.01 to 0.04 in.) than microfibers. Synthetic microfibers have a diameter less than 0.3 mm and a length between 13 to 57 mm, while synthetic macrofibers have a diameter greater than 0.3 mm and lengths between 38 to 57 mm (Harrington and Fick 2014). Steel macrofibers have a length of 19 to 64 mm (Harrington and Fick 2014). Round steel macrofibers are typically 0.25 to 1.0 mm in diameter, while flat steel macrofibers are 0.15 to 0.40 mm thick and 0.25 to 0.90 mm wide (Bentur and Mindess 2007).

One important characteristic of the fiber size is known as the aspect ratio, which is the ratio of the fiber's length to its effective diameter. Many fibers are not manufactured with a circular cross-section, and therefore an effective fiber diameter is calculated based on the cross-sectional area. As the fiber aspect ratio increases, the total surface area for concrete-fiber bonding increases. A fiber with a smaller aspect ratio may pull out of the concrete matrix before it fully reaches its maximum energy absorption potential. Conversely, a fiber with a longer aspect ratio may have such a strong bond that the fiber fractures before debonding from the concrete matrix. Additionally, larger fiber aspect ratios increase the potential for fiber "balling," which is when the fibers clump together during the mixing process and cause issues with consolidation and non-

uniform distribution; balling can be generally accommodated by adjusting the mixture design and batching procedure. Macrofibers are designed with a material, aspect ratio, and surface texture that allows them to debond and pull out of the concrete matrix in order to maximize their energy absorption potential.

3.1.2 Texture and Shape

Fibers can be manufactured with various shapes, textures, and embossings. These different geometric features are intended to provide mechanical interlock or friction for the fiber as it is pulling out of the concrete matrix. A description of the manufactured shape, texture, or embossing is sometimes given by the manufacturer. For example, synthetic fibers are sometimes described as being monofilament (a single strand of fiber material, often with multiple chopped fibers of the same length), multifilament (a mixture of monofilament fibers of various lengths), or fibrillated (fiber material manufactured to have a branched network structure for a greater micro-surface area). Examples of different fiber shapes and textures are shown in Figure 3.1.



Figure 3.1. Examples of different macrofiber types, top to bottom: crimped, embossed, bi-tapered, and twisted synthetic; straight fibrillated synthetic (two images); hooked-end and crimped steel; and twisted basalt

Both synthetic and steel fibers can also be embossed, twisted, crimped, or hooked-end (in which the fiber is pressed in a die to change the profile of the fiber along the length). In one study of polypropylene fibers, it was found that a crimped texture offered the greatest bond pullout strength compared to other textures (e.g., straight, twisted, hooked-end, sinusoidal) (Won et al. 2006).

Steel fiber textures and shapes vary depending on the manufacturing and processing methods, but steel fibers commonly have a circular, semicircular, or rectangular cross-section, and the discrete fibers can be straight, hooked-end, deformed (crimped), or enlarged-end. The deformed steel fiber category is very broad, encompassing any number of surface textures and shapes meant to increase the surface area and/or mechanical bonding properties.

3.1.3 Packaging

Fiber packaging varies depending on the fiber type and the manufacturer. Although the fiber packaging method is not intended to alter the purpose of the fiber, the specific fiber packaging method may affect the fiber dispersion, the fresh concrete properties, and potentially the hardened concrete properties. Synthetic macrofibers may be packaged loose or in bundles (Figure 3.2).

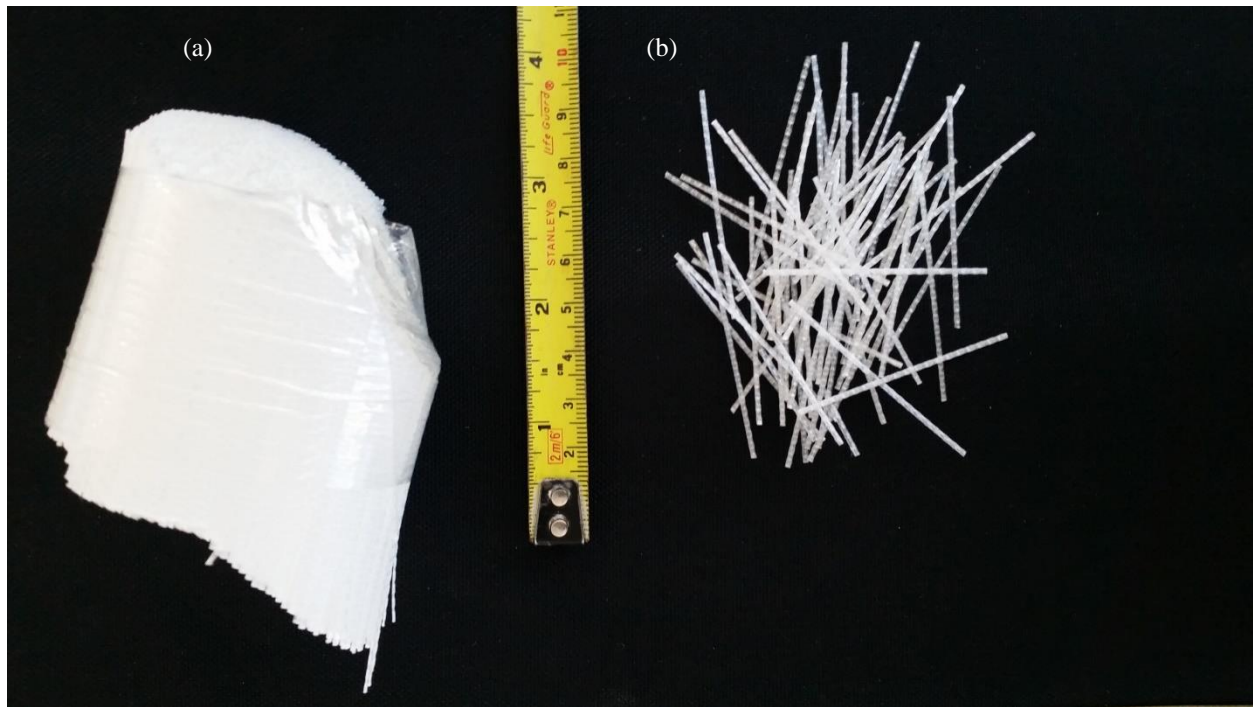


Figure 3.2. Synthetic macrofibers packaged in (a) a discrete bundle or (b) loose

Typically, synthetic fibers are sold in bags at a fixed weight in order to simplify the dosage calculation as the number of bags to add to a given concrete batch. The fiber bags may be dissolvable, such that the entire bag is added to the mixer during the concrete batching process. Sometimes concrete producers instead open the packaging bags and pour the contents directly into the concrete mixer. Bundled fibers typically come in a dissolvable wrapping. The dissolvable bags and bundle wrapping should not affect the mixture's performance. Fibrillated synthetic macrofibers may be pre-bundled (as is the case with entangled or twisted fiber strands), and the shearing action of the mixing process properly disperses this type of fiber.

Steel macrofibers are often packaged loose or in glued bundles. Depending on the manufacturing process, some of the glued steel macrofibers may also require the shearing action of the concrete mixer for their dispersion. The glue is often water-soluble and should not affect the concrete mixture's performance (Bentur and Mindess 2007).

3.2 Fiber Material Types

Fiber material can be classified as synthetic, steel, glass, or natural. These materials are defined in ASTM C1116, Standard Specification for Fiber-Reinforced Concrete, in terms of the FRCs that are made with them. The four FRC classifications are summarized as follows:

- **Type I: Steel Fiber-Reinforced Concrete.** This classification is for concrete made with carbon steel, alloy steel, or stainless steel fibers, as specified further by ASTM A820.
- **Type II: Glass Fiber-Reinforced Concrete.** This classification is for concrete made with alkali-resistant glass fibers, as specified further by ASTM C1666.
- **Type III: Synthetic Fiber-Reinforced Concrete.** This classification is for concrete made with synthetic fibers that have been proven to be resistant to deterioration by the cement paste environment (e.g., moisture, alkaline pore solution, chemical admixtures) over the useful life of the structure. Currently, only polyolefin fibers have a standard specification for use in concrete, which is described in ASTM D7508.
- **Type IV: Natural Fiber-Reinforced Concrete.** This classification is for concrete made with natural fibers that have been proven to be resistant to deterioration by the cement paste environment (e.g., moisture, alkaline pore solution, chemical admixtures) over the useful life of the structure. Currently, only cellulose fibers have a standard specification for use in concrete, which is described in ASTM D7357. Other natural fibers have been used in concrete but do not have their own standard specifications at this time. Examples of natural fibers include bamboo fibers, jute fibers, and basalt fibers.

For FRC pavement overlays, synthetic and steel macrofibers have predominantly been used. Some typical properties of synthetic and steel macrofibers are shown in Table 3.1.

Table 3.1. Typical macrofiber or microfiber properties

Fiber Type	Material	Tensile Strength (MPa)	Tensile Modulus (MPa)	Elastic Modulus (GPa)	Tensile Strain, (% max to min.)	Fiber Diameter (μm)	Relative Adhesion to Cement Matrix
Synthetic	Polypropylene	200 to 700	0.5 to 9.8	3.5 to 10	15 to 10	10 to 150	Poor
	Polyvinyl alcohol	800 to 1500	29 to 40	29 to 36	10 to 6	14 to 600	Excellent
	Polyethylene	400	2 to 4	5	400 to 100	300 to 1000	Good
Steel	Carbon steel	1000	200	210	2 to 1	50 to 85	Excellent
	Stainless steel	1000	200	210	2 to 1	50 to 85	Excellent

Source: Bentur and Mindess 2007, Banthia et al. 2012

In general, for composite FRC to have greater strength, elastic modulus, or toughness properties relative to unreinforced concrete, the macrofibers should have properties similar to or greater than those of plain concrete. Because the elastic modulus for paving concrete can be assumed to range from 4,000 to 6,000 ksi (27.6 to 41.4 GPa), it can be seen in Table 3.1 that steel macrofibers have a greater elastic modulus than paving concrete while synthetic macrofibers may have a comparable or lower elastic modulus. To meet or exceed concrete strength and modulus properties, some “high-tenacity” synthetic macrofibers have been developed. These are polymer macrofibers with slightly greater elastic modulus and strength properties compared to typical polymer macrofibers.

3.2.1 Synthetic (Polymer) Fibers

Synthetic fibers are the most common type of fibers used in FRC overlays, with 92% of all fiber-reinforced concrete overlays in the United States reported to contain synthetic macrofibers (Hansen et al. 2016). These fibers are polymeric, consisting of polypropylene, polyolefin, polyester, or blends of these polymers. Nylon fibers have also been used for some asphalt concrete applications because of its higher melting point. Synthetic fibers do not affect mix water batching because they do not absorb moisture. At higher fiber dosages, synthetic fibers can exhibit balling (Figure 3.3).



Figure 3.3. Example of fiber balling in a hardened BCOA application in a parking lot, shown with a lens cap 60 mm in diameter

For FRC overlays, synthetic macrofibers have been dosed at 3 to 5 lb/yd³ but can be dosed at even higher levels, e.g., 7.5 lb/yd³, as long as there is enough cementitious paste to coat the fibers and fiber balling is controlled (Harrington and Fick 2014).

Polypropylene and polyethylene are the most common commercially available synthetic or polymer materials and are classified as polyolefins. Numerous specifications use the term polyolefin to specify synthetic fibers because this is the term used in ASTM D7508-10. The term polyolefin is broad, and ASTM D7508-10 specifies that this term is used to describe any long-chain polymer containing at least 85% by weight ethylene and/or propylene monomer units. This means that polypropylene and polyethylene are two types of polymers that are acceptable for use as synthetic fibers in concrete mixtures.

The following are some advantages, disadvantages, and characteristics of the various polymer fiber types:

- **Polypropylene (PP).** Some advantages of PP include low cost, high alkali resistance, and high melting point (165°C), while some disadvantages include lower modulus of elasticity, poor bond with the cementitious matrix, and degradation with extended exposure to sunlight and oxygen (Bentur and Mindess 2007). PP fibers are available in many forms, including monofilament and fibrillated, and some high-tenacity forms are available. PP is hydrophobic, which affects its dispersion and bonding properties, so it is often manufactured with a surface treatment to improve dispersion and bonding when used for concrete applications. The theoretical critical volume of PP fibers (i.e., the minimum volume after which the concrete may exhibit strain hardening) is 3% (Bentur and Mindess 2007). However, the maximum

practical volume fractions of PP fibers are around 0.5% to 1% because of fiber balling tendencies.

- **Polyethylene (PE).** Most PE fibers have an elastic modulus around 5 GPa, although high-modulus (15 to 31 GPa) PE fibers have been reported. PE fibers have been mixed into concrete at volumes as high as 4%, at which point strain hardening behavior has occurred (Bentur and Mindess 2007). Similar to PP, PE fibers can also exhibit fiber balling, so the practical maximum volume fraction of PE fibers is also around 0.5 to 1%.
- **Polyolefin.** This type of fiber includes any combination of polypropylene and polyethylene polymers. ASTM D7508, Standard Specification for Polyolefin Chopped Strands for Use in Concrete, classifies polyolefin fibers into micro-polyolefin fibers, macro-polyolefin fibers, and hybrid fibers (a blend of micro- and macro-polyolefin fibers). Micro-polyolefin fibers have a denier (mass density) of < 580 , which typically equates to a fiber diameter of < 0.3 mm, and are chopped to lengths of 3 to 50 mm. Macro-polyolefin fibers have a denier of ≥ 581 which equates to fiber diameters of ≥ 0.3 mm, and are chopped to a length of 12 to 65 mm. The tensile strength of macro-polyolefin must be at least 50 ksi (345 MPa) per ASTM D7508. Hybrid fibers must meet the necessary criteria for the corresponding micro- and macro-polyolefin fiber contents.
- **Polyvinyl alcohol (PVA).** These fibers have a high strength and a high elastic modulus (see Table 3.1). Because PVA is naturally hydrophilic, PVA fibers sometimes bond too well with the cement and are supplied with a coating to optimize the chemical bond. PVA fibers have been used to produce high-performance FRC (e.g., ECC, a strain-hardening FRC) at fiber contents as low as 2%. In conventional concrete, research studies have used PVA fibers at contents from 0.5% to 4% by volume, with 1% being common.

3.2.2 *Steel Fibers*

FRCs with steel macrofibers have been studied since the 1960s, initially as a method to replace secondary reinforcement intended for crack control, but later the toughness benefits of steel macrofibers for concrete applications was realized (Bentur and Mindess 2007). Steel macrofiber dosage levels for concrete pavements are typically from 30 to 70 lb/yd³, with the dosage depending on the project inputs and design requirements.

Steel macrofibers had been used in FRC overlays historically, but more recently synthetic macrofibers have been overwhelmingly specified. Some reasons suggested to explain why steel macrofibers are no longer as popular include concerns related to corrosion potential (Marcos-Meson et al. 2018), concerns that surface steel fibers may puncture tires, difficulty in introducing the fibers in the batching process, and the higher costs of steel versus polymeric fiber material.

The highly alkaline pore solution of concrete in theory protects the passivation layer on the steel, preventing the corrosion of steel fibers encased in concrete. However, some concrete degradation mechanisms, such as carbonation or chloride ingress, affect this passivation layer and can

increase the risk of corrosion, especially near the surface and in the presence of cracks of larger widths (Marcos-Meson et al. 2018). Stainless steel and coated steel fibers have been made available to reduce the risk of corrosion, but these also come at a higher cost. With proper concrete mixture design and fiber selection, the probability of internal steel fiber corrosion can be minimized. Furthermore, many successful applications of FRC with steel macrofibers have been reported. The risk of corrosion is discussed in more detail in Sections 4.2.6 and 5.3.8 and Table 5.4.

There has been no evidence that steel fibers regularly puncture tires, mainly because any surface fibers often bend or break away easily at the surface or corrode and break off because they are directly exposed to the environment. For paving projects, synthetic macrofibers are simpler to introduce to the concrete batching process relative to steel macrofibers.

ASTM A820, Standard Specification for Steel Fibers for Fiber-Reinforced Concrete, classifies five types of steel fibers for use in FRC: Type I (cold-drawn wire), Type II (cut sheet), Type III (melt-extracted), Type IV (mill cut), and Type V (modified cold-drawn wire). These classifications are based on the process used to produce the fiber, and, regardless of the classification, the fiber can be straight or deformed. Straight steel fibers are uncommon in FRC because a greater bonding condition is achieved with deformed fibers, and therefore many commercial steel fibers are manufactured with a rough surface, crimping, hooked ends, or enlarged ends (see Figure 3.1). ASTM A820 also specifies that the minimum tensile strength of steel fibers for FRC should be 50 ksi (345 MPa). Steel fibers offer a greater tensile strength and tensile modulus compared to synthetic fibers (Table 3.1). Due to their higher material density, a larger weight dosage of steel fibers is required for the same volume fraction of synthetic fibers.

3.2.3 Natural, Glass, and Other Fibers

Natural fibers are produced or processed from a local, organic source, such as cellulose, coconut husks, hemp, sisal, jute, bamboo, etc. One laboratory study showed that cellulose microfibers can reduce and potentially eliminate drying shrinkage cracking in an FRC overlay of an existing concrete substrate (Banthia and Gupta 2006). Some other fiber types, such as glass, carbon, and mineral (e.g., asbestos or basalt) fibers, have been studied for use in cement or concrete but have not been applied significantly to FRC pavements and therefore are not discussed in this report.

3.3 Deflection Hardening versus Softening Behavior

There are three primary interactions at the fiber-cement matrix interface that affect the response and performance of FRC: fiber-cement adhesion (physical and chemical), friction between the fiber and the matrix, and mechanical bonding (such as that due to the texture of the fiber) (Bentur and Mindess 2007). Designing an FRC pavement with these interactions in mind assists in the selection of the appropriate fiber to begin performance testing (e.g., fiber type, texture, size, aspect ratio, and so on).

Macrofibers are added to improve the tensile behavior of the concrete, and therefore FRC exhibits either a strain hardening or a strain softening response under direct tension loading. This means that after the FRC material cracks, the fibers either carry a tensile stress higher than the tensile strength of the concrete or the fibers carry a tensile stress lower than the concrete tensile strength. Concrete pavements are designed to undergo flexural loading, which is a combination of compression and tension. If an FRC material that exhibits tensile strain softening (i.e., the material carries stress after cracking that is lower than the tensile strength of the concrete) is tested under flexural loading, it can be further classified as having deflection hardening or deflection softening behavior (Naaman and Reinhardt 2006). Similar to direct tension, as the FRC material cracks under flexural loading, the FRC exhibits a flexural capacity that is either greater than the concrete flexural strength (deflection hardening) or lower than the concrete flexural strength (deflection softening).

Given that concrete pavements resist loading through flexural stresses, FRC performance is typically associated with deflection softening or hardening behavior, as summarized in Figure 3.4.

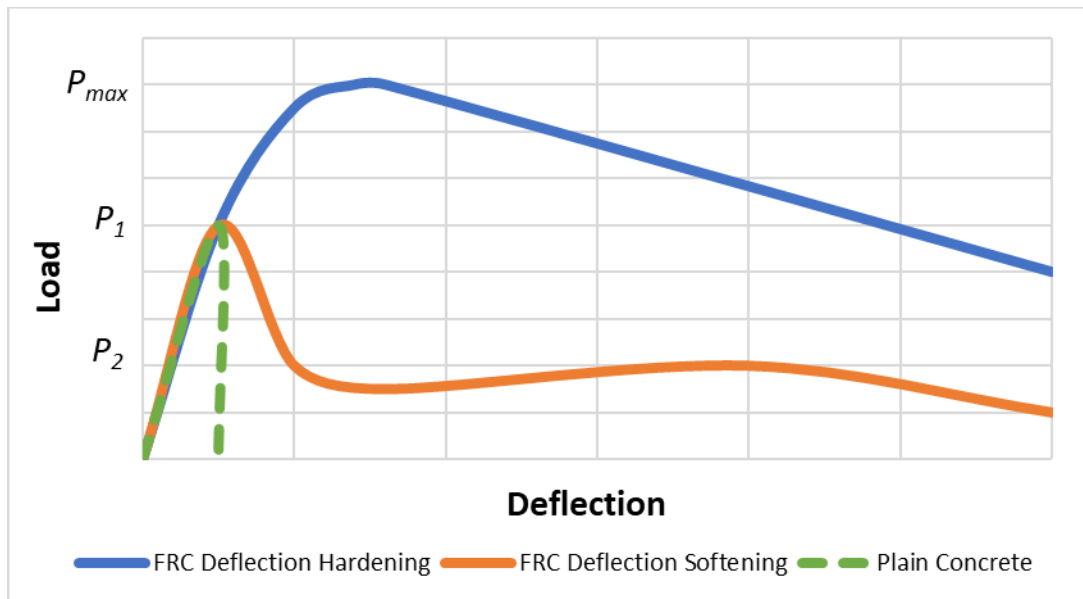


Figure 3.4. Schematic of deflection hardening and softening response under flexural loading for plain concrete and FRC

All three concrete specimens represented in Figure 3.4 macro-crack at load P_1 . The FRC with deflection hardening behavior reaches an ultimate load of P_{max} , while the FRC with deflection softening behavior reaches a maximum post-cracking residual load of P_2 . The plain concrete has no significant residual load carrying capacity after load P_1 .

As the local material strength is reached, cracking propagation progresses until the specimen's flexural strength is reached (P_1). If fibers are present across the macro-crack, a deflection hardening response is exhibited when the applied load continues to increase with increasing deflection. After P_1 , if the applied load decreases with increasing deflection, then deflection

softening behavior exists for the FRC material. In strain hardening and deflection hardening materials, the composite material sustains greater stresses than the concrete matrix alone. Bond failure and slippage at the cement-fiber interface are the primary contributors to the deflection hardening behavior.

Several important properties are calculated from the simply supported beam flexural test of FRC materials, as shown in Figure 3.4. FRC under flexural stress produces a distinct macro-crack at a certain load level, which is known as the first crack load (P_1) or the limit of proportionality for deflection hardening materials (Figure 3.4).

For plain concrete and deflection softening FRC, P_1 is the load used to compute the flexural strength or modulus of rupture. With continued deformations, a deflection hardening material reaches a maximum load (P_{max}), which can be defined as the ultimate load carrying capacity of the specimen. For deflection softening materials, a secondary peak or residual load (P_2) often occurs at higher displacement levels and is inherently lower in magnitude than P_1 . Even though a deflection softening FRC beam specimen does not exceed the first crack load of plain concrete, the same FRC material can increase the flexural load carrying capacity of a concrete slab.

In general, higher volume fractions, larger aspect ratios, and greater fiber stiffnesses produce a higher post-cracking load response. In a study summarized in Table 3.2 (Kim and Bordelon 2017a), deflection hardening behavior was noted for FRC with higher fiber volumes and certain steel macrofiber types, while deflection softening behavior was seen for all synthetic polypropylene macrofibers tested.

Table 3.2. Fiber characteristics and volumes resulting in deflection hardening or deflection softening behavior for concrete overlay mixtures

Fiber Characteristics	Fiber Volume	Behavior
Steel, hooked-end, 35 mm length, 0.55 mm diameter	0.5%	Deflection softening
	1.0%	Deflection hardening
Steel, hooked-end, 60 mm length, 0.9 mm diameter	0.5%	Deflection hardening
	1.0%	Deflection hardening
Polypropylene, 40 mm length, 0.11 mm thick, 1.4 mm wide	0.5%	Deflection softening
	1.0%	Deflection softening
Polypropylene, 50 mm length, 0.4 mm thick, 1.2 mm wide	0.5%	Deflection softening
	1.0%	Deflection softening

Source: Kim and Bordelon 2017a

Almost all FRC materials used in concrete overlays have deflection softening responses based on the macrofiber type and volume fractions that have been specified for pavement projects.

4 BEHAVIOR OF FRC MATERIALS FOR CONCRETE PAVEMENTS

The properties of FRC materials in general are influenced by the fiber (e.g., its type, volume, orientation, dispersion, texture, geometry, and size), the concrete matrix (e.g., its strength and aggregate properties), and the interactions between the fiber and the concrete matrix. The properties of FRC test specimens are affected by the specimen size, the method of sample preparation, and the loading rate or test configuration (Bentur and Mindess 2007). The procedures for standardized tests and other experimental FRC test methods are discussed in Chapter 7, while this chapter focuses on the general fresh and hardened concrete properties that can be expected from FRC materials.

4.1 Fresh Concrete Properties

FRC workability is defined as how readily the FRC can be mixed, placed, consolidated, and finished. The factors affecting the workability of FRC materials include the type of fiber and its length, the fiber content of the mixture, and the type of admixtures added to the concrete mixture. For moderate to high macrofiber additions ($\leq 1.5\%$ by volume), a slump loss between 1 and 4 in. (25 and 100 mm) can be expected after the macrofibers are added to the mixture (Harrington and Fick 2014). The greater the amount of macrofibers in the mixture, the greater the reduction in slump that should be expected. To compensate for the reduction in workability, it may be necessary to increase the water-reducing admixture dosage and/or, if necessary, increase the total cementitious content of the concrete mixture. Increasing the total cementitious content may be preferred over adjusting the dosage of the water-reducer to ensure that the macrofibers are coated and that an adequate bond is achieved. Either of these mixture design changes also improves the finishability of the FRC pavement.

Macrofibers can be dispersed into the concrete by hand, through pre-packaged bags or bundles, or through an automated system. During mixing, there may be a tendency for fiber “balls” to form, especially when a mixture is not adjusted to accommodate the fiber dosage or the charging of the macrofibers has not been properly sequenced. Macrofiber balling can occur as a result of any combination of factors, including the properties of macrofiber type selected for the mixture, the volume fraction of the macrofibers, the mixture’s workability, the charging sequence of the mixture’s constituents, the type and speed of the concrete mixer, and the condition of the fines in the mixing system. The fiber manufacturer’s recommendations regarding the mixing procedure should be followed to minimize balling. For example, adding the macrofibers to the mixture before or simultaneously with the aggregates, as opposed to adding the macrofibers at the end of the concrete mixing stage, may help reduce some macrofiber balling. Synthetic macrofibers and glued steel macrofibers require the shearing action of the mixer to assist with dispersion. Changing the aggregates so that they have a more angular shape and changing the aggregate gradation to achieve a well-graded particle size distribution may also assist with fiber dispersion and minimize fiber balling. A recommended well-graded blending, such as the ones listed in Table 4.1, has been found to reduce the formation of fiber balls and improve the workability of FRCs with steel fibers (ACI Committee 544 2009).

Table 4.1. Recommended aggregate gradations for FRC

Sieve Size	Percent Passing for Maximum Aggregate Size of				
	3/8 in. (10 mm)	0.5 in. (13 mm)	0.75 in. (19 mm)	1 in. (25 mm)	1.5 in. (38 mm)
2 in. (51 mm)	100	100	100	100	100
1.5 in. (38 mm)	100	100	100	100	85-100
1 in. (25 mm)	100	100	100	94-100	65-85
0.75 in. (19 mm)	100	100	94-100	76-82	58-77
0.5 in. (13 mm)	100	93-100	70-88	65-76	50-68
3/8 in. (10 mm)	96-100	85-96	61-73	56-66	46-58
#4 (5 mm)	72-84	58-78	48-56	45-53	38-50
#8 (2.4 mm)	46-57	41-53	40-47	36-44	29-43
#16 (1.1 mm)	34-44	32-42	32-40	29-38	21-34
#30 (0.6 mm)	22-33	19-30	20-32	19-28	13-27
#50 (0.3 mm)	10-18	8-15	10-20	8-20	7-19
#100 (150 μ m)	2-7	1-5	3-9	2-8	2-8
#200 (75 μ m)	0-2	0-2	0-2	0-2	0-2

Source: ACI Committee 544 2009

The fresh concrete unit weight changes slightly depending on the macrofiber type and dosage. Since synthetic macrofibers have a lower specific gravity than cement and aggregate, the unit weight of FRC is only minimally reduced for normal to moderate volume fractions of synthetic macrofibers. Conversely, steel macrofibers have a significantly greater specific gravity than cement and aggregate, and therefore the unit weight of FRC increases corresponding to the volume fraction of the steel macrofibers.

For air-entrained concrete, the air content may be affected by the addition of fibers, primarily because of the fibers' negative impact on workability. In such cases, it is recommended that trial batches be made to assess whether target air contents will be influenced by a given dosage of fibers. In general, it may be necessary to slightly increase the dosage of the air-entraining admixture when mixing FRC materials.

4.2 Hardened Concrete Properties

4.2.1 Strength and Elastic Modulus

The amount of macrofibers that would fundamentally increase the strength of an FRC composite is called the theoretical critical fiber volume. This critical fiber volume is reported to be about 1% to 3% for discrete, discontinuous macrofibers randomly oriented in the cement matrix (Bentur and Mindess 2007). Because practical macrofiber dosages for FRC pavement overlays are much lower than this critical volume fraction (e.g., < 0.5%), no change in compressive and flexural strength or elastic modulus should be expected. In some cases, the addition of fibers can reduce the strength of an FRC. Overwhelmingly, however, these examples of reductions in

strength are often linked to poor fiber dispersion, fiber balling, or problems with FRC specimen placement and consolidation.

Some specific mixtures with steel or synthetic macrofibers have shown some increase in reported concrete strength, especially at very high (2%) steel volume fractions, with greater increases possible if the macrofibers are aligned in the direction of the tensile stress (Bentur and Mindess 2007). Likewise, the flexural strength of concrete has been reported to increase by as much as 100% with the addition of high volumes of steel macrofibers, with the flexural strength increasing as the steel macrofiber volume and fiber aspect ratio increase and when deformed instead of straight macrofibers are used (Bentur and Mindess 2007).

4.2.2 Toughness and Fracture

The most significant impact of macrofibers on concrete behavior is the increase in post-cracking toughness, energy absorption, and fracture energy. Figure 4.1 shows an example of an FRC beam sample that has been tested past the peak load capacity of the concrete; nevertheless, the composite still retains load carrying capacity (residual strength) via the macrofibers bridging the crack.



Figure 4.1. Example of the post-cracking behavior of notched FRC beam specimen with synthetic macrofiber volume of 0.43%

The toughness of FRC with steel and macro-synthetic fibers can be as high as one to two orders of magnitude greater than that of plain concrete, with toughness increasing as a function of macrofiber content and fiber aspect ratio.

In order to quantify the impact of macrofibers on toughness, energy absorption, and fracture energy, measurement standards have been created to calculate the residual strength of the

concrete after cracking. ASTM C1609 is one test method available to measure the residual strength of FRC (see Section 7.2.1.1). Table 4.2 shows sample results from ASTM C1609 for two synthetic macrofibers at two volume fractions. The results show that residual strength increases with macrofiber volume fraction and is affected by the type of macrofiber.

Table 4.2. ASTM C1609 results for two macro-synthetic fibers at two fiber volumes

Fiber Characteristics	Hybrid twisted bundle of 54 mm monofilament and 38 mm fibrillated PP fibers		Embossed 48 mm PP fibers	
	0.27%	0.38%	0.27%	0.38%
Total Fiber Volume	0.27%	0.38%	0.27%	0.38%
Compressive Strength, MPa (psi)	54.8 (7950)	52.5 (7610)	53.3 (7730)	53.8 (7800)
Flexural Strength, f_1 , MPa (psi)*	5.05 (730)	5.05 (735)	5.05 (730)	5.20 (750)
Residual Strength at L/600, f_{600} , MPa (psi)*	0.65 (95)	1.20 (175)	1.10 (160)	1.75 (255)
Residual Strength at L/150, f_{150} , MPa (psi)*	0.65 (90)	1.05 (155)	0.90 (135)	1.55 (225)

*Tested with a beam size of 150 x 150 mm (6 x 6 in.) and a span length of 450 mm (18 in.).

Additionally, Table 4.3 shows the effect of macrofiber type, macrofiber volume, and concrete age on residual strength.

Table 4.3. ASTM C1609 residual strength values for FRCs with different fiber types, fiber volumes, and concrete ages

Fiber Type	Fiber Volume	Residual Strength at L/150, f_{150} (MPa)*					
		3 days	7 days	14 days	28 days	56 days	90 days
Steel, hooked-end, 35 mm length, 0.55 mm diameter	0.5%	N/A	2.40	2.62	2.83	2.61	2.48
	1.0%	2.71	3.08	3.26	3.21	4.03	4.53
Steel, hooked-end, 60 mm length, 0.9 mm diameter	0.5%	2.71	2.99	3.45	4.18	N/A	4.19
	1.0%	4.06	4.60	4.61	6.51	4.77	5.26
Polypropylene, 40 mm length, 0.11 mm thick, 1.4 mm wide	0.5%	2.22	1.64	1.97	1.10	1.79	1.25
	1.0%	2.87	3.05	4.22	2.73	3.20	2.62
Polypropylene, 50 mm length, 0.4 mm thick, 1.2 mm wide	0.5%	1.68	2.10	1.97	2.29	3.27	2.34
	1.0%	2.99	3.00	4.39	4.49	3.68	4.26

Tested with a beam size of 150 x 150 mm (6 x 6 in.) and a span length of 450 mm (18 in.).

Source: Kim and Bordelon 2017a

In general, the residual strength increases as macrofiber volume, fiber aspect ratio, and fiber stiffness increase. The residual strength may not continue to increase with concrete age depending on the strength of the fiber-concrete matrix, type of fiber, and fiber content.

The concrete fracture properties can differ between plain concrete and FRC as well as between FRCs with different types and volume fractions of fibers. As seen in Table 4.4, a dramatic increase in the total fracture energy can be realized with the addition of macrofibers to concrete with limestone or recycled concrete aggregates.

Table 4.4. Average 7-day strength and fracture properties of FRC

Aggregate Type Concrete Type	Limestone (Roesler et al. 2007a)		Limestone (Bordelon et al. 2009)		RCA (Bordelon et al. 2009)	
	Plain	FRC*	Plain	FRC**	Plain	FRC**
Compressive Strength (MPa)	33.1	31.4	31.2	30.3	27.8	23.8
Split Tensile Strength (MPa)	3.44	4.22	2.61	2.93	2.45	2.86
Modulus (GPa)	N/A	N/A	26.0	26.0	28.0	28.2
Critical Stress Intensity Factor, K_{Ic} (MPa-m ^{1/2})	1.01	1.03	0.94	1.09	0.91	0.95
Total Fracture Energy (N/m)	120	3530	86	310***	56	262***

* 0.78% volume fraction of synthetic macrofibers

** 0.2% volume fraction of synthetic macrofibers

*** Calculated at a crack mouth opening displacement of 4 mm

The critical stress intensity factor does not change significantly with the addition of macrofibers because this property is primarily controlled by the properties of the concrete constituents and the matrix.

Table 4.5 shows the effect of different macrofiber types, macrofiber volumes, and concrete ages on the total fracture energy. For all macrofiber types, the total fracture energy increases with increasing macrofiber volume and age, with certain macrofiber types yielding a greater increase in total fracture energy.

Table 4.5. Effect of fiber type, fiber volume, and concrete age on the wedge splitting total fracture energy

Fiber Type	Fiber Volume	Total Fracture Energy (N/m)*		
		7 days	28 days	90 days
Plain concrete		81	88	107
Steel, hooked-end, 35 mm length, 0.55 mm diameter	0.5%	728	751	1325
	1.0%	955	1046	1621
Steel, hooked-end, 60 mm length, 0.9 mm diameter	0.5%	425	1142	2137
	1.0%	1051	1749	2740
Polypropylene, 40 mm length, 0.11 mm thick, 1.4 mm wide	0.5%	490	512	648
	1.0%	531	510	717
Polypropylene, 50 mm length, 0.4 mm thick, 1.2 mm wide	0.5%	525	689	821
	1.0%	703	991	901

* Total fracture energy until complete separation for the plain concrete and until an opening deflection of 2.5 mm for the FRC

Source: Kim and Bordelon 2017a

4.2.3 Fatigue

The effect of macrofibers on the fatigue properties of concrete has also been investigated. In general, steel macrofibers have been found to have limited to no effect on the compressive fatigue of concrete but do improve the flexural fatigue properties by increasing the endurance limit, reducing crack sizes, and increasing the amount of energy absorbed before failure (Bentur and Mindess 2007).

Table 4.6 shows the beam fatigue data for three different steel macrofibers. The results demonstrate that FRC exhibits better fatigue performance than plain concrete.

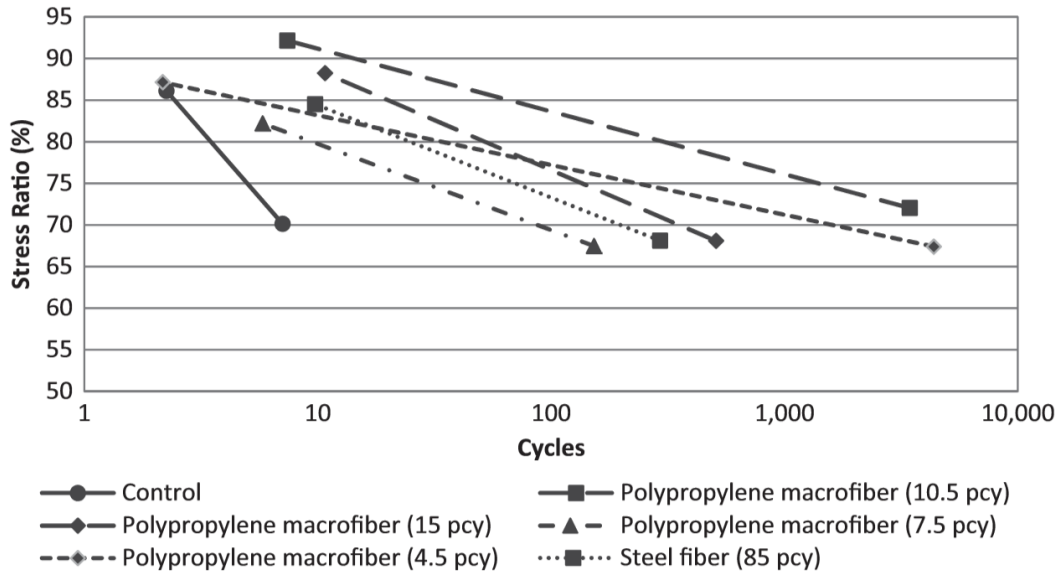
Table 4.6. Beam fatigue testing for FRC with steel fibers

Stress Ratio	Plain Concrete		FRC Steel Fiber 1		FRC Steel Fiber 2		FRC Steel Fiber 3	
	Maximum Stress (psi)	Average Number of Cycles	Maximum Stress (psi)	Average Number of Cycles	Maximum Stress (psi)	Average Number of Cycles	Maximum Stress (psi)	Average Number of Cycles
100	741	1	872	1	778	1	759	1
95			828	1,193	739	1,547	721	860
90	667	2,200	785	2,903	702	3,417	683	4,320
85			741	28,053	661	51,440	645	68,100
80	593	60,183	698	98,303	622	175,987	607	185,100
75			654	233,547	584	375,047	567	330,117
70	519	322,413	611	>1,000,000	545	>1,000,000	531	>1,000,000
60	445	>1,000,000						

Steel macrofiber volumes were 0.46% for all FRC mixtures. Steel fiber 1 was a 1.13 in. deformed fiber with an aspect ratio of 45. Steel fiber 2 was a 1.5 in. deformed fiber with an aspect ratio of 60. Steel fiber 3 was a 1.18 in. hooked-end fiber with an aspect ratio of 60. Replicate concrete beams were tested under four-point flexural bending until failure or until 1 million cycles.

Source: Nanni 1991

Figure 4.2 shows the results of low-cycle fatigue testing of FRC with synthetic or steel macrofibers. These results also confirm that the number of cycles to failure for FRC is significantly greater than that of plain concrete (Mulheron et al. 2015, Kevern et al. 2016).



Mulheron et al. 2015

Figure 4.2. Low-cycle fatigue of concretes containing different macrofibers at different volume fractions

Table 4.7 demonstrates that FRC with steel or synthetic macrofibers retains toughness even after fatigue for 2 million cycles with and without freeze/thaw damage.

Table 4.7. Flexural strength and toughness of FRC exposed to freeze/thaw and fatigue

Condition*	Plain Concrete	Steel Fiber 1	Steel Fiber 2	Polyolefin Fiber
<i>Flexural Strength (MPa)</i>				
90-day Unconditioned	6.60	7.09	6.66	6.55
Freeze/Thaw only	4.65	6.11	5.59	5.51
Fatigue (10-40%) only	4.78	5.34	5.10	4.76
Fatigue (10-45%) only	5.34	7.06	6.53	N/A
Freeze/Thaw then Fatigue (10-40%)	5.55	5.73	6.30	6.43
Freeze/Thaw then Fatigue (10-45%)	5.75	4.93	6.00	6.21
Fatigue (10-40%) then Freeze/Thaw	5.25	6.00	5.51	5.35
<i>Residual Strength (Toughness) per JSCE SF-4 (MPa)</i>				
90-day Unconditioned	N/A	4.67	3.92	4.32
Freeze/Thaw only	N/A	5.66	4.18	3.59
Fatigue (10-40%) only	N/A	4.02	3.29	3.52
Fatigue (10-45%) only	N/A	5.19	3.88	N/A
Freeze/Thaw then Fatigue (10-40%)	N/A	4.59	3.92	3.95
Freeze/Thaw then Fatigue (10-45%)	N/A	4.93	3.98	4.01
Fatigue (10-40%) then Freeze/Thaw	N/A	5.10	4.16	3.89

Fiber volumes were 0.5% steel and 1.67% polyolefin. The fiber shapes were hooked-end (steel fiber 1), corrugated (steel fiber 2), and straight (polyolefin).

* Fatigue testing was for 2 million cycles at 10% to 40% or 10% to 45% of the 90-day flexural strength. Freeze/thaw testing was for 300 cycles. Samples were exposed to freeze/thaw only, fatigue only, freeze/thaw followed by fatigue, and fatigue followed by freeze/thaw.

Source: Forgeron and Trottier 2004

4.2.4 Load Transfer Efficiency

Very few studies have been conducted on the impact of macrofibers on joint load transfer efficiency. Macrofibers have been demonstrated to control crack widths, and therefore macrofibers should enhance the LTE across contraction joints and cracks through better aggregate interlock. Research conducted at the University of Pittsburgh (Barman 2014, Barman et al. 2015) compared FRC beams to plain concrete beams subjected to repeated shear loading, similar to the vertical movement of joints at a given crack width. The tested beams were standard 6 by 6 by 24 in. The study found that FRCs containing either 0.36% by volume of straight synthetic or 0.43% by volume of crimped synthetic macrofibers both exhibited a 20% increase in LTE compared to plain concrete, with the joints in the FRCs maintaining the same LTE for several million load repetitions. Field measurements of joint LTE on several plain concrete or FRC overlays have shown that FRCs perform well (King and Roesler 2014), but there is still limited field data to make strong conclusions about the long-term benefits of macrofibers to LTE given the impacts that support conditions, slab-base bonding, joint spacing, and climate have on joint crack widths.

4.2.5 *Shrinkage*

Traditionally, microfibers have been successfully applied to control and minimize plastic shrinkage cracking in very early-age concrete. Plastic shrinkage cracking has also been reported to be mitigated with as little as 0.1% by volume polypropylene macrofibers (Bentur and Mindess 2007), although greater resistance to plastic shrinkage cracking is commonly obtained through the use of synthetic microfibers (ACI Committee 544 2010) instead of macrofibers. The research findings regarding the effects of macrofibers on concrete drying shrinkage have been somewhat conflicting. Steel macrofibers may reduce free drying shrinkage, with greater shrinkage improvements as the macrofiber volume increases and for deformed rather than straight macrofibers. Steel macrofibers have been confirmed to reduce cracking and crack widths under restrained shrinkage conditions (Bentur and Mindess 2007). In a restrained shrinkage test, the addition of 0.5% by volume steel macrofibers was found to reduce the maximum crack width by 90% and the average crack width by 80% compared to plain concrete, while 0.5% by volume polypropylene macrofibers reduced the maximum crack width by 70% and the average crack width by 70% (Shah et al. 1994). While stress development in concrete under restrained ring shrinkage is similar for both plain concrete and FRC, the addition of macrofibers can delay the formation of visible cracks, and in FRC with steel macrofiber volumes of at least 0.5% the macrofibers may be able to transfer stress across the cracks under continued shrinkage conditions (Shah and Weiss 2006).

4.2.6 *Durability*

Because macrofibers hold cracks together after the concrete has cracked, FRC has the potential to improve durability to deleterious materials compared to plain concrete through lower permeability and reduced crack widths. For concrete with crack widths greater than 100 μm , the addition of steel macrofibers has been shown to reduce concrete permeability compared to cracked plain concrete (Rapoport et al. 2002). Furthermore, the permeability of FRC is lower than that of plain concrete even under applied mechanical stress (Banthia and Bhargava 2007).

Depending on the aggregate quality, the hardness of the concrete, and the testing configuration and loading speed, steel macrofibers can significantly increase the abrasion resistance of concrete (Bentur and Mindess 2007). Published results have demonstrated that synthetic fibers do improve the abrasion resistance of concrete (Grdic et al. 2012).

Studies of the freeze/thaw durability of FRC have shown that, similar to plain concrete, the amount of air entrainment is a critical factor for FRC (ACI Committee 544 2010), so the same air content requirements applied during the design of conventional concrete should be followed for the design of FRC. In one study, after exposure to 300 freeze/thaw cycles, concrete with macrofiber volumes of 0.5% steel or 1.67% polyolefin experienced a 15% reduction in flexural strength, compared to the 30% reduction found for plain concrete. However, the flexural fatigue endurance limit was only marginally improved by the presence of the macrofibers after freeze/thaw damage (i.e., an endurance limit of 64% was found for plain concrete versus 68% to 70% for FRC relative to the 90-day flexural strength) (Forgeron and Trottier 2004). Despite

reductions in flexural strength after freeze/thaw exposure, Table 4.7 demonstrates that FRC retains suitable residual strength.

With steel macrofibers, one potential degradation mechanism is corrosion of the fibers. In general, with proper mixture design formulation, the risk of corrosion can be minimized. Concrete durability as it relates to the corrosion of steel macrofibers is discussed in more detail in Section 5.3.8. Concerning the corrosion of conventional reinforcing steel in concrete, one study demonstrated that the presence of polypropylene macrofibers along with conventional reinforcing steel reduced the corrosion rate of the embedded steel in concrete exposed to restrained shrinkage conditions and a chloride ion solution (Sanjuán et al. 1997).

4.3 Selection of Fiber Type for Pavement Design

As described in Chapter 3 and the earlier sections of Chapter 4, many options related to fiber characteristics are available that can influence the design of a pavement with FRC. The decision of whether a specific fiber should be used is often based on some or all of the following parameters:

- Availability of the selected fiber type
- Toughness or fracture energy: Will the fiber need to perform and carry stress after concrete cracking?
- Fatigue and durability: Will the fiber material withstand the concrete and pavement loading and the environmental conditions?
- Cost of the fiber type at the determined required dosage rate (Note that the FRC would need to be tested or the manufacturer would need to be consulted to estimate the dosage rate.)

Several DOTs that have had experience with FRC or that intend to use FRC in the future may have a pre-approved list of fiber types from which the fiber used for a project must be selected. Such lists present information about different aspects of the fibers or the effects that the fibers have on the concrete so that the designer is aware of performance aspects that have been investigated or may be improved upon in the future as manufacturers further optimize and refine the fibers used in concrete. Some parameters, such as load transfer efficiency, are important, but the amount of research performed at this time is insufficient to identify the particular aspects of a given fiber type that will improve LTE.

5 CONCRETE PAVEMENT DESIGN METHODOLOGY WITH FRC MATERIALS

Given that the addition of macrofibers to plain concrete slabs can increase the slabs' flexural and ultimate capacities (see Section 2.3.1), an FRC material property (f_{150}^D) is needed to quantify the benefits that macrofibers provide to concrete slabs. Whereas the beam flexural strength shows similar values between plain concrete and FRC, the residual strength of the FRC beam (f_{150}^D) has been shown to be a representative material property that describes the effects of macrofibers on concrete slab behavior (Altoubat et al. 2008). For concrete pavement overlay design with macrofibers, it has been proposed that an effective or modified flexural strength, f_{eff} , based on the measurements from ASTM C1609, be used instead of the standard flexural strength (Altoubat et al. 2008, Roesler et al. 2008, Covarrubias et al. 2010, Bordelon and Roesler 2012).

The effective flexural strength, f_{eff} , is calculated in equation (5-1) using the residual strength f_{150}^D from ASTM C1609 (see Section 7.2.1.1) and the actual concrete flexural strength (f_1). In previous publications and methods, the residual strength ratio (R_{150}) shown in equation (5-2) was utilized for the FRC pavement design equations, but it has been superseded by the residual strength. Because the flexural strength of the concrete mixture f_1 increases with age, the R_{150} value can sometimes decrease even for a consistent fiber amount and residual strength. Therefore, the residual strength f_{150}^D is used because it reflects the effectiveness of the macrofiber reinforcement once concrete cracking has occurred. For the macrofiber volume fractions used for FRC overlays, a minimum R_{150} of 20% has been recommended (Bordelon and Roesler 2012), which corresponds to f_{150}^D values between 100 and 150 psi.

$$f_{\text{eff}} = f_1 + f_{150}^D \quad (5-1)$$

$$R_{150} = 100 \left(\frac{f_{150}^D}{f_1} \right) \quad (5-2)$$

The effective flexural strength considering the effects of the macrofibers is then used to determine the stress ratio, $SR = \sigma/f_{\text{eff}}$, where σ is the tensile stress in the concrete pavement. This stress ratio is applied to the plain concrete fatigue equations used for jointed concrete pavement design for both new construction and overlays (Roesler et al. 2008, Bordelon and Roesler 2012). Figure 5.1 shows BCOA thickness design examples for different panel sizes, for plain concrete or FRC material, and for varying traffic levels in terms of equivalent single axle loads (ESALs).

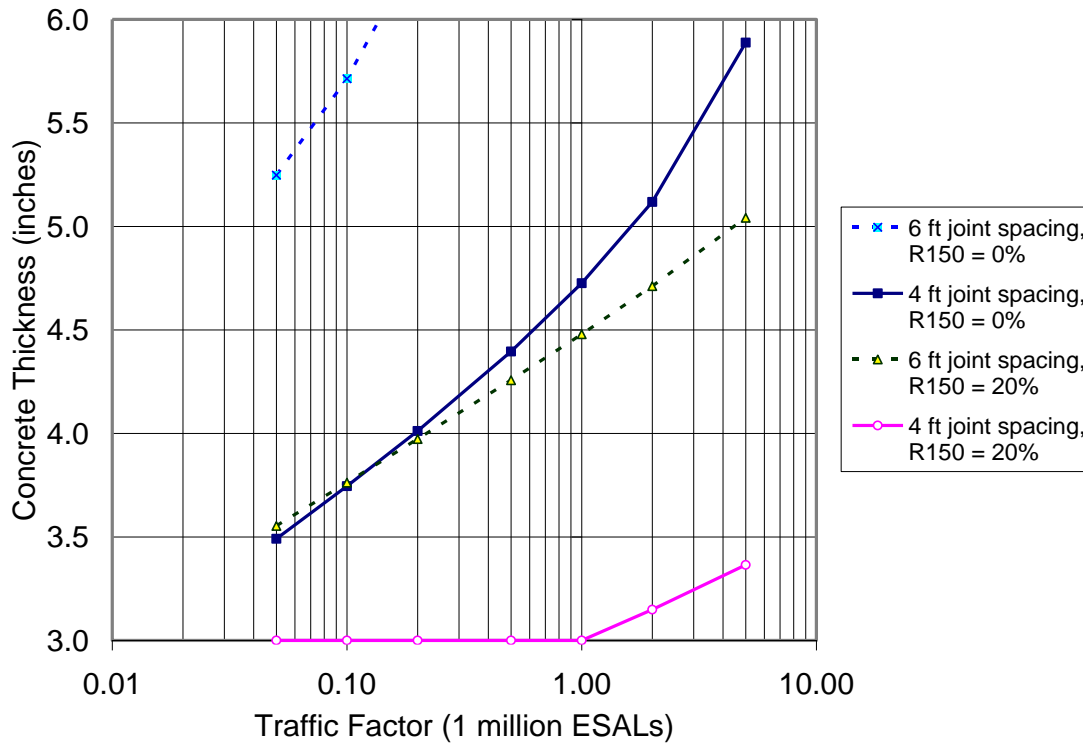


Figure 5.1. Fatigue-based design examples for FRC ($R_{150} = 20\%$ or $f_{150}^D = 150$ psi) and plain concrete with two slab sizes: 6 ft (1.8 m) and 4 ft (1.2 m)

The design charts in Figure 5.1 are for BCOA over a 4 in. (10 cm) asphalt pavement with a stiffness of 350 ksi (2.4 GPa). See Bordelon and Roesler (2012) for more information.

The design chart demonstrates that a thinner slab for a fixed traffic volume can be achieved by utilizing FRC and/or a smaller slab size. The Bonded Concrete Overlay of Asphalt - Mechanistic-Empirical (BCOA-ME) design procedure (Vandenbossche et al. 2017) also uses the effective flexural strength in the stress ratio and fatigue equations, with R_{150} being estimated by an empirical relationship based on the macrofiber type and the macrofiber dosage (Li et al. 2016).

Several design procedures and software applications are available for bonded and unbonded overlays, as summarized in Table 5.1.

Table 5.1. Summary of existing concrete overlay design procedures

Overlay Type	Traffic (Millions of ESALs)	Typical Concrete Slab Thickness	Typical Joint Spacing (ft)	Range of Existing Pavement Condition	Recommended Design Procedure^{a,b}
<i>Bonded Overlay</i>					
Over Asphalt Pavement	Up to 15	3–6 in.	=1.5 times thickness (in.)	Fair to Good	1, 2, 8
Over Concrete Pavement	Up to 15	3–6 in.	Match existing cracks and joints and cut intermediate joints	Fair to Good	3, 4, 5
Over Composite Pavement	Up to 15	3–6 in.	=1.5 times thickness (in.)	Fair to Good	1, 2, 8
Thin Fibrous Overlays of Asphalt Pavement	Up to 15	2–3 in.	4–6 ft	Fair to Good	7
<i>Unbonded Overlay</i>					
Over Asphalt Pavement	Up to 100	4–11 in.	Slab < 6 in.: 1.5 times thickness (in.) Slab ≥ 6 in.: 1.5 times thickness (in.) Slab > 7 in.: 15 ft	Deteriorated to Fair	3, 4, 5
Over Concrete Pavement	Up to 100	4–11 in.	Slab < 6 in.: 1.5 times thickness (in.) Slab ≥ 6 in.: 1.5 times thickness (in.) Slab > 7 in.: 15 ft	Deteriorated to Fair	3, 4, 5
Over Composite Pavement	Up to 100	4–11 in.	Slab < 6 in.: 1.5 times thickness (in.) Slab ≥ 6 in.: 1.5 times thickness (in.) Slab > 7 in.: 15 ft	Deteriorated to Fair	3, 4, 5

Overlay Type	Traffic (Millions of ESALs)	Typical Concrete Slab Thickness	Typical Joint Spacing (ft)	Range of Existing Pavement Condition	Recommended Design Procedure^{a,b}
Short-jointed Concrete Slabs over Asphalt, Concrete, or Composite Pavement	Up to 100	> 3 in.	4–8 ft	Poor to Fair	6

^a Recommended design procedures:

1. Bonded Concrete Overlay on Asphalt Thickness Designer (ACPA): <http://apps.acpa.org/applibrary/BCOA/>
2. BCOA-ME (Vandenbossche et al. 2017, Li et al. 2016):
<http://www.engineering.pitt.edu/Vandenbossche/BCOA-ME/>
3. AASHTO Guide for Design of Pavement Structures (AASHTO 1993)
4. AASHTO Pavement ME (AASHTO 2008)
5. Pavement Designer (ACPA): <https://pavementdesigner.org/>
6. Optipave 2 (TCPavements): <http://www.tcpavements.cl/eng/software>
7. Flowable Fibrous Concrete for Thin Concrete Inlays (Bordelon and Roesler 2011)
8. Illinois DOT design of bonded concrete inlay/overlay of asphalt pavements (Roesler et al. 2008)

^b Macrofiber reinforcement is permitted directly in design procedures 1, 2, 6, 7, and 8 and indirectly in 3, 4, and 5. Source: Harrington and Fick 2014

The option of using macrofiber reinforcement can be directly included in some of these design methods, as noted in Table 5.1. Other overlay design methods must employ the effective flexural strength approach to account for the impact of macrofibers on slab behavior. Several of the design procedures listed in Table 5.1 are further explained and can be referenced in the *Guide to the Design of Concrete Overlays Using Existing Methodologies* (Torres et al. 2012).

5.1 Residual Strength Estimation Software for FRC Overlay Design

To accompany this report, a new software tool, shown in Figure 5.2, was developed to assist the pavement design engineer in selecting the appropriate FRC residual strength (f_{150}^D) and effective flexural strength (f_{eff}) values to be used in pavement design software that may not incorporate the benefits of fibers.

Residual Strength Estimator for Fiber-Reinforced Concrete Overlays

Instructions: Run an overlay design software to determine the design inputs. Select design choices from the drop-down menus below to narrow down the recommended performance requirement of FRC for the proposed overlay pavement. Determine the effective flexural strength to input into overlay design software instead of design concrete flexural strength. Prepare specifications to achieve design residual strength of FRC material.

Design Input Choices

Type of Overlay Road	<input type="text" value="Local Road/Street"/>	
Millions of ESALS in Design Life	<input type="text" value="0.01 to 5.0 million ESALS"/>	
Asphalt Pre-Condition*	<input type="text" value="Fair"/>	*refer to Tech Report to example estimates of asphalt pre-condition
Desired New Concrete Thickness	<input type="text" value="3 to 4.5 inch PCC thickness"/>	
Remaining HMA Thickness after Milling	<input type="text" value="4.5 to 6 inches HMA remaining"/>	
Overlay Slab Size	<input type="text" value="6ft joint spacing"/>	
Desired Performance Enhancements <i>(this will generate a higher residual strength, but not included in effective flexural strength)</i>	<input type="text" value="basic FRC overlay"/>	
Plain Unreinforced Concrete Flexural Strength (<i>MOR</i>) <i>based on 28 day Four Point Bending (ASTM C78 or ASTM C1609)</i>	<input type="text" value="600"/>	psi

Design Suggestions/Warnings:

Recommended Residual Strength (f_{150})

Use value within this range for the Material Specification:

100 to **150** psi (target value from ASTM C1609 test results of FRC)

Effective Flexural Strength (f_{eff})

Replace the *MOR* from the Pavement Design Software with this value:

700 psi

NOTE: Actual fiber dosage rates are dependent on fiber type, fiber dimensions, concrete mixing/placement technique, cement content and fiber content or volume fraction. The intended fiber and dosage rate should be verified by ASTM C1609 test method. These recommended values are based off of previous field and laboratory testing of fibers used in concrete overlay pavements. Refer to the Tech Guide or Tech Report for more details.

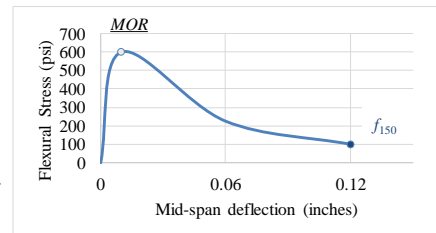


Figure 5.2. Screenshot of the Residual Strength Estimator software tool for local road/street design

The screenshot in Figure 5.2 shows a case with 0.01 to 5 million ESALs, an asphalt pavement in fair condition, a new concrete overlay 3 to 4.5 in. thick, an amount of HMA remaining after milling estimated to be 4.5 to 6 in., and an intended overlay slab size of 6 ft. The tool has calculated the recommended residual strength to be 100 to 150 psi. For a concrete flexural strength of 600 psi, the effective FRC flexural strength is 700 psi.

The Residual Strength Estimator software is Excel-based. It does not design the pavement overlay thickness but rather only provides estimates of the residual strength and effective flexural strength based on the intended pavement design inputs. The pavement engineer should preferably choose a mechanistic-empirical concrete overlay design software tool that allows for the estimated residual strength to be incorporated into an effective flexural strength based on the recommendations from the Excel-based tool shown in Figure 5.2. Since some of the existing concrete overlay design software applications already incorporate fiber reinforcement (e.g.,

ACPA BCOA Thickness Designer or Opti-Pave), pavement engineers need to make sure that the benefits of fibers are not double-counted in the design. The technical details of the Residual Strength Estimator software are provided in Appendix A.

5.2 Concrete Overlay Thickness and FRC Material Design Process

The following steps summarize the procedure that should be followed to select the correct FRC for a new concrete overlay design utilizing the Residual Strength Estimator software and a mechanistic-empirical overlay design procedure:

1. Determine the existing pavement conditions and gather the initial design inputs.
2. Decide whether the new concrete overlay is a bonded or unbonded system based on the existing pavement's condition and the initial pavement design inputs.
3. Run the Residual Strength Estimator tool to determine the FRC's residual strength value (f_{150}) for concrete overlay design and the effective flexural strength value (f_{eff}).
4. Design the concrete overlay with an existing mechanistic-empirical pavement design program using the effective flexural strength value from the Residual Strength Estimator.
5. Select potential macrofiber types and amounts based on previous experimental data and/or consultation with the manufacturer.
6. Design the concrete mixture(s) with macrofibers and cast trial batches for each fiber type. It is recommended that at least two volume fractions of FRC beams be cast, e.g., 0.25% and 0.50%.
7. Run ASTM C1609 at a fixed age (e.g., 7 or 14 days) for the trial batches and calculate the residual strength (f_{150}) versus fiber volume fraction for each fiber type.
8. Select the fiber volume fraction (%) or fiber content (lb/yd³) for the specified residual strength.
9. During construction, verify that the selected macrofiber type and content achieve the specified residual strength in the field.

These steps are also shown in Figure 5.3.

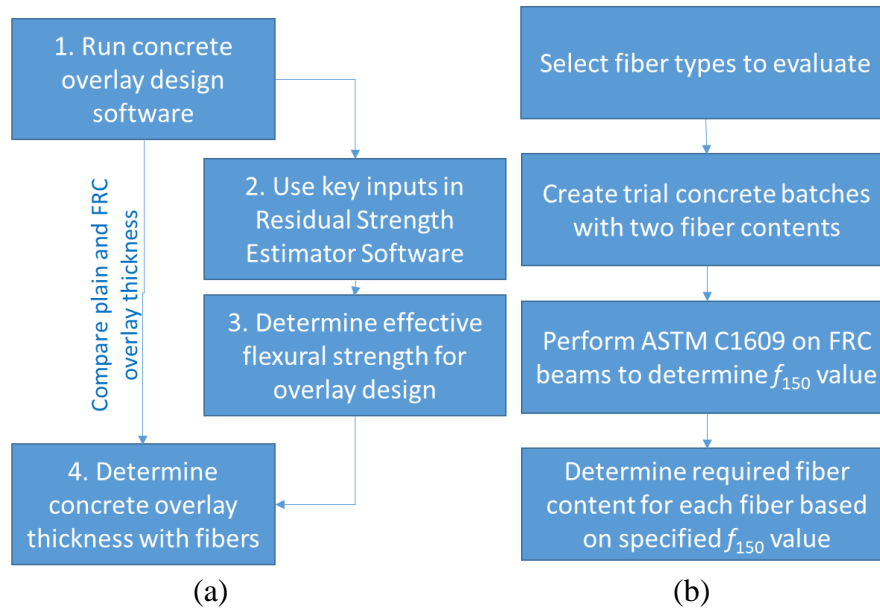


Figure 5.3. Flow chart showing the steps involved in (a) designing an FRC overlay and comparing its thickness to that of plain concrete and (b) determining the amount of fibers necessary to meet the design specification

In the following sections, two specific examples are shown to demonstrate how the Residual Strength Estimator software can be combined specifically with the BCOA-ME software. The BCOA-ME inputs do allow for macrofibers, but the software does not distinguish between different fiber characteristics, only the fiber material type. Therefore, the current BCOA-ME input option for fiber reinforcement is not utilized in the examples below.

5.2.1 Bus Pad Example Using BCOA-ME and Residual Strength Estimator

This example represents an overlay for a bus pad with a design traffic of 75,000 ESALs. The existing asphalt is in poor to fair condition and will have 3 in. remaining after milling. It is anticipated that the new overlay will be 4 in. thick and have a 6 ft joint spacing. The new concrete flexural strength is 600 psi. When this information is inserted into the BCOA-ME software with the no-fiber option, the resulting overlay design thickness is 5 in. The Residual Strength Estimator software is also run to estimate the macrofiber content using the key inputs. The residual strength (f_{150}) recommended is between 150 and 225 psi. An effective flexural strength of 725 psi is recommended for this design. A new simulation in BCOA-ME is now run with the effective flexural strength updated from 600 to 725 psi while all other inputs are fixed (with “No Fibers” still selected in the BCOA-ME software). The new FRC overlay thickness for this bus pad is 4 in., which is 1.0 in. thinner than the plain concrete (no-fiber) design.

5.2.2 Local Road Example Using BCOA-ME and Residual Strength Estimator

This example represents an overlay for a local road with approximately 4 million ESALs. The existing asphalt has some localized potholes but otherwise moderate distresses and will have 3

in. of asphalt remaining after milling. It is anticipated that the new overlay will be 4.5 to 6 in. thick and have a 6 ft joint spacing. The concrete flexural strength is 600 psi. When these inputs are inserted into the BCOA-ME software with the no-fiber option, the resulting overlay design thickness is 5.75 in. Using the same key inputs, the Residual Strength Estimator software recommends an f_{150} of 150 to 225 psi and an effective flexural strength of 725 psi. The software warns that an unbonded concrete overlay should be considered and that any asphalt sections in poor condition should be repaired first. Assuming that a bonded concrete overlay is nevertheless designed, a new simulation in BCOA-ME is now run with an effective flexural strength of 725 psi (with “No Fibers” selected). The new FRC overlay design thickness for this local road is 4.5 in., which is 1.25 in. thinner than the plain concrete (no-fiber) design.

5.3 Common FRC Overlay Questions and Answers

5.3.1 When Should I Consider Using Macrofibers in a Concrete Overlay?

The main advantages of FRC slabs over plain concrete slabs are improved load carrying capacity, smaller crack widths, reduction in the rate of crack deterioration, and extended service life, as summarized in Figure 5.4.

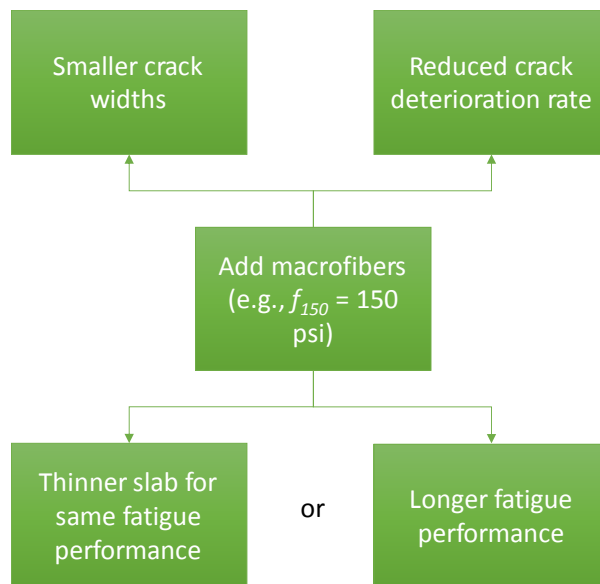


Figure 5.4. Benefits of using macrofibers in concrete overlays

FRC can be designed with a thinner slab compared to plain concrete (Bordelon and Roesler 2012) and can be especially useful where a thinner slab is required to accommodate a vertical height restriction (Harrington and Fick 2014). Additionally, FRC could also be considered for higher traffic areas with heavier repeated loadings and locations in need of an increased design or service life at the same slab thickness.

Macrofibers in concrete have been shown to control crack widths and to reduce the rate of crack deterioration. FRC pavement overlays can also accommodate variability in the support's thickness, stiffness, and materials (Harrington and Riley 2012). FRC can help reduce slab movement, slab misalignment, and/or crack widening and can help control plastic shrinkage cracking (Harrington and Fick 2014). Furthermore, round dowels can be problematic when slip-form paving an overlay that is ≤ 7 in. thick, so undoweled FRC joints may be a viable design alternative to consider for certain traffic levels (Harrington and Fick 2014).

5.3.2 *How Do Macrofibers Affect Contraction Joints?*

At this time, FRC materials should not be used as a substitute for dowel bars if dowel bars are required for the pavement design. Researchers have shown macrofibers can enhance the LTE of contraction joints (Barman et al. 2015), and thus FRC can be thought of as acting more like a tied joint than a doweled joint. No significant findings or recommendations have been made that warrant the replacement of required doweled joints with macrofibers. Sawn longitudinal contraction joints for FRC overlays typically do not need tie bars, but tie bars should definitely be considered for longitudinal construction joints to minimize the slab migration that has been observed in many thin concrete overlays (Figure 5.5).



Figure 5.5. Example of slab migration in BCOA without macrofibers

5.3.3 *How Do I Quantify the Existing Pavement Condition in FRC Overlay Design?*

The Residual Strength Estimator software accepts input values of poor, localized poor (meaning a pavement in mostly fair or good condition with some areas in poor condition), fair, or good

condition for the existing pavement. This is a subjective rating system, and it mainly affects whether the overlay pavement will likely be bonded or unbonded. Some suggested criteria for selecting the existing pavement condition are listed in Table 5.2.

Table 5.2. Examples of criteria for selecting the condition of the pre-existing asphalt

	Poor and Localized Poor	Fair	Good +
HMA Structural Number (Odoki and Kerali 2008)	2		5
HMA Stiffness (Bordelon and Roesler 2012)	100 ksi (0.7 GPa)	350 ksi (2.4 GPa)	600 ksi (4.1 GPa)
HMA Seasonal Resilient Modulus (Mu and Vandenbossche 2010)	430 ksi (3 GPa)		580 ksi (4 GPa)
HMA Distresses	Stripping, delaminations, poor drainage, excessive rutting, moderate fatigue cracking, transverse cracking		Rutting, some surface cracks, aging

5.3.4 What Is the Difference between Bonded and Unbonded Overlays with FRC?

FRC overlays can be bonded or unbonded. The choice between an unbonded or bonded overlay is primarily determined based on the condition of the existing pavement and the expected concrete overlay thickness and not the presence of fibers. The addition of macrofibers should not be used to convert an unbonded concrete overlay design to a bonded overlay design. If the existing pavement is in good to fair condition, then a bonded overlay can likely be designed with fibers, but if the existing pavement is in a poor and deteriorated condition, then an unbonded overlay design should be chosen. A number of possible design methodologies are available depending on whether a bonded or unbonded overlay is chosen, as summarized in Table 5.1. The *Guide to Concrete Overlays* (Harrington and Fick 2014) and the *Guide to the Design of Concrete Overlays using Existing Methodologies* (Torres et al. 2012) provide a very thorough discussion of the selection process when considering an unbonded versus a bonded overlay.

5.3.5 What Macrofiber Dosage Is Required for a Concrete Overlay?

The specific dosage amount of fiber to use depends on several input, design, and concrete mixture factors. Fiber contents for concrete overlays can range from 0.2% to 1% by volume of the total concrete mixture, and the necessary fiber content primarily depends on the objective that the addition of macrofibers is intended to achieve, e.g., to increase flexural capacity, increase service life, minimize crack widths, and/or reduce the crack deterioration rate. FRC applications for pavements and industrial floors commonly employ a macrofiber volume of around 0.5% or less (Brandt 2008), which balances the added benefits with the increased costs.

The manufacturer can typically provide suggested fiber dosages to meet the specified f_{150}^D performance values from ASTM C1609. However, trial batches should be tested in the laboratory with several fiber types and volume fractions to determine the required dosage levels for each fiber type because the concrete constituents and proportions can impact the residual strength values. Two independent sets of potential residual strength values from ASTM C1609 for different macrofiber types and contents are shown in Figure 5.6 and Table 5.3. Note that in Figure 5.6 residual strength (f_{150}) is calculated at a deflection of 3 mm.

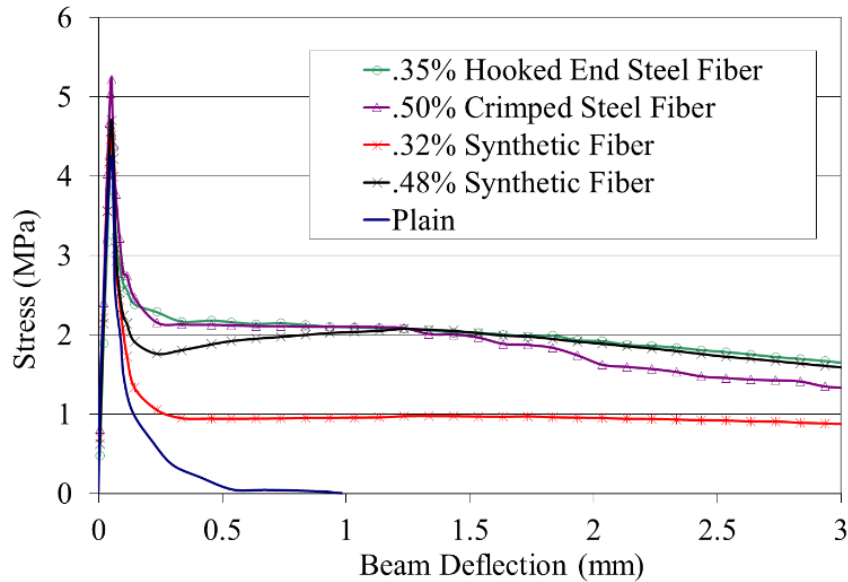


Figure 5.6. Example ASTM C1609 load-deflection results for several fiber types and amounts with the same concrete mixture design

Table 5.3. Example residual strength values for different fiber types and amounts

Fiber type	Age, days	Fiber volume, percent of total concrete volume	Fiber dosage, lb/yd ³ [kg/m ³]	f ₁₅₀ value, psi [MPa]
Synthetic Fiber #1	14	0.27%	4.0 (2.4)	90 (0.65)
Synthetic Fiber #1	28	0.38%	5.8 (3.4)	155 (1.05)
Synthetic Fiber #2	28	0.27%	4.1 (2.5)	160 (1.10)
Synthetic Fiber #2	28	0.38%	5.8 (3.5)	225 (1.10)
Synthetic Fiber #3	28	0.50%	7.6 (4.5)	160 (1.10)
Steel Fiber	28	0.19%	25.1 (14.9)	175 (1.21)

The macrofiber content depends on the type of overlay, the condition of the existing pavement, and elevation restrictions. For example, in Quebec a minimum steel macrofiber volume of 0.5% provided satisfactory performance, primarily through crack stabilization, on FRC overlays of existing concrete pavements (Chanvillard et al. 1989). For FRC overlays of asphalt parking lots, a minimum synthetic macrofiber dosage of 4 lb/yd³ (0.26% by volume) has been recommended

(Harrington and Riley 2012). For BCOA, a minimum residual flexural strength (f_{150}^D) of 100 to 150 psi should be specified (Roesler et al. 2008, Bordelon and Roesler 2012). The macrofiber type and volume fraction can be adjusted according to the residual strength requirement.

5.3.6 *Do I Need to Update the Concrete Mixture Design when Adding Macrofibers?*

Generally, it is not necessary to change the concrete mixture design to accommodate macrofiber volumes less than 0.5% (Bentur and Mindess 2007), but achieving a workable FRC mixture is key to successfully mixing and dispersing the fibers as well as consolidating and finishing without fiber balling. In some instances, water reducing or superplasticizing admixtures are needed to offset the negative impact of macrofibers on a particular concrete mixture. At higher macrofiber dosages, aggregate gradation, volume, and coarse-to-fine ratio should be re-evaluated to ensure suitable packing density.

5.3.7 *What Specific Fiber Type Should I Use, and Do I Need to Consider the Fiber Type when Determining the Fiber Dosage?*

While both steel and synthetic macrofibers have successfully been implemented in FRC overlays, synthetic macrofibers have become more prevalent because they are easier to handle, less prone to balling, do not corrode (Harrington and Fick 2014), and avoid the common perception that steel fibers may puncture vehicle tires. Regardless of the fiber type and geometry, the macrofiber content can be adjusted to achieve the specified residual strength performance. For example, in one study residual strength ratios (R_{150}) of around 20% were achieved using macrofiber volumes of 0.26% synthetic (straight fiber), 0.40% synthetic (crimped fiber), 0.5% synthetic (twisted fiber), 0.19% steel (hooked-end fiber), or 0.50% steel (crimped fiber) (Bordelon and Roesler 2012). Therefore, the concrete residual strength (from ASTM C1609) should always be specified first instead of fiber content, and then laboratory testing can be conducted to determine a suitable fiber type and required fiber volume fraction.

5.3.8 *Will I Have Corrosion Issues if I Use Steel Fibers?*

Corrosion of steel in concrete—whether that steel is in the form of rebar, dowels, or fibers—is the result of a very complex interaction among multiple variables. The alkalinity of the concrete pore solution retains the passivation of the steel, thereby preventing any corrosion. Reduction of the alkalinity, such as by carbonation or the presence of chloride ions, depassivates the steel and increase the probability of corrosion. Various alterations to the concrete mixture and pavement designs can minimize the potential for steel macrofiber corrosion, especially near the concrete overlay surface.

Exposure to chlorides or to carbonation can increase the risk of steel fiber corrosion. A recent review of the literature revealed that the following factors are relevant for FRC with steel fibers exposed to either chlorides or carbonation (Marcos-Meson et al. 2018):

1. Fiber Characteristics

- a. *Chloride exposure.* Stainless steel fibers offer greater corrosion resistance compared to carbon steel fibers, although the comparison is inconclusive for coated steel fibers. The effects of fiber dimensions and fiber manufacture type (cold-drawn wire, melt-extracted, mill cut, or cut sheet) on corrosion resistance are either inconclusive or cannot be determined due to insufficient data.
 - b. *Carbonation exposure.* Carbon steel fibers appear to corrode in cracked concrete, but the extent of corrosion may not be very severe in carbonated uncracked concrete. Stainless steel fibers perform well even in cracked samples, and galvanized and coated steel fibers may perform similarly to carbon steel fibers. Limited data are available on the effect of fiber manufacture type (cold-drawn wire, melt-extracted, mill cut, or cut sheet) on corrosion resistance, and no data are available on the effect of fiber dimensions.
2. Presence of Cracks
- a. *Chloride exposure.* There is limited evidence of corrosion in uncracked quality concrete samples, although long-term exposure may yield corrosion in the top 1 to 5 mm of the concrete. Concrete with wide cracks (> 0.5 mm) offers a high probability of carbon steel fiber corrosion. The evidence of carbon steel fiber corrosion in concrete with narrow cracks (between 0.2 and 0.5 mm) is inconclusive, although galvanized steel or stainless steel may delay or prevent corrosion at these crack widths. Literature suggests that minimal corrosion of carbon steel fibers may occur when crack widths are less than 0.15 to 0.2 mm or 0.05 to 0.1 mm, although other studies suggest that no crack width limit exists and that any cracked concrete with carbon steel fibers is compromised.
 - b. *Carbonation exposure.* There is limited evidence of corrosion in uncracked quality concrete samples, except for possible damage in the top 1 to 10 mm of the concrete. Initiation of carbonation-induced corrosion is more likely in the presence of wide cracks (> 0.5 mm), with the depth of carbonation potentially affecting up to 90% of the fiber cross-section and causing a 30% to 40% reduction in residual tensile strength. Similarly, the depth of carbonation in the presence of narrow cracks (between 0.2 and 0.5 mm) may affect up to 70% to 90% of the fibers bridging the cracks and cause a 30% to 40% reduction in total energy absorption relative to pre-cracked samples. Evidence of corrosion has been found in 10% to 40% of the fibers in smaller cracks (0.1 to 0.2 mm wide), which yielded minimal reductions in energy absorption capability.

Based on a recent literature review (Marcos-Meson et al. 2018), Table 5.4 provides some recommended limits for and the corrosion durability behavior of steel fibers in FRC.

Table 5.4. Recommended limits for and corrosion durability of steel fibers in concrete

	Carbonation		Chlorides	
	Mild exposure (XC2, XC3)	Aggressive exposure (XC4)	Mild exposure (XS-1, XS-2, XD-1, XD-2)	Aggressive exposure (XS-3, XD-3)
Maximum water-to-cementitious materials (w/cm) ratio	0.5–0.6	0.4–0.5	0.5	0.4–0.5
Supplementary cementitious materials*	SF	SF	FA, GGBFS	FA, GGBFS
Type of steel fiber	Carbon, galvanized	Carbon, galvanized, stainless	Carbon	Carbon, stainless
Critical crack width (mm)	0.3–0.5	< 0.3	0.2–0.3	< 0.2
Cracking or spalling	No	No	No	No
Loss in compressive strength	None	None	None	Low to none
Loss in tensile strength	None	Low to none	None	Low to none
Loss in residual tensile strength				
Uncracked	Low to none	Low to none	Low to none	Low to none
Wide cracks (> 0.5 mm)	Low	High	Medium	High
Narrow cracks (< 0.5 mm)	Low	Medium	Medium	High to medium
Hairline cracks (< 0.2 mm)	Low to none	Medium to none	Low to none	Medium to none

* SF = silica fume, FA = fly ash, GGBFS = ground granulated blast furnace slag
Source: Marcos-Meson et al. 2018

The recommendations in Table 5.4 are categorized based on mild or aggressive exposure to carbonation or chlorides. The exposure conditions are according to European Standard EN 206: carbonation (XC), chlorides from seawater (XS), and chlorides from sources other than seawater (XD). For chloride exposure, pavements are categorized as XD-3.

6 CONSTRUCTION MODIFICATIONS WITH FRC PAVEMENT OVERLAYS

6.1 Existing Pavement Surface Preparation

An FRC overlay can be placed over any existing pavement structure that has been properly prepared. FRC overlays generally have superior performance compared to other rehabilitation alternatives (e.g., unreinforced concrete or asphalt), especially where there might be reflective cracking and localized distress such as aged, spalled, or cracked asphalt. To ensure a good BCOA or sound surface for an unbonded overlay with macrofibers, the existing pavement should be milled and water-cleaned to remove any loose debris, which is the same recommendation for plain concrete overlays.

6.2 FRC Mixture Proportioning

In general, for FRC pavement overlays with moderate or low macrofiber dosages (0.5% by volume), the concrete mixture design does not necessarily need to be changed (Bentur and Mindess 2007). At higher macrofiber dosages (1% by volume or more), the aggregate gradation, aggregate size, and fineness modulus need to be re-evaluated to ensure a suitable packing density. Other modest changes to the cementitious contents can be made and the use of water reducers can be considered to ensure a good fiber-cement bond. Trial batches are recommended to assess whether the mixture design is suitable for the pavement construction application.

The total cementitious content should be high enough such that there is enough cementitious paste to coat the macrofibers to provide sufficient mixing, placement workability, consolidation, and finishability. Because a slump loss of up to 2 to 4 in. can be expected with the addition of macrofibers (Harrington and Fick 2014), the concrete may need to be mixed for a higher slump than normal so that the desired slump is achieved after the macrofibers are added and mixed. In order to compensate for the anticipated slump loss when fibers are added, water reducers and superplasticers are commonly utilized to maintain mixing, placement, and consolidation workability.

The water-to-cementitious materials (w/cm) ratio should be selected for the desired workability and strength performance. In general, FRCs used for overlays have the following mixture proportions: w/cm ratios of 0.38 to 0.45, air contents of 5% to 7%, supplementary cementitious material (e.g., fly ash or ground granulated blast furnace slag) replacements of cement of 15% to 35%, and well-graded aggregates (Harrington and Fick 2014). Table 6.1 provides concrete mixture designs for a pavement overlay with synthetic macrofibers at two dosage levels.

Table 6.1. Concrete constituents and mixture proportions for a pavement overlay with synthetic macrofibers at two dosage levels

Constituent	Concrete Mixture, kg/m ³ (lb/yd ³)	
	Fiber Mix 2.5A	Fiber Mix 3.5A
Cement	284.8 (480.0)	284.8 (480.0)
Fly Ash	71.2 (120.0)	71.2 (120.0)
Coarse Aggregate (25 mm)	1112.7 (1875.5)	1112.7 (1840.5)
Fine Aggregate	681.4 (1148.6)	678.5 (1143.7)
Water	150.0 (252.9)	150.0 (252.9)
Synthetic Macrofibers	2.5 (4.2)	3.5 (5.9)
Superplasticizer*	200 (3.0)	260 (4.0)

* In units of mL per 100 kg cementitious (fl. oz. per 100 lb cementitious)

Macrofiber balling (i.e., clumping and entanglement of fibers) has been reported to occur under several conditions: the macrofibers are added pre-bundled or in bags without adequate shearing during mixing, the macrofiber volume is too high, the macrofibers have a high aspect ratio (> 60), there is an insufficient amount of cementitious paste, and/or the coarse aggregate is too large (e.g., ASTM C33 #467 is used instead of #567 or #67).

Macrofibers can be successfully added at any phase in the mixing process, but the manufacturer’s recommendation should be closely followed. If macrofibers are added at the end of the mixing process or at the job site, manufacturers recommend using a “charging speed” for the mixer. Likewise, macrofibers can be discharged on a conveyor belt with the aggregates prior to mixing, blown into the drum mixer, or manually dispersed into the drum mixer in order to minimize fiber balling. ACI Committee 544 on fiber reinforcement states that a minimum of 40 revolutions at normal mixing speed, or “until the mixture is satisfactory,” is considered to be sufficient to mix and disperse the macrofibers in a concrete truck mixer (ACI Committee 544 2008). Also, balling has been found to occur if the mixer has worn out blades, the concrete is mixed too long after the macrofibers are added, the macrofibers are added too quickly (e.g., 132 lb/min of steel macrofibers is too fast according to D. Parham of Bekaert S.A. [personal communication, September 16, 2013]), and/or the macrofibers are added to the mixer before other ingredients (Bentur and Mindess 2007, ACI Committee 544 2009). Pre-bundled macrofibers effectively have a lower aspect ratio, allowing more gradual dispersion of the macrofibers over the mixing cycle.

6.3 FRC Batching and Mixing

Either a central drum or a ready-mix truck can be used for batching and mixing. Ideally, introducing and mixing the macrofibers at the batch plant is preferred, but this depends on the application and the available equipment. The main decision when batching FRC is how the fibers should be charged with the other concrete constituents and mixed properly to avoid fiber balling. Initially, the batching and mixing of macrofibers should follow the manufacturer’s recommendation based on the type, size, aspect ratio, and packaging of the macrofiber. When possible, a trial batch should be mixed to verify the proper batch sequencing and the dispersion

of macrofibers in the concrete mixture without the appearance of fiber balling at either the batch plant or the construction site.

Macrofiber balling can occur under any combination of the following conditions: the macrofibers are added too quickly, the macrofiber volume is too high, the macrofibers are already clumped together in the delivery bags, the mixer is inefficient or has worn blades, the mixture is too stiff, the concrete is mixed too long after the macrofibers are added, or the macrofibers are added to the mixer before other ingredients. See Section 6.2 for more information about mixture proportioning strategies that help prevent balling. Once the macrofibers are added, a minimum number of revolutions (e.g., 40) at a normal mixing speed, or “until the mixture is satisfactory,” should be sufficient to mix and disperse the macrofibers (ACI Committee 544 2008).

6.4 Placement and Consolidation

Conventional concrete construction practices and equipment can be used for FRC overlays (see Figure 6.1, which shows placement of FRC with a synthetic macrofiber dosage of 4 lb/yd³), particularly for the moderate macrofiber volumes ($\leq 0.5\%$).



Figure 6.1. Construction of an FRC overlay in Iowa

FRC materials for an overlay can be placed using chutes, buckets, buggies, conveying, pumping, or placers. Slip-form pavers and other mechanical placing equipment such as vibrating or laser screeds are well suited for placing FRC overlays. The internal vibrators are sufficient to consolidate the concrete without segregating the lower density macrofibers to the concrete surface. Overvibration should be avoided with steel or synthetic fibers because it can cause the fibers to sink or come to the surface, respectively. Because the addition of macrofibers can reduce the concrete’s workability, any expected slump loss should be adjusted for when using side-form paving, slip-form paving, and hand placement. Self-consolidating concrete has also been used for FRC overlays, such as with flowable fibrous concrete inlays (Bordelon and Roesler 2011).

6.5 Finishing

Conventional finishing equipment is employed for FRC overlays. Magnesium bull floats, channel radius floats, or highway straightedges can be used. These establish the desired surface

by closing any tears or open areas remaining after the paving screed passes. Wood floats should not be used because they tend to pull the macrofibers up to the surface. Tilting the blades of any float at too great of an angle also exposes the macrofibers to the surface. Macrofibers near the surface may be partially exposed or pulled out when a surface texture is applied, but this does not affect the overall performance of the FRC overlay. Macrofibers partially embedded in the concrete surface eventually wear off due to a combination of traffic and weathering. Experience has shown that the overlay surface is easier to finish at macrofiber volumes less than 0.4% (Harrington and Riley 2012).

6.5.1 *Balling and Surface Appearance*

Intermittent fiber balls should be removed immediately with a hoe or rake. The contractor should adjust the batching and mixing procedure to avoid the further creation of fiber balls as soon as they are noticed on a project. Fiber balls or clumps that are within the mixture when it is placed may migrate to the pavement surface or edge during paver-auger placement, causing consolidation and finishing issues. The surface of an external FRC pavement has a noticeable surface finish, with the discrete fibers visible and potentially providing a “hairy” look, particularly for synthetic macrofibers (Figure 6.2).



Figure 6.2. Examples of the surface appearance of FRC with a slipform pavement edge (upper left), with the use of transverse tining and curing compound (upper right), and for a hand-finished troweled surface (bottom)

This hairy appearance is more common with macrofibers that have a lower flexural stiffness. Polymeric macrofibers degrade with ultraviolet light exposure over a long period of time, so they will eventually disappear from the surface. Often abrasion from traffic tires will remove any loose or exposed surface fibers. Steel macrofibers have historically been thought to puncture tires if they happen to stick out of the surface. However, steel macrofibers typically bend at the surface and break off instead of puncturing tires. Discrete steel fibers directly exposed to air and water can locally corrode, but the internal steel fibers remain functional without any corrosion occurring.

6.5.2 Texturing and Tining

To provide friction and texture to the surface of an FRC overlay, texturing and tining must be completed (see Figure 6.2 for an example of transverse tining). Burlap drags and tining rakes can be used, but caution must be used to avoid significant disturbance and removal of macrofibers from the surface. Brooms or tining rakes should be held at a small angle to the horizontal surface to prevent lifting or exposing the macrofibers. Texturing should also be done only in one direction and should never pull against the established pattern. Examples of a good burlap drag and tining for FRC overlays are shown in Figure 6.3 and Figure 6.4, respectively.



Figure 6.3. FRC overlay with 4 lb/yd³ of synthetic macrofiber showing excellent finishability



Figure 6.4. FRC overlays with synthetic macrofibers and longitudinal tining

6.5.3 *Curing*

Curing is critical, especially for thinner FRC overlays, which are more sensitive to early-age temperature contractions and moisture loss. Curing of an FRC overlay should follow the same practices that are implemented for conventional concrete pavement. Certain solvent-based curing compounds may make the macrofibers at the surface more visible (Harrington and Fick 2014). Therefore, manufacturers of curing compounds should be consulted to confirm that no negative interactions between the macrofiber and the specific chemicals in the curing compound can occur.

6.6 Joints

In general, an early-entry saw should first be considered to create joints, especially for thinner overlays, where the surface area to volume ratio is especially high. Sawcut timing is more critical for FRC overlays than for plain concrete overlays because the concrete material is more resistant to crack growth and the shorter panel sizes used for FRC overlays do not generate as much internal stress in the material. Sawing should be commenced shortly after final set. If sawcutting is performed too early, then excessive raveling of the joints can occur, which had been an issue with early BCOA applications due to the large lineal footage of the contraction joints. If joint raveling is observed due to fibers being pulled out or aggregate movement, then the sawing should be delayed for another 30 minutes. A new, clean saw blade is recommended to achieve the best sawcut edges and to avoid pulling out macrofibers from the matrix.

Field observations of FRC overlay joints have shown that contraction joint activation can occur from 1 in 4 to 1 in 20 joints (Roesler et al. 2008). These initially activated joints are dominant joints with wider crack widths. Longer-term monitoring has shown that many more contraction joints activate over time, especially under traffic loading. Contraction joints in FRC overlays should be sawcut as early as possible and not cast or tooled. Joints should first be sawed in a trial section (4 to 6 ft long) to ensure acceptable amounts of joint raveling.

Transverse contraction joints should be cut to 1/4 of the depth of the pavement or at least 1 in., depending on the type of saw and assuming that the joint cutting is properly timed. Longitudinal joints should be sawcut deeper, to approximately 1/3 of the depth of the pavement (ACI Committee 544 2008), given the relatively low transverse stress state in FRC overlays. Extra saws are required for small-panel FRC overlays given the large number of contraction joints that are required to be cut per lineal foot of pavement. If there is a significantly greater number of joints to be cut (in slab sizes of 4 or 6 ft) and weather conditions (high temperatures and wind speeds) are significantly affecting setting time, it is recommended that the transverse joints be cut first at every 24 or 36 ft, and then the remaining joints should be cut to the design panel size; this process, known as skip sawing, should only be used when absolutely necessary because it may otherwise encourage the formation of dominant joints.

6.7 Maintenance

The typical practice for FRC overlays is to not seal the contraction joints, but this practice depends on the design life of the overlay, the number of lanes, the panel size, and other environmental factors. Since macrofibers maintain tight joint openings (less than 1 mm is common with macrofibers), there is generally no need to add joint sealant. If a crack forms in the mid-panel and remains tight, there is no need to seal the crack. If it is decided to remove and replace an FRC panel, the existing FRC joints will require full-depth sawcutting in order to remove the distressed panel. When a new FRC mixture is placed as the new panel, the benefits of the fibers in that panel bridging with the adjacent panels will not be available. In such cases, a thicker replacement panel may be required to offset the higher expected stresses in the slab.

If the FRC overlay eventually exhibits high International Roughness Index (IRI) values or faulting, diamond grinding may be used to improve the ride and friction. The presence of macrofibers, especially steel, may require significantly more effort to perform the grinding operation.

7 FRC TEST METHODS

The FRC properties that are most important and therefore need to be measured are typically application specific. This chapter covers only the FRC test methods that have been used or proposed for concrete overlay applications. The following is a brief summary of the properties that are particularly important to FRC overlays:

- **Fresh properties.** Workability is extremely important for FRC pavements because it enables proper mixing, placement of the mixture on the site, consolidation under vibration, and finishing with mechanical equipment. For consistency, the common test methods used for plain concrete, including slump, air content, and unit weight, are often used for FRC. More advanced fresh property tests have also been proposed to measure the batched macrofiber content and plastic shrinkage cracking potential.
- **Strength and modulus.** For FRC overlays with low to moderate macrofiber contents (< 1% by volume), the flexural and compressive strengths and elastic modulus are not significantly impacted by the macrofibers. Measuring these mechanical properties, however, is still necessary for design and quality control/quality assurance purposes.
- **Fracture energy and toughness.** The primary benefit of FRC is the enhancement of the concrete's fracture energy or toughness, i.e., its energy absorption capacity. Tests have been proposed to measure these properties in order to accurately predict the benefits of FRC in terms of concrete pavement cracking resistance, crack deterioration, and crack width control.
- **Shrinkage and durability.** For FRC overlays with low to moderate macrofiber contents (< 1% by volume), the shrinkage and durability properties are not expected to be impacted. Measuring these properties, however, is still necessary for ensuring the long-term performance of the concrete pavement overlay.

7.1 Fresh Property Testing

The common fresh concrete tests—such as slump (ASTM C143), air content (ASTM C173, ASTM C231), and unit weight (ASTM C138)—can be applied equally to FRC and plain concrete. The recently developed Vibrating Kelly Ball (VKelly) test may have some potential for evaluating FRC materials for slip-form paving (Taylor et al. 2015). Note that the presence of macrofibers may complicate the routine execution of these tests, such as by reducing the slump or preventing a tight seal on the air meter; however, with additional care and caution, an experienced operator can successfully apply these tests to FRC. One additional workability test was created for evaluating FRC, ASTM C995, Standard Test Method for Time of Flow of Fiber-Reinforced Concrete Through Inverted Slump Cone, but it has been withdrawn without replacement.

The macrofiber content in fresh concrete can be verified by a washout test, similar to the method specified in ASTM C1229 for glass microfiber-reinforced concrete. In general, a washout test

procedure collects a known volume of fresh FRC and then extracts the fibers by washing the concrete over a certain mesh or sieve size. Steel fiber content and dispersion can be verified through magnetic or electrical conductivity methods or again with a washout test when the concrete is in the fresh state (Ferrara et al. 2012). Synthetic macrofiber content must be determined either by the washout method or through X-ray computed tomographic imaging of the hardened material (Bordelon and Roesler 2014, ACI Committee 544 2017).

Plastic shrinkage cracking potential can be tested using ASTM C1579, Standard Test Method for Evaluating Plastic Shrinkage Cracking of Restrained Fiber Reinforced Concrete (Using a Steel Form Insert). This test compares the plastic shrinkage cracking of a freshly cast FRC mixture to that of a control concrete mixture when both are exposed to severe drying conditions. Concrete panels (355 mm by 560 mm and 100 mm thick) are cast on top of triangular stress risers, which provide the restraint to induce cracking. The crack widths are measured after 24 hours, and a crack reduction ratio is computed based on the ratio of the average crack widths of the FRC to those of the plain concrete control specimen.

7.2 Hardened Property Testing

Nearly all standard hardened concrete tests are applicable to FRC, such as compressive strength (ASTM C39), flexural strength (ASTM C78, ASTM C293), split tensile strength (ASTM C496), elastic modulus (ASTM C469), linear free drying shrinkage (ASTM C157), restrained ring shrinkage (ASTM C1581), freeze/thaw durability (ASTM C666), etc. However, several standardized and non-standardized tests methods have been specifically developed for FRC. These tests will be the primary focus of this section.

One important caveat that test operators need to be aware of concerns the post-cracking behavior of FRC. Because FRC has some amount of residual strength after a peak load is reached, it is possible to obtain errant readings of additional load after failure, particularly with the standard concrete strength tests (i.e., ASTM C496 and sometimes ASTM C39). It is recommended that test operators follow the ASTM standards but pay close attention and stop the tests after a peak stress is attained and the specimen is cracked even though the loading apparatus may continue reading an increase in applied stress.

A nuclear density gauge with the ability to measure moisture content, such as those commonly utilized to verify the quality of asphalt and roller compacted concrete (RCC) pavement construction and soil compaction, can be used to estimate the synthetic macrofiber content in FRC, provided that a calibration curve has been developed (Amirkhanian 2012). An experimental study reported a 5% error in the macrofiber content determination for a 30 cm (12 in.) concrete slab.

7.2.1 Residual Strength and Toughness

The most significant FRC-specific tests for concrete overlays involve measurement of the concrete's residual strength through testing of a beam specimen (see Figure 7.1).

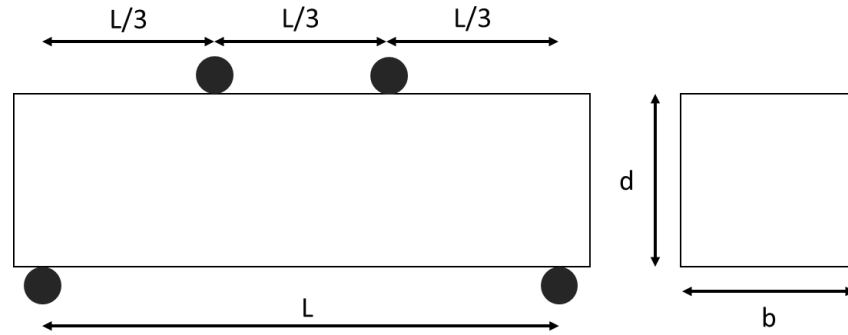


Figure 7.1. Geometry of the ASTM C1609 beam specimen and test configuration setup

Common testing methods include ASTM C1609, ASTM C1399, EN 14651, ASTM C1550, and the double-punch test (also known as the Barcelona test). These FRC-specific tests were developed for different fiber types and applications. One method designed for use in pavements, ASTM C1018, has been withdrawn by ASTM International and is therefore not a recommended test method. Currently, the most commonly used FRC toughness test for determining the required residual strength for concrete overlay applications is ASTM C1609. The details of the preferred residual strength test method (ASTM C1609-12) and other residual strength and toughness tests are described in the remainder of this section.

7.2.1.1 Residual Strength by ASTM C1609-12

ASTM C1609-12, Standard Test Method for Flexural Performance of Fiber-Reinforced Concrete (Using Beam with Third-Point Loading), uses a standard flexural strength concrete beam specimen and a similar testing configuration to that of ASTM C78. Under third-point (four-point) loading, a deflection measuring device, e.g., a linear variable displacement transducer (LVDT), is attached at either the top or the bottom of the beam at the midspan (see Figure 7.2).



Figure 7.2. ASTM C1609 test setup showing the LVDT measuring the deflection at the top of the beam at midspan and the ASTM C1812 roller assembly

The testing is controlled by the beam's vertical deflection (measured by the LVDT) in order to capture the post-peak load and deflection response, as shown in Figure 7.3.

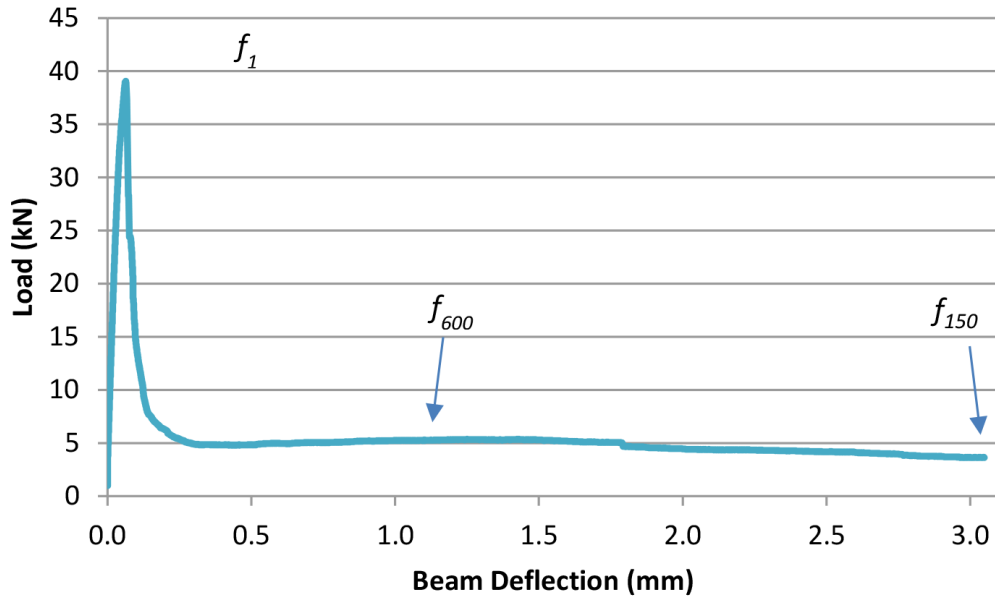


Figure 7.3. Load-deflection response curve from an ASTM C1609 test for a concrete specimen with 0.27% by volume synthetic macrofibers tested at an age of 56 days

The nominal square cross-section of the beam shown in Figure 7.3 is 150 mm (6 in.) with a span of 460 mm (18 in.). The peak load corresponds to a flexural strength, f_1 , of 4.85 MPa (700 psi). The residual strengths, f_{600}^D and f_{150}^D , are 0.65 MPa (90 psi) and 0.45 MPa (65 psi), respectively.

The ASTM C1609-12 standard allows for either 100 mm (4 in.) or 150 mm (6 in.) square cross-section beam specimens. It has been shown that the test can produce very different residual strength values for 100 and 150 mm specimens made with the same FRC material, regardless of whether the FRC uses steel or synthetic macrofibers (Altoubat et al. 2004). Therefore, use of the 150 mm beam depth is recommended for concrete pavement overlays. Figure 7.1 shows the geometry of the ASTM C1609 beam, with the width (b), height (d), and span length (L). The nominal geometry should be $b = d = L/3$. The test is conducted until a deflection of $L/150$ is reached (3 mm for a 150 mm beam depth), which is the significant load-deflection parameter linked to FRC slab performance.

The beam stress equation for third-point loading in equation (7-1) is used to compute the flexural strength at first crack load, f_1 (note that this is from load P_1 in Figure 3.4).

$$f_1 = \frac{P_1 L}{bd^2} \quad (7-1)$$

The residual strength of the beam is computed using the same beam equation but instead using the corresponding loads at deflections of $L/600$ and $L/150$, e.g., see equation (7-2). These residual strength values are f_{600}^D and f_{150}^D , respectively (see Figure 7.3), with the latter value being the residual strength most referred to in FRC overlay design, i.e., f_{150} .

$$f_{150}^D = \frac{P_{150}^D L}{bd^2} \quad (7-2)$$

Residual strength values can be thought of as the ability of the FRC to carry load at some magnitude of deflection and crack width.

The equivalent flexural strength ratio, $R_{T,150}^D$, is also determined by ASTM C1609. This value represents the overall toughness or residual strength of the FRC relative to the concrete strength. It is determined by equation (7-3), where T_{150}^D is the area under the load-deflection curve up to a deflection of $L/150$. $R_{T,150}^D$ was initially used to design and specify FRC materials for concrete overlays but has subsequently been replaced by just the residual strength (f_{150}).

$$R_{T,150}^D = \frac{150 T_{150}^D}{f_1 b d^2} \quad (7-3)$$

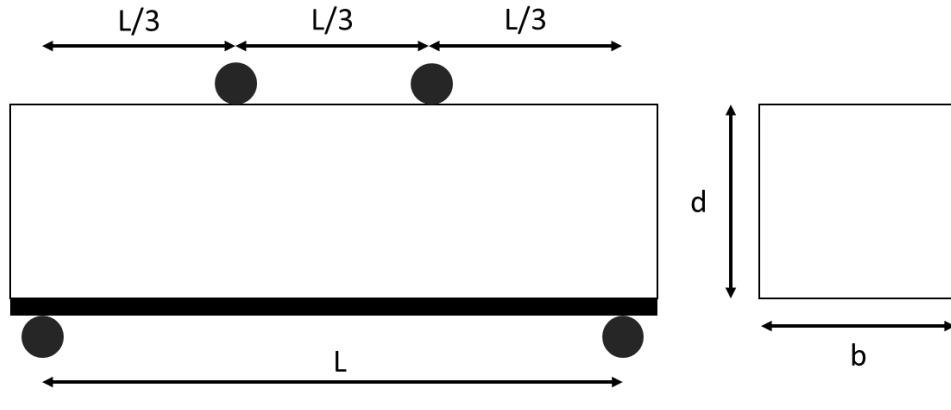
One commonly reported problem with the ASTM C1609 test is that the post-peak load-deflection response may not be obtained because of sudden crack propagation near the peak load, which is difficult to control on many types of testing machines. When this does occur, it frequently happens when conducting the test at the recommended displacement rates specified in ASTM C1609. The lack of control near the peak load is often attributed to a combination of the stiffness of the testing apparatus, the sensitivity and feedback control of the LVDT, the rigidity of the rollers, and the configuration and rigidity of the yoke that holds the LVDT. Furthermore, the age of the beam and the volume fraction of the macrofibers can also control the success of the test on a given testing machine, especially with less-than-ideal control and stiffness.

To overcome these complications, some solutions have included (1) conducting the test at a slower loading rate than specified in the standard (Banthia and Islam 2013); (2) reconfiguring the control method (Bernard 2009), test apparatus, and/or yoke; (3) utilizing “unlimited travel” rollers (Bernard 2014), which are now specified in ASTM C1812; (4) adding a notch (see Section 7.2.1.3); or (5) testing the beams at earlier ages.

7.2.1.2 Residual Strength by ASTM C1399-10

ASTM C1399, Standard Test Method for Obtaining Average Residual-Strength of Fiber-Reinforced Concrete, estimates the residual strength of an FRC beam using a steel plate beneath the simply supported beam, as shown in Figure 7.4.

Part 1: Load concrete beam with a steel plate until a crack forms



Part 2: Reload the specimen with the steel plate removed

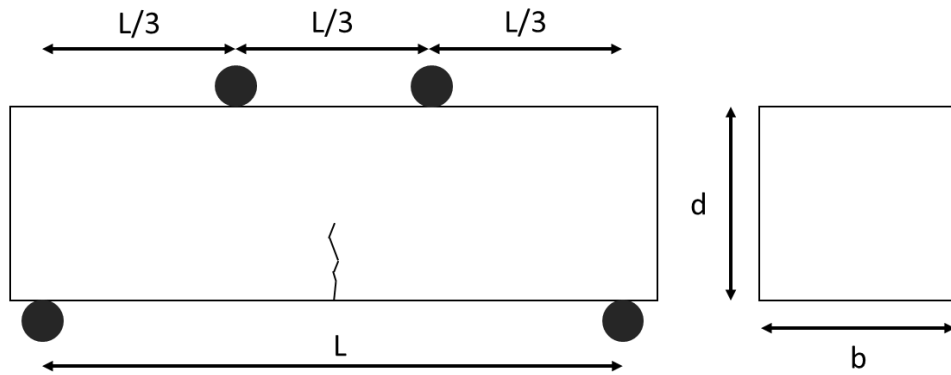


Figure 7.4. Geometry of the ASTM C1399 beam setup, where $L = 300$ mm, $d = b = 100$ mm, and the thickness of the steel plate is 12 mm

The steel plate is placed at the bottom of the beam in order to achieve a more stable crack initiation without the need for the closed-loop servo-hydraulic system required for ASTM C1609. After the concrete peak strength is reached, the steel plate is removed and the beam is reloaded to determine the residual strength of the FRC (Figure 7.5).

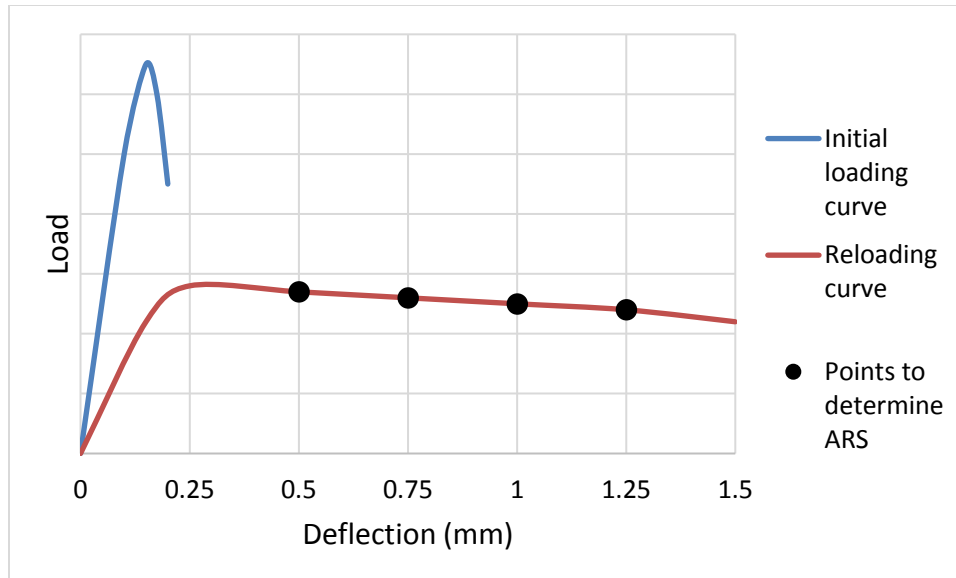


Figure 7.5. Schematic example of load-deflection response for the ASTM C1399 test

The specimen size specified in this standard is a 100 mm (4 in.) square cross-section beam with a 350 mm (14 in.) length with the third-point loading configuration over a span length of 300 mm (12 in.). Because a steel plate is employed, the peak load and calculated strength obtained from this configuration is not equivalent to the standard concrete flexural strength from ASTM C78. Using this specimen size for materials with larger nominal maximum aggregate sizes may affect the residual strength results. Figure 7.4 shows the geometry of the ASTM C1399 beam, with $b = d = L/3$.

During the execution of ASTM C1399, an LVDT (or similar device) is fixed to the beam, similarly to ASTM C1609. The test is operated in displacement control of the loading frame head and not in deflection control of the LVDT. A 12 mm (0.5 in.) steel plate is placed beneath the FRC beam, and the composite beam is loaded until both a peak load is reached (and the beam cracks) and the beam deflects to 0.2 mm (0.008 in.). The beam is then unloaded, the steel plate is removed, and the beam is reloaded until the beam deflection reaches 1.25 mm (0.05 in.). The average residual load (F_{avg}) is computed by averaging the loads (F_A , F_B , F_C , and F_D) that correspond to the respective deflections of 0.5 mm (0.02 in.), 0.75 mm (0.03 in.), 1.0 mm (0.04 in.), and 1.25 mm (0.05 in.) during the beam reloading portion of the test.

The average residual strength (ARS) is computed using equation (7-4) by inputting the average residual load in the beam equation. Note that the residual strength values obtained from ASTM C1399 are not the same as the values derived from ASTM C1609, even with the same concrete mixture and fiber content.

$$ARS = \frac{F_{avg}L}{bd^2} = \frac{F_A + F_B + F_C + F_D}{4} \left(\frac{L}{bd^2} \right) \quad (7.4)$$

7.2.1.3 Residual Strength by EN 14651

European Standard EN 14651, Test Method for Metallic Fibered Concrete – Measuring the Flexural Tensile Strength (Limit of Proportionality (LOP), Residual), is a residual strength test method for FRC. The test is similar to ASTM C1609, except that the beam specimen is notched and under a three-point bending configuration, as shown in Figure 7.6.

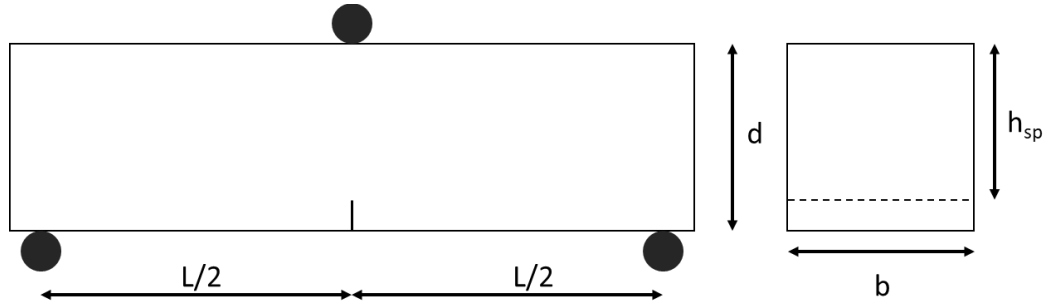


Figure 7.6. Geometry of the EN 14651 notched beam setup, where $L = 500$ mm, beam depth and width is 150 mm, and notch depth is ≤ 5 mm

While the title of the standard mentions metallic fibers, the test has been applied to all macrofiber types. The beam geometry has a nominal width (b) of 150 mm, a depth (d) of 150 mm, and a span length (L) of 500 mm. The sawcut notch should be ≤ 5 mm wide, with a notch depth of 25 mm. A closed-loop servo-hydraulic apparatus is needed to perform the test either in deflection control, similar to the LVDT measurement for ASTM C1609, or in crack mouth opening displacement (CMOD) control, similar to fracture testing (see Section 7.2.2). Example setups of deflection and CMOD control are shown in Figure 7.7.



Figure 7.7. EN 14651 setup, with an LVDT measuring deflection at the beam mid-span (left) and a clip-on gauge measuring CMOD (right)

Depending on the measurement configuration, the test produces load-deflection or load-CMOD curves. The standard provides an approximation equation to convert from deflection to CMOD or vice versa. The residual flexural strength ($f_{R,j}$) is determined in equation (7-5), where F_j is the load corresponding to $CMOD = 0.5$ mm ($j = 1$), 1.5 mm ($j = 2$), 2.5 mm ($j = 3$), and 3.5 mm ($j =$

4) and h_{sp} is the beam depth minus the notch height. Because this beam geometry includes a notch, the cracking behavior around the peak load is more stable when compared to that of unnotched specimens (e.g., those used in ASTM C1609). The residual strength obtained from EN14651 is not the same as that obtained from ASTM C1609 or C1399.

$$f_{R,j} = \frac{3F_j L}{2bh_{sp}^2} \quad (7.5)$$

7.2.1.4 ASTM C1550 FRC Round Panel Test

ASTM C1550, Standard Test Method for Flexural Toughness of Fiber Reinforced Concrete (Using Centrally Loaded Round Panel), quantifies FRC toughness using a panel rather than a beam geometry (Figure 7.8).

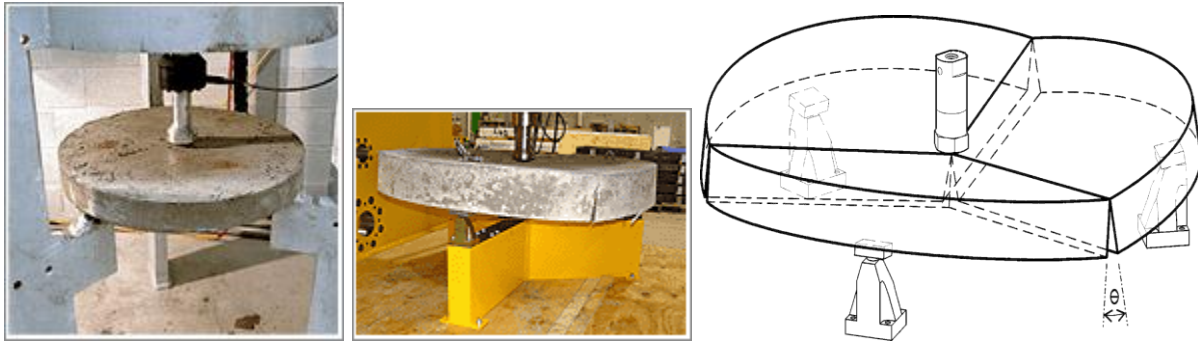


Figure 7.8. ASTM C1550 round panel test setup and failure mode

An 800 mm (31.5 in.) diameter circular panel, 75 mm (3 in.) thick, is supported by three pivots that are equally spaced and placed 25 mm (1 in.) from the panel edge. The panel is then centrally loaded at a fixed rate until a displacement of 45 mm (1.8 in.). After accounting for extraneous deformations and the compliance of the test apparatus, the energy absorption of the FRC specimen is computed as the area under the load-deflection curve, typically to deflections of 5 mm (0.2 in.), 10 mm (0.4 in.), 20 mm (0.8 in.), or 40 mm (1.6 in.). For a test result to be considered valid, at least three radial cracks need to have formed during the test.

The ASTM C1550 is a common test method for fiber-reinforced shotcrete (FRS). As such, it is recommended that the specimens be manufactured by either casting or spraying. For FRS, it has been shown that the results from tests that use beam geometries can be correlated with the results from panel tests, the latter of which have been found to be more reliable and produce less variability (Bernard 2002).

7.2.1.5 Double-Punch Test (Barcelona Test)

The double-punch test, also known as the Barcelona test, measures toughness using FRC cylinders (Molins et al. 2009) or cube specimens (Pujadas et al. 2014, Galeote et al. 2017). The test is detailed in the Spanish standard UNE 83515, Fibre Reinforced Concrete – Determination

of Cracking Strength, Ductility and Residual Tensile Strength - Barcelona Test. In this test configuration, an FRC cylinder (150 mm diameter) or cube (150 mm side length) is loaded at the top and bottom of the sample with circular, steel punches (37.5 mm diameter). For the cylindrical sample configuration, a circumferential extensometer is placed at the mid-height of the cylinder to measure the total circumferential opening displacement (TCOD), as shown in Figure 7.9.



Figure 7.9. Barcelona test (double-punch test) setup with a circumferential extensometer attached at the mid-height of the FRC cylinder to measure TCOD

As a simplification, the test can be conducted with the axial displacement of the loading head, which is then correlated to the TCOD (Pujadas et al. 2013). The toughness or energy absorbed is inferred from the area under the load-TCOD curve until a given TCOD value (e.g., 1 mm, 2 mm, 3 mm, and 4 mm). While the toughness value from the double-punch test configuration is not the same as that determined from a beam test configuration, a correlation has been reported between the results from both configurations (Molins et al. 2009), and a method to develop correlations between the two tests has been proposed (Galeote et al. 2017).

7.2.2 Fracture Test Geometries

Currently, there is no standardized fracture test procedure specifically designed for plain or fiber-reinforced concrete. However, several fracture tests and geometries have been altered and informally adopted for FRC materials in order to evaluate their critical stress intensity factor (K_{IC}), critical crack tip opening displacement ($CTOD_C$), and total fracture energy (G_F).

Notched beams under three-point loading have commonly been used to quantify concrete fracture parameters. The common analysis methods include the two-parameter fracture model (Jenq and Shah 1985), the size effect model (Bažant and Planas 1997), and the total fracture energy model (Hillerborg 1985). Modifications to these methods have been needed in order to apply the tests to FRC materials, given the significantly greater beam deflections of FRCs. In notched beam testing, similar to EN 14651, the test is conducted under crack opening

displacement (COD) control, and the results can be measured using a clip-on gauge (extensometer) attached to knife edges placed at the notch. To account for the greater COD range needed for FRC, a string potentiometer can be attached (Figure 7.10) and calibrated against the clip-on gauge to provide COD values.



Figure 7.10. Notched beam fracture testing of FRC showing (a) the clip-on gauge attached to knife edges on the bottom of the beam across the notch, (a, b) the string potentiometer attached to the exterior of the beam, and (b) the fractured specimen

For an 80 mm (3.1 in.) by 150 mm (6 in.) rectangular cross-section beam with a 50 mm (2 in.) notch, a string potentiometer with a total stroke of at least 75 mm (3 in.) has been found to be sufficient. The fracture properties of plain concrete and FRC notched beam specimens have been well documented in the literature (Roesler et al. 2007b, Park et al. 2010).

A test using another fracture geometry, known as the wedge split tension test, was developed for plain concrete (Brühwiler and Wittmann 1990) but has been applied to FRC materials (Elser et al. 1996, Löfgren et al. 2005, Kim and Bordelon 2017a). The wedge split fracture test has been reported to be more reliable than tests using the notched beam geometry and produces more stable crack growth while removing the influence of the specimen's self-weight. A cube-shaped specimen with dimensions of 6 in. (150 mm) or 8 in. (200 mm) is cast, as shown in Figure 7.11.

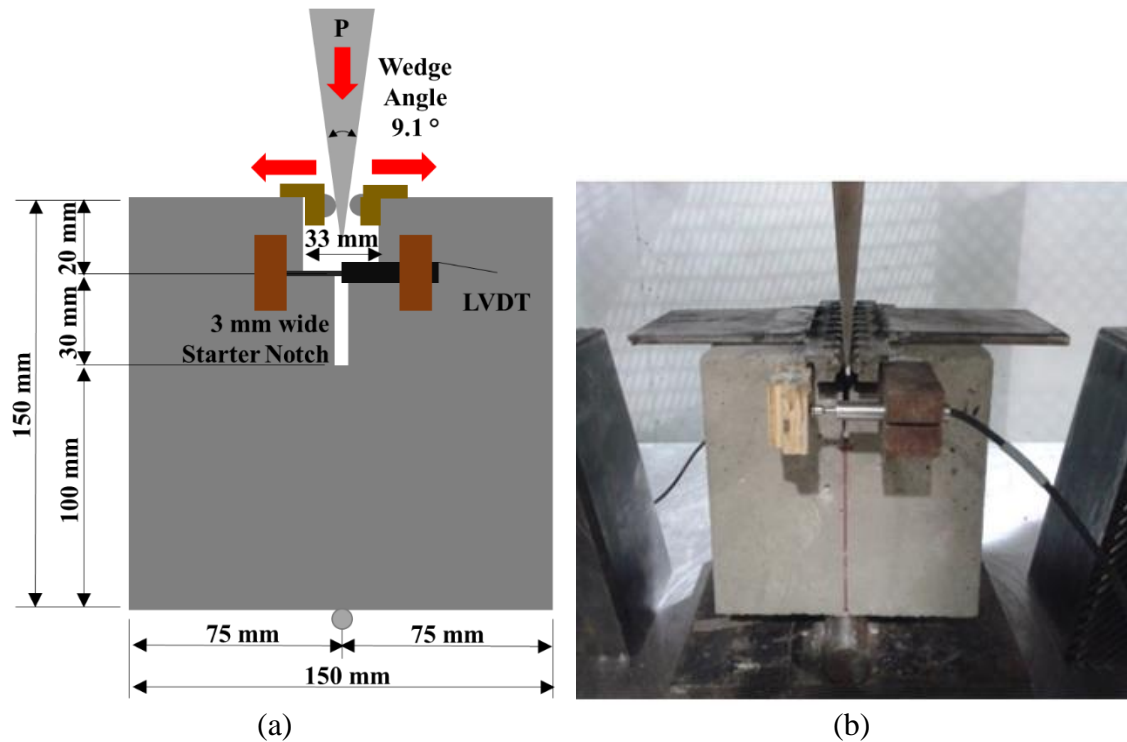


Figure 7.11. (a) Schematic showing the dimensions of a 150 mm wedge split test specimen, with the wedge vertically thrust between the roller bearings to induce a horizontal tensile splitting force, and (b) test specimen being loaded with the wedge split tension apparatus and LVDTs mounted on either side of the specimen

The notch of the fracture specimen is typically cut with a saw rather than formed in the mold for more consistent concrete at the notch tip. Different gauges can be used to record opening displacement, such as a set of LVDTs on either side of the cube or a crack width opening displacement gauge mounted at the top notch.

Yet another fracture geometry is used by the disk-shaped compact tension (DCT) test. This test was developed for plain concrete (Amirkhanian et al. 2015) but has more recently been applied to FRC (Brand et al. 2013, LaHucik et al. 2017). The advantages of the DCT test are that the geometry of the specimen removes the influence of the specimen's self-weight and the testing configuration and apparatus are currently used for testing asphalt pavement mixtures (e.g., ASTM D7313). In the DCT test, a sample is cut and prepared from a typical 6 in. (150 mm) diameter concrete cylinder and then pulled in tension from either side of the notch (see Figure 7.12).



Figure 7.12. Fracture geometry of the DCT test for FRC (a) during and (b) after testing

8 EXAMPLE FRC OVERLAY SPECIFICATION

Based on the design methodology discussed in Chapter 5, it is recommended that the FRC residual strength and a method to verify the quantity of macrofibers added per unit volume in the fresh state be specified. The following is an example specification for FRC overlays:

The material must comply with the following requirements from the Special Provision for Portland Cement Concrete Inlay or Overlay:

Synthetic fibers shall be Type III according to ASTM C1116. The synthetic fiber shall be a monofilament or bundled monofilament with a minimum length of 1.0 in (25 mm) and a maximum length of 2 ½ in. (63 mm), and shall have a maximum aspect ratio (length divided by the equivalent diameter of the fiber) of 150. The quantity of synthetic fibers added to the concrete mixture shall be sufficient to have a residual strength (f_{150}) of 125 psi according to ASTM C1609, measured at an age of 7 days. The maximum dosage rate shall not exceed 6.0 lb/yd³ (4.2 kg/m³), unless the manufacturer can demonstrate through a field demonstration that the concrete mixture will be workable and fiber balling is not a problem as determined by the Engineer. The minimum dosage rate shall not be less than 3.0 lb/yd³ (1.8 kg/m³). Synthetic fibers shall be added to the concrete and initially mixed per the manufacturer's recommendation.

The Department will maintain a qualified product list of synthetic fibers, which will include the minimum required dosage rate. The manufacturer shall provide the following to the Department:

- The specific product brand name
- Independent laboratory test results that show that the product meets department specifications of residual strength (f_{150})

By adopting a performance-based specification for residual strength, nearly any macrofiber type can be utilized, provided that the specified residual strength is met by some minimum macrofiber volume. Based on the current FRC overlay design experience, it is recommended that ASTM C1609 testing be specified (with the roller assembly specified by ASTM C1812), with the residual strength varying dependent on the recommendations of the Residual Strength Estimator software, e.g., 100 to 250 psi.

9 RESEARCH NEEDS FOR FRC OVERLAYS

While FRC has undergone significant improvements since the 1960s, there are still a number of important research topics worth investigating, particularly regarding FRC pavement design. Some ongoing and future research needs are summarized as follows:

- **Load transfer efficiency (LTE).** While LTE has been evaluated for FRC overlays based on limited finite element analysis, laboratory-scale beam tests, large-scale slab tests, and field tests (e.g., Roesler et al. 2012, Barman 2014, Barman et al. 2015), there is still insufficient evidence on the long-term contributions of FRC to contraction joint LTE and ways to quantify this contribution in FRC design.
- **Service and design life of FRC.** The currently available field data are insufficient to assess whether the design or service life of a concrete overly can be confidently extended using FRC. Nearly 90 FRC overlays have been documented in the United States as of April 2018, two-thirds of which have been constructed since 2000 (see Section 2.2).
- **Reduced thickness effects.** Using the effective flexural strength design method (Chapter 5), a thinner FRC overlay can be designed (Bordelon and Roesler 2012). Initial performance observations (King and Roesler 2014) suggest that the concept is working, but there are insufficient data on the long-term performance of FRC overlays designed and constructed to have reduced thicknesses.
- **Bottom-Up versus Top-Down Failure Cracks.** Using the effective flexural strength design method (Chapter 5), an FRC overlay with a reduced slab thickness can enhance a pavement's fatigue performance (Bordelon and Roesler 2012), which has also been demonstrated by accelerated pavement testing (Roesler et al. 2012). However, the long-term performance of FRC overlays designed and constructed to have top-down versus bottom-up cracking modes of failure is still undetermined.
- **Removal of dowel bars.** While both dowel bars and macrofibers act as types of reinforcement at joints, it is still unclear from the literature and experience whether macrofibers can be substituted for dowel bars under certain circumstances in concrete overlays. FRC pavements without dowel bars and an erodible base have been reported to develop faulting prematurely in a few projects in South America. For very thin (3 to 5 in.) concrete overlays, dowel bars are impractical, and therefore FRC joints are a possible solution. As truck traffic increases, however, the pavement design will eventually require dowelled joints. Modeling of undoweled FRC overlays has shown that crack widths can be reduced by a factor of 1.3 relative to undoweled plain concrete overlays (Kim and Bordelon 2017b). Another study found that for two similarly designed FRC overlay test sections, one with dowel bars and the other without, the section with dowel bars experienced significantly less faulting than the section without dowel bars (Vandenbossche and Barman 2010).

10 SUMMARY OF FRC OVERLAYS FOR PAVEMENTS

The selection of the appropriate type and design of a concrete overlay is significantly linked to the existing pavement condition, traffic levels, and roadway elevation constraints. Macrofibers have been shown to improve the flexural and ultimate capacity of concrete slabs, and these improvements can be used in the structural design of the concrete overlay thickness and slab size. Numerous macrofibers are available that have different materials (steel or polymeric), shapes and diameters (round, rectangular, etc.), lengths, and surface textures and embossments. The effectiveness of a macrofiber is related to its material properties, geometry, surface enhancements, and interaction with the concrete matrix.

The residual strength at 3 mm deflection (f_{150}^D) per ASTM C1609-12 has been shown to quantify the added benefit of a particular macrofiber type to the capacity of a concrete slab. By adding the residual strength (f_{150}^D) to the plain concrete flexural strength (f_1), an effective flexural strength value (f_{eff}) is obtained that can be used in existing structural design programs for concrete overlays (e.g., AASHTO Pavement ME). Residual strength values for concrete overlay applications typically range between 100 and 225 psi.

A Residual Strength Estimator spreadsheet has been developed to help engineers determine the appropriate f_{150} given the existing pavement conditions and initial design inputs. The design residual strength value should be incorporated into the specifications for FRC materials used in overlays. Macrofibers should not be specified by volume fraction or weight because different fiber properties and geometries produce the same residual strength at different fiber contents.

The proper batching and mixing of macrofibers is important to the successful construction of FRC overlays. Ideally, the macrofibers should be continuously added to the concrete mixture at the central drum plant with the other concrete constituents, but adjustments may need to be made based on the available equipment and the pre-packaging of the specific macrofibers. Best practices for concrete paving should generally be followed, with slight adjustments for finishing and texturing to avoid pulling out fibers from the surface. Proper timing and depth of the sawcut contraction joints ensures that the joints in the FRC overlay activate as soon possible and helps avoid premature cracking and the formation of dominant joints. FRC materials should not be used to replace dowel bars but can be considered similar in function to tie bars at contraction joints.

REFERENCES

- Altoubat, S., J. R. Roesler, and K. A. Rieder. 2004. Flexural Capacity of Synthetic Fiber Reinforced Concrete Slabs on Ground Based on Beam Toughness Results, in di Prisco, M., Felicetti, R., and Plizzari, G. A. eds. *Proceedings of the Sixth International RILEM Symposium on Fibre-Reinforced Concretes*. RILEM, pp. 1063–1072.
- Altoubat, S. A., J. R. Roesler, D. A. Lange, and K. A. Rieder. 2008. Simplified Method for Concrete Pavement Design with Discrete Structural Fibers, *Construction and Building Materials*, Vol. 22, No. 3, pp. 384–393. doi: 10.1016/j.conbuildmat.2006.08.008.
- AASHTO. 1993. *Guide for Design of Pavement Structures*. 4th Edition. American Association of State Highway Officials, Washington, DC.
- . 2008. *Mechanistic-Empirical Pavement Design Guide: A Manual of Practice*. 2nd Edition. American Association of State Highway Officials, Washington, DC.
- ACI Committee 544. 2008. *Guide for Specifying, Proportioning, and Production of Fiber-Reinforced Concrete*. ACI 544.3R-08. American Concrete Institute, Farmington Hills, MI.
- . 2009. *Report on Fiber Reinforced Concrete*. ACI 544.1R-96 (reapproved 2009). American Concrete Institute, Farmington Hills, MI.
- . 2010. *Report on the Physical Properties and Durability of Fiber-Reinforced Concrete, ACI 544.5R-10*. American Concrete Institute, Farmington Hills, MI.
- . 2017. *Report on the Measurement of Fresh State Properties and Fiber Dispersion of Fiber-Reinforced Concrete*. ACI 544.2R-17. American Concrete Institute, Farmington Hills, MI.
- Armaghani, J. and D. Tu. 1999. Rehabilitation of Ellaville Weigh Station with Ultrathin Whitetopping, *Transportation Research Record: Journal of the Transportation Research Board*, No. 1654, pp. 3–11. doi: 10.3141/1654-01.
- Amirkhanian, A. N. 2012. *Properties of Functionally Graded Concrete Slabs*. University of Illinois at Urbana-Champaign.
- Amirkhanian, A. N., D. W. Spring, J. R. Roesler, and G. H. Paulino. 2015. Forward and Inverse Analysis of Concrete Fracture Using the Disk-Shaped Compact Tension Test, *Journal of Testing and Evaluation*, Vol. 44, No. 1, pp. 625–634.
- Amirkhanian, A. and J. Roesler. 2019. *Overview of Fiber-Reinforced Concrete Bridge Decks*. National Concrete Pavement Technology Center, Iowa State University, Ames, IA.
- Banthia, N. and R. Gupta. 2006. Repairing with Fiber-Reinforced Concrete: Cellulose Fibers Enhance Overlay Performance, *Concrete International*, Vol. 28, No. 11, pp. 36–39.
- Banthia, N. and A. Bhargava. 2007. Permeability of Stressed Concrete and Role of Fiber Reinforcement, *ACI Materials Journal*, Vol. 104, No. 1, pp. 70–76. doi: 10.14359/18497.
- Banthia, N., V. Bindiganavile, J. Jones, and J. Novak. 2012. Fiber-Reinforced Concrete in Precast Concrete Applications: Research Leads to Innovative Products, *PCI Journal*, Vol. 57, No. 3, pp. 33–46.
- Banthia, N. and S. T. Islam. 2013. Loading Rate Concerns in ASTM C1609, *Journal of Testing and Evaluation*, Vol. 41, No. 6, pp. 1032–1036. doi: 10.1520/JTE20120192.
- Barman, M. 2014. *Joint Performance Characterization of Bonded Whitetopping Overlays*. PhD dissertation, University of Pittsburgh, PA.

- Barman, M. and B. Hansen. 2018. *Comparison of Performances of Structural Fibers and Development of a Specification for Using Them in Thin Concrete Overlays*. Minnesota Department of Transportation, St. Paul, MN.
<http://www.dot.state.mn.us/research/reports/2018/201829.pdf>.
- Barman, M., J. M. Vandenbossche, and Z. Li. 2015. Characterization of Load Transfer Behavior for Bonded Concrete Overlays on Asphalt, *Transportation Research Record: Journal of the Transportation Research Board*, No. 2524, pp. 143–151. doi: 10.3141/2524-14.
- Barros, J. A. O. and J. A. Figueiras. 1998. Experimental Behavior of Fiber Concrete Slabs on Soil, *Mechanics of Cohesive-Frictional Materials*, Vol. 3, pp. 277–290.
- Bažant, Z. P. and J. Planas. 1997. *Fracture and Size Effect in Concrete and Other Quasibrittle Materials*. CRC Press, Boca Raton.
- Beckett, D. 1990. Comparative Tests on Plain, Fabric Reinforced and Steel-Fibre Reinforced Concrete Ground Slabs, *Concrete*, Vol. 24, No. 3, pp. 43–45.
- Beckett, D. and J. Humphreys. 1989. *Comparative Tests on Plain, Fabric Reinforced and Steel Fibre Reinforced Concrete Ground Slabs*. Thames Polytechnic School of Civil Engineering, Dartford.
- Bentur, A. and S. Mindess. 2007. *Fibre Reinforced Cementitious Composites*. 2nd Edition. Taylor & Francis, London.
- Bernard, E. S. 2002. Correlations in the Behaviour of Fibre Reinforced Shotcrete Beam and Panel Specimens, *Materials and Structures*, Vol. 35, No. 3, pp. 156–164. doi: 10.1007/BF02533584.
- Bernard, E. S. 2009. Influence of Test Machine Control Method on Flexural Performance of Fiber Reinforced Concrete Beams, *Journal of ASTM International*, Vol. 6, No. 9, pp. 1–16. doi: 10.1520/jai102327.
- Bernard, E. S. 2014. Influence of Friction in Supporting Rollers on the Apparent Flexural Performance of Third-Point Loaded Fiber Reinforced Concrete Beams, *Advances in Civil Engineering Materials*, Vol. 3, No. 1, pp. 158–176. doi: 10.1520/ACEM20130098.
- Bordelon, A., V. Cervantes, and J. R. Roesler. 2009. Fracture Properties of Concrete Containing Recycled Concrete Aggregates, *Magazine of Concrete Research*, Vol. 61, No. 9, pp. 665–670. doi: 10.1680/macr.2008.61.9.665.
- Bordelon, A. and J. Roesler. 2011. Flowable Fibrous Concrete for Thin Concrete Inlays, in Al-Qadi, I. and Murrell, S. eds. *1st Transportation and Development Institute Congress*. American Society of Civil Engineers, pp. 874–883.
- . 2012. Design with Fiber-Reinforcement for Thin Concrete Overlays Bonded to Asphalt, *Journal of Transportation Engineering*, Vol. 138, No. 4, pp. 430–435. doi: 10.1061/(ASCE)TE.1943-5436.0000339.
- . 2014. Spatial Distribution of Synthetic Fibers in Concrete with X-Ray Computed Tomography, *Cement and Concrete Composites*, Vol. 53, pp. 35–43. doi: 10.1016/j.cemconcomp.2014.04.007.
- Brand, A. S., A. N. Amirkhanian, and J. R. Roesler. 2013. *Flexural Capacity of Rigid Pavement Concrete Slabs with Recycled Aggregates*. University of Illinois at Urbana Champaign, Urbana, IL.
- . 2014. Flexural Capacity of Full-Depth and Two-Lift Concrete Slabs with Recycled Aggregates, *Transportation Research Record: Journal of the Transportation Research Board*, No. 2456, pp. 64–72. doi: 10.3141/2456-07.

- Brandt, A. M. 2008. Fibre Reinforced Cement-Based (FRC) Composites After Over 40 Years of Development in Building and Civil Engineering, *Composite Structures*, Vol. 86, No. 1–3, pp. 3–9. <https://www.sciencedirect.com/science/article/pii/S0263822308000597>.
- Brühwiler, E. and F. H. Wittmann. 1990. The Wedge Splitting Test, A New Method Of Performing Stable Fracture Mechanics Tests, *Engineering Fracture Mechanics*, Vol. 35, No. 1–3, pp. 117–125. doi: 10.1016/0013-7944(90)90189-N.
- Burnham, T. R. 2005. *Forensic Investigation Report for MnRoad Ultrathin Whitetopping Test Cells 93, 94, and 95*. Minnesota Department of Transportation, St. Paul, Minnesota.
- Chanvillard, G., P.-C. Aïtcin, and C. Lupien. 1989. Field Evaluation of Steel-Fiber Reinforced Concrete Overlay with Various Bonding Mechanisms, *Transportation Research Record: Journal of the Transportation Research Board*, No. 1226, pp. 48–56.
- Covarrubias, J. P. and J. P. Covarrubias. 2008. “TCP Design” for Thin Concrete Pavement. *9th International Conference on Concrete Pavements*, August 17–21, San Francisco, CA, pp. 905–917.
- Covarrubias, J. P., J. Roesler, and J. P. Covarrubias. 2010. Design of Concrete Slabs with Optimized Geometry. 11th International Symposium on Concrete Roads, October 13–15, Seville, Spain.
- Dahal, S., J. Roesler, P. Gupta, et al. 2019a. *Performance Monitoring of Re-Engineered CRCP Test Sections: Volume 2*. Illinois Center for Transportation, University of Illinois at Urbana-Champaign, Urbana, IL.
- Dahal, S., J. Roesler, S. Gillen, and D. Gancarz. 2019b. Re-Engineering CRCP Design. 13th International Symposium on Concrete Roads, June 19–22, Berlin, Germany.
- Del Rio, P. and J. P. Covarrubias. 2016. Repavimentación Camino La Pólvara, Ruta 60 Ch En Chile, Utilizando Hormigón Reforzado Con Fibra Estructural Y Diseñado Con Sistema De Losas De Geometría Optimizada (Roadway Rehabilitation of La Polvora Route 60 in Chile Utilizing FRC and Designed with Slabs with Optimized Geometry). XVIIIth Argentine Congress of Roads and Traffic, October 24–28, Rosario, Santa Fe, Argentina.
- Elsaigh, W. A. 2001. *Steel Fiber Reinforced Concrete Ground Slabs*. Master’s thesis, University of Pretoria, South Africa.
- Elser, M., E. K. Tschegg, and S. E. Stanzl-Tschegg. 1996. Fracture Behaviour of Polypropylene-Fibre-Reinforced Concrete under Biaxial Loading: An Experimental Investigation, *Composites Science and Technology*, Vol. 56, No. 8, pp. 933–945. doi: 10.1016/0266-3538(96)00057-7.
- Falkner, H., Z. Huang, and M. Teutsch. 1995. Comparative Study of Plain and Steel Fiber Reinforced Concrete Ground Slabs, *Concrete International*, Vol. 17, No. 1, pp. 45–51.
- Falkner, H. and M. Teutsch. 1993. *Comparative Investigations of Plain and Steel Fibre Reinforced Industrial Ground Slabs*, No. 102. Institut für Baustoffe, Massivbau und Brandschutz, Technical University of Brunswick, Braunschweig, Germany.
- Ferrara, L., P. Bamonte, A. Caverzana, A. Musa, and I. Sanal. 2012. A Comprehensive Methodology to Test the Performance of Steel Fibre Reinforced Self-Compacting Concrete (SFR-SCC), *Construction and Building Materials*, Vol. 37, pp. 406–424. doi: 10.1016/j.conbuildmat.2012.07.057.
- Folliard, K., D. Sutfin, R. Turner, and D. P. Whitney. 2006. *Fiber in Continuously Reinforced Concrete Pavements*. Center for Transportation Research, University of Texas, Austin, TX.

- Forgeron, D. P. and J.-F. Trottier. 2004. Evaluating the Effects of Combined Freezing and Thawing and Flexural Fatigue Loading Cycles on the Fracture Properties of FRC. In *High Performance Structures and Materials II*. WIT Press, pp. 177–188.
- Galeote, E. A. Blanco, S. H. P. Cavalaro, and A. de la Fuente. 2017. Correlation between the Barcelona Test and the Bending Test in Fibre Reinforced Concrete, *Construction and Building Materials*, Vol. 152, pp. 529–538. doi: 10.1016/j.conbuildmat.2017.07.028.
- Grdic, Z. J. G. A. Toplicic Curcic, N. S. Ristica, and I. M. Despotovic. 2012. Abrasion Resistance of Concrete Micro-Reinforced with Polypropylene Fibers, *Construction and Building Materials*, Vol. 27, No. 1, pp. 305–312. doi: 10.1016/j.conbuildmat.2011.07.044.
- Hansen, B., M. Barman, and T. U. Rahman. 2016. *Comparison of Performances of Structural Fibers and Development of a Specification for using Structural Fibers in Thin Concrete Overlays: Task 1 Report-Literature Review*. University of Minnesota, Duluth, MN.
- Harrington, D. and G. Fick. 2014. *Guide to Concrete Overlays: Sustainable Solutions for Resurfacing and Rehabilitating Existing Pavements*. 3rd Edition. National Concrete Pavement Technology Center, Iowa State University, Ames, IA.
- Harrington, D. S. and R. C. Riley. 2012. *Guide to Concrete Overlays of Asphalt Parking Lots*. National Concrete Pavement Technology Center, Iowa State University, Ames, IA.
- Henschen, J. A. Amir Khanian, J. Roesler, and D. Lange. 2014. Field Evaluation of Alternative Isolation Joints at O’Hare International Airport. 2014 FAA Worldwide Airport Technology Transfer Conference: Innovations in Airport Safety and Pavement Technology, August 5–7, Galloway, NJ.
- Herrin, S. M. and J. E. Naughton, III. 2003. 10 Year Performance of Innovative Pavements Greater Rockford Airport. Airfield Pavements Specialty Conference 2003, September 21–24, Las Vegas, NV. doi: 10.1061/40711(141)11.
- Hillerborg, A. 1985. The Theoretical Basis of a Method to Determine the Fracture Energy G_F of Concrete, *Materials and Structures*, Vol. 18, No. 4, pp. 291–296.
- Jenq, Y. and S. P. Shah. 1985. Two Parameter Fracture Model for Concrete, *Journal of Engineering Mechanics*, Vol. 111, No. 10, pp. 1227–1241. doi: 10.1061/(ASCE)0733-9399(1985)111:10(1227).
- Kannemeyer, L., B. D. Perrie, P. J. Strauss, and L. du Plessis. 2008. Ultra Thin Continuously Reinforced Concrete Pavement Research in South Africa. 9th International Conference on Concrete Roads, August 17–21, San Francisco, CA.
https://researchspace.csir.co.za/dspace/bitstream/handle/10204/1320/Kannemeyer_2007.pdf?sequence=1&isAllowed=y.
- Kevern, J., T. Rupnow, M. Mulheron, Z. Collier, and P. Icenogle. 2016. *Evaluation of the Fatigue and Toughness of Fiber Reinforced Concrete for Use as a New Highway Pavement Design*. Louisiana Transportation Research Center, Baton Rouge, LA.
http://www.ltrc.lsu.edu/pdf/2016/FR_559.pdf.
- Kim, M. O. and A. C. Bordelon. 2017a. Age-Dependent Properties of Fiber-Reinforced Concrete for Thin Concrete Overlays, *Construction and Building Materials*, Vol. 137, pp. 288–299. doi: 10.1016/j.conbuildmat.2017.01.097.
- . 2017b. *Cracking and Debonding of a Thin Fiber Reinforced Concrete Overlay*. Mountain-Plains Consortium and University of Utah, Salt Lake City, UT. doi: 10.13140/RG.2.2.27297.20322.

- King, D. and J. R. Roesler. 2014. *Structural Performance of Ultra-Thin Whitetopping on Illinois Roadways and Parking Lots*. Illinois Center for Transportation, University of Illinois at Urbana-Champaign, IL.
- LaHucik, J., S. Dahal, J. Roesler, and A. N. Amirkhanian. 2017. Mechanical Properties of Roller-Compacted Concrete with Macro-Fibers, *Construction and Building Materials*, Vol. 135, pp. 440–446. doi: 10.1016/j.conbuildmat.2016.12.212.
- Li, Z., N. Dufalla, F. Mu, and J. M. Vandenbossche. 2016. *Bonded Concrete Overlay of Asphalt Pavements Mechanistic-Empirical Design Guide (BCOA-ME): Theory Manual*. University of Pittsburgh, PA.
- Löfgren, I., J. F. Olesen, and M. Flansbjer. 2005. *Application of WST-Method for Fracture Testing of Fibre-Reinforced Concrete*. Chalmers University of Technology, Göteborg, Sweden.
- Marcos-Meson, V., A. Michel, A. Solgaard, G. Fischer, C. Edvardsen, and T. L. Skovhus. 2018. Corrosion Resistance of Steel Fibre Reinforced Concrete - A Literature Review, *Cement and Concrete Research*, Vol. 103, pp. 1–20. doi: 10.1016/j.cemconres.2017.05.016.
- Meda, A., G. A. Plizzari, L. Sorelli, and B. Rossi. 2004. Fracture Mechanics for SFRC Pavement, in *Proceedings of the CEB-FIB Symposium*. Avignon, France. <http://www.afgc.asso.fr/images/stories/pub/Avignon-2004/027-Meda.pdf>.
- Melhem, H. G., R. Swart, and S. Walker. 2003. *Accelerated Testing for Studying Pavement Design and Performance (FY 2000): Effectiveness of Fiber Reinforced and Plain, Ultra-Thin Concrete Overlays on Portland Cement Concrete Pavement (PCCP)*. Kansas State University, Manhattan, KS.
- Molins, C., A. Aguado, and S. Saludes. 2009. Double Punch Test to Control the Energy Dissipation in Tension of FRC (Barcelona Test), *Materials and Structures/Materiaux et Constructions*, Vol. 42, No. 4, pp. 415–425. doi: 10.1617/s11527-008-9391-9.
- Mu, F. and J. Vandenbossche. 2010. Temperature Effects on Overlay Bond Characteristics and the Overlay Response to Dynamic Loads for Bonded PCC Overlays Placed on Asphalt Pavements, in *7th International DUT-Workshop on Design and Performance of Sustainable and Durable Concrete Pavements*. October 10–11, Seville, Spain.
- Mulheron, M., J. T. Kevern, and T. D. Rupnow. 2015. Laboratory Fatigue and Toughness Evaluation of Fiber-Reinforced Concrete, *Transportation Research Record: Journal of the Transportation Research Board*, No. 2508, pp. 39–47. doi: 10.3141/2508-05.
- Naaman, A. E. and H. W. Reinhardt. 2006. Proposed Classification of HPFRC Composites Based on their Tensile Response, *Materials and Structures*, Vol. 39, No. 5, pp. 547–555. doi: 10.1617/s11527-006-9103-2.
- Nanni, A. 1991. Fatigue Behaviour of Steel Fiber Reinforced Concrete, *Cement and Concrete Composites*, Vol. 13, No. 4, pp. 239–245. doi: 10.1016/0958-9465(91)90029-H.
- Newbolds, S. A. and J. Olek. 2008. *Evaluation of Performance and Design of Ultra-Thin Whitetopping (Bonded Concrete Resurfacing. Using Large-Scale Accelerated Pavement Testing*. Joint Transportation Research Program, Purdue University, West Lafayette, IN. doi: 10.5703/1288284314322.
- Nguyen, M. I., J. M. Balay, C. Sauzeat, H. Di Benedetto, K. Bilodeau, F. Olard, and B. Ficherouille. 2012. Accelerated Pavement Testing Experiment of a Pavement Made of Fiber-Reinforced Roller-Compacted Concrete. In *Advances in Pavement Design through Full-scale Accelerated Pavement Testing*. 4th International Conference on Accelerated Pavement Testing, September 19–21, Davis, CA. pp. 299–311.

- Odoki, J. B. and H. G. R. Kerali. 2008. *Highway Development & Management – 4: Deterioration of Bituminous Roads*. World Bank. Available at: <http://siteresources.worldbank.org/INTROADSHIGHWAYS/Resources/338993-1115667319236/1095944-1229373148786/05HDM-4DeteriorationBituminousRoads2008-10-22.pdf>.
- Park, K., G. H. Paulino, and J. Roesler. 2010. Cohesive Fracture Model for Functionally Graded Fiber Reinforced Concrete, *Cement and Concrete Research*, Vol. 40, No. 6, pp. 956–965.
- Parker, F., Jr., 1974. *Steel Fibrous Concrete for Airport Pavement Applications*. FAA-RD-74-31. Federal Aviation Administration and U.S. Army Engineer Waterways Experiment Station, Vicksburg, MS.
- Pujadas, P., A. Blanco, S. Cavalaro, A. de la Fuente, and A. Aguado. 2013. New Analytical Model to Generalize the Barcelona Test using Axial Displacement, *Journal of Civil Engineering and Management*, Vol. 19, No. 2, pp. 259–271. doi: 10.3846/13923730.2012.756425.
- Pujadas, P., A. Blanco, S. H. P. Cavalaro, A. de la Fuente, and A. Aguado. 2014. Multidirectional Double Punch Test to Assess the Post-Cracking Behaviour and Fibre Orientation of FRC, *Construction and Building Materials*, Vol. 58, pp. 214–224. doi: 10.1016/j.conbuildmat.2014.02.023.
- Rajan, S., J. Olek, T. L. Robertson, K. Galal, T. Nantung, and W. J. Weiss. 2001. Analysis of Performance of the Ultra-Thin Whitetopping Subjected to Slow Moving Loads in an Accelerated Pavement Testing Facility. 7th International Conference on Concrete Pavements: The Use of Concrete in Developing Long-Lasting Pavement Solutions for the 21st Century, September 9–13, Orlando, FL.
- Rapoport, J., C.-M. Aldea, S. P. Shah, B. Ankenman; and A. Karr. 2002. Permeability of Cracked Steel Fiber-Reinforced Concrete, *Journal of Materials in Civil Engineering*, Vol. 14, No. 4, pp. 355–358. doi: 10.1061/(ASCE)0899-1561(2002)14:4(355).
- Roberts-Wollmann, C. L., M. Guirola, and W. S. Easterling. 2004. Strength and Performance of Fiber-Reinforced Concrete Composite Slabs, *Journal of Structural Engineering*, Vol. 130, No. 3, pp. 520–528. doi: 10.1061/(ASCE)0733-9445(2004)130:3(520).
- Roesler, J. 2006. Fatigue Resistance of Concrete Pavements. 6th International DUT–Workshop on Fundamental Modelling of Design and Performance of Concrete Pavements, September 15–16, Old-Turnhout, Belgium.
- Roesler, J. R., D. A. Lange, S. A. Altoubat, K.-A. Rieder, and G. R. Ulrich. 2004. Fracture of Plain and Fiber-Reinforced Concrete Slabs under Monotonic Loading. *Journal of Materials in Civil Engineering*, Vol. 16, No. 5, pp. 452–460. doi: 10.1061/(ASCE)0899-1561(2004)16:5(452).
- Roesler, J. R., S. A. Altoubat, D. A. Lange, K.-A. Rieder, and G. R. Ulrich. 2006. Effect of Synthetic Fibers on Structural Behavior of Concrete Slabs-On-Ground, *ACI Materials Journal*, Vol. 103, No. 1, pp. 3–10.
- Roesler, J., G. Paulino, C. Gaedicke, A. Bordelon, and K. Park. 2007a. Fracture Behavior of Functionally Graded Concrete Materials for Rigid Pavements. *Transportation Research Record: Journal of the Transportation Research Board*, No. 2037, pp. 40–49. doi: 10.3141/2037-04.
- Roesler, J., G. H. Paulino, K. Park, and C. Gaedicke. 2007b. Concrete Fracture Prediction using Bilinear Softening. *Cement and Concrete Composites*, Vol. 29, No. 4, pp. 300–312.

- Roesler, J. A. Bordelon, A. Ioannides, M. Beyer, and D. Wang. 2008. *Design and Concrete Material Requirements for Ultrathin Whitetopping*. Illinois Center for Transportation, University of Illinois at Urbana Champaign.
- Roesler, J. R., V. G. Cervantes, and A. N. Amirkhania. 2012. Accelerated Performance Testing of Concrete Pavement with Short Slabs, *International Journal of Pavement Engineering*, Vol. 13, No. 6, pp. 494–507.
- Rollings, R. S. 1986. *Field Performance of Fiber-Reinforced Concrete Airfield Pavements*. DOT/FAA/PM-86/26, U.S. Army Corps of Engineers and Federal Aviation Administration, Washington, DC.
- Sanjuán, M. A., C. Andrade, and A. Bentur. 1997. Effect of Crack Control in Mortars Containing Polypropylene Fibers on the Corrosion of Steel in a Cementitious Matrix, *ACI Materials Journal*, Vol. 94, No. 2, pp. 134–141.
- Shah, H. R. and J. Weiss. 2006. Quantifying Shrinkage Cracking in Fiber Reinforced Concrete using the Ring Test, *Materials and Structures*, Vol. 39, No. 293, pp. 887–899. doi: 10.1617/s11527-006-9089-9.
- Shah, S. P., M. Sarigaphuti, and M. E. Karaguler. 1994. Comparison of Shrinkage Cracking Performance of Different Types of Fibers and Wiremesh. In *Fiber Reinforced Concrete Developments and Innovations*. SP-142. American Concrete Institute, Farmington Hills, MI. pp. 1–18.
- Shoenberger, J. E. and J. G. Tom. 1992. *Polypropylene Fibers in Portland Cement Concrete Pavements*. DOT/FAA/RD-92-9. U.S. Army Engineer Waterways Experiment Station, Vicksburg, MS, and Federal Aviation Administration, Washington, DC.
- Snyder, M. B. 2009. Lessons Learned from MnROAD (1992–2007): Whitetopping Design, Construction, Performance and Rehabilitation. Transportation Research Board 88th Annual Meeting, January 11–15, Washington DC.
- Sorelli, L. G., A. Meda, and G. A. Plizzari. 2006. Steel Fiber Concrete Slabs on Ground: A Structural Matter, *ACI Structural Journal*, Vol. 103, No. 4, pp. 551–558. doi: 10.14359/16431.
- Taylor, P., X. Wang, and X. Wang. 2015. *Concrete Pavement Mixture Design and Analysis (MDA): Development and Evaluation of Vibrating Kelly Ball Test (VKelly) Test for the Workability of Concrete*. National Concrete Pavement Technology Center, Iowa State University, Ames, IA.
https://intrans.iastate.edu/app/uploads/2018/03/MDA_vibrating_Kelly_ball_test_w_cvr-1.pdf.
- Torres, H. N., H. Roesler, R. O. Rasmussen, and D. Harrington. 2012. *Guide to the Design of Concrete Overlays using Existing Methodologies*. National Concrete Pavement Technology Center, Iowa State University, Ames, IA.
https://intrans.iastate.edu/app/uploads/sites/7/2018/08/Overlays_Design_Guide_508-1.pdf.
- Vandenbossche, J., M. Barman, F. Mu, and K. Gatti. 2011. *Development of Design Guide for Thin and Ultra-thin Concrete Overlays of Existing Asphalt Pavements, Task 1 Report: Compilation and Review of Existing Performance Data and Information*. Minnesota Department of Transportation, St. Paul, MN.
<http://www.dot.state.mn.us/materials/tpf5165/DEVELOPMENT/COMPILATION%20AND%20REVIEW%20OF%20EXISTING%20PERFORMANCE%20DATA%20AND%20INFORMATION.pdf>.

- Vandenbossche, J. and M. Barman. 2010. Bonded Whitetopping Overlay Design Considerations for Prevention of Reflection Cracking, Joint Sealing, and the Use of Dowel Bars, *Transportation Research Record: Journal of the Transportation Research Board*, No. 2155, pp. 3–11. doi: 10.3141/2155-01.
- Vandenbossche, J. M., N. Dufalla, and Z. Li. 2017. Bonded Concrete Overlay of Asphalt Mechanical-Empirical Design Procedure, *International Journal of Pavement Engineering*, Vol. 18, No. 11, pp. 1004–1015. doi: 10.1080/10298436.2016.1141410.
- Vandenbossche, J. M. and D. Rettner. 1998. The Construction of US-169 and I-94 Experimental Thin and Ultra-thin Whitetopping Sections in Minnesota, Report MN/RC – 2001-07. Minnesota Department of Transportation, St. Paul, MN.
- Won, J.-P., D.-H. Lim, and C.-G. Park. 2006. Bond Behaviour and Flexural Performance of Structural Synthetic Fibre-Reinforced Concrete, *Magazine of Concrete Research*, Vol. 58, No. 6, pp. 401–410. doi: 10.1680/mac.2006.58.6.401.
- Zhang, J. and V. C. Li. 2002. Monotonic and Fatigue Performance in Bending of Fiber-Reinforced Engineered Cementitious Composite in Overlay System, *Cement and Concrete Research*, Vol. 32, No. 3, pp. 415–423. doi: 10.1016/S0008-8846(01)00695-0.
- Zhang, Z., Q. Zhang, A. Qian, and V. C. Li. 2015. Low E Modulus Early Strength Engineered Cementitious Composites Material: Development for Ultrathin Whitetopping Overlay, *Transportation Research Record: Journal of the Transportation Research Board*, No. 2481, pp. 41–47. doi: 10.3141/2481-06.
- Zhang, Z., S. Qian, H. Liu, and V. Li. 2017. Ductile Concrete Material with Self-Healing Capacity for Jointless Concrete Pavement Use, *Transportation Research Record: Journal of the Transportation Research Board*, No. 2640, pp. 78–83. doi: 10.3141/2640-09.

APPENDIX A: DESCRIPTION OF RESIDUAL STRENGTH ESTIMATOR SOFTWARE FOR FRC CONCRETE OVERLAYS

The Residual Strength Estimator software has been developed in Microsoft Excel so that it can be easily updated at a later date when more FRC overlay performance data are available. Two screenshots of the software with different inputs can be seen in Figure 5.2 in the report and in Figure A.1 in this appendix.

Residual Strength Estimator for Fiber-Reinforced Concrete Overlays

Instructions: Run an overlay design software to determine the design inputs. Select design choices from the drop-down menus below to narrow down the recommended performance requirement of FRC for the proposed overlay pavement. Determine the effective flexural strength to input into overlay design software instead of design concrete flexural strength. Prepare specifications to achieve design residual strength of FRC material.

Design Input Choices

Type of Overlay Road	Local Road/Street	
Millions of ESALS in Design Life	0.01 to 5.0 million ESALS	
Asphalt Pre-Condition*	Fair	*refer to Tech Report to example estimates of asphalt pre-condition
Desired New Concrete Thickness	3 to 4.5 inch PCC thickness	
Remaining HMA Thickness after Milling	4.5 to 6 inches HMA remaining	
Overlay Slab Size	6ft joint spacing	
Desired Performance Enhancements <i>(this will generate a higher residual strength, but not included in effective flexural strength)</i>	basic FRC overlay	
Plain Unreinforced Concrete Flexural Strength (<i>MOR</i>) <i>based on 28 day Four Point Bending (ASTM C78 or ASTM C1609)</i>	600	psi

Design Suggestions/Warnings:

Recommended Residual Strength (f_{150})
Use value within this range for the Material Specification:

100 to **150** psi (target value from ASTM C1609 test results of FRC)

Effective Flexural Strength (f_{ef})
Replace the *MOR* from the Pavement Design Software with this value:

700 psi

NOTE: Actual fiber dosage rates are dependent on fiber type, fiber dimensions, concrete mixing/placement technique, cement content and fiber content or volume fraction. The intended fiber and dosage rate should be verified by ASTM C1609 test method. These recommended values are based off of previous field and laboratory testing of fibers used in concrete overlay pavements. Refer to the Tech Guide or Tech Report for more details.

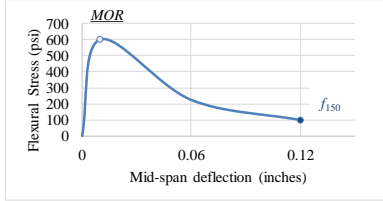


Figure A.1. Screenshot of the Residual Strength Estimator software

The options for the design inputs, shown in the tan boxes, are inserted into the software by navigating to Data > Data Validation > List. The lists of options are stored in the Index Values tab so that the possible options and the effects on the recommendations can be adjusted when updates to the software tool are required. When a specific input item is selected, the spreadsheet looks up an index value corresponding to this input from the Index Values tab. The current list of design input options and their corresponding index values are shown in Table A.1.

Table A.1. Input choices and index values in the FRC Residual Strength Estimator software

Pull-down Menu Choices	Unbonded Index Value; “1” indicates user should consider unbonded design	f_{150} Index Value	Added increase in f_{150} (if applicable)
Local Road/Street		0	
Collector Street		0	
Arterial		0	
Highway		0	
Bus Pad		100	
Parking Lot		100	
Unknown		20	
< 0.01 million ESALs		0	
0.01 to 5.0 million ESALs		20	
5 to 15 million ESALs		50	
> 15 million ESALs	1	50	
Poor Throughout	1	50	
Localized Poor	1	35	
Fair		20	
Good		0	
> 6 in. PCC thickness	1	0	
4.5 to 6 in PCC thickness		20	
3 to 4.5 in. PCC thickness		20	
< 3 in. PCC thickness	not tried yet, not in software		
< 3 in. HMA remaining	1		50
3 to 4.5 in. HMA remaining			25
4.5 to 6 in. HMA remaining			
> 6 in. HMA remaining			
4 ft joint spacing		5	
6 ft joint spacing		20	
12 ft joint spacing	not recommended, not in software		
basic FRC overlay			0
enhanced load transfer efficiency			50
reduced crack rate deterioration			50

In addition to an index value, the software also looks up whether or not an unbonded pavement design should be recommended. An unbonded design should be considered by the designer if a “1” is listed in first index column of the Index Values tab next to the corresponding design input. For some specific situations, such as if the remaining HMA is thin or the user would like to specify a higher fiber content, the user can indicate that indirectly through the options under the “Desired Performance Enhancement” input. The options for this input do not increase the effective flexural strength but only the specified recommended f_{150} range that the material tests should yield. The amount of increase to the recommended f_{150} is also shown in the last column of Table A.1.

In the software, index values are used to calculate a recommended FRC performance value or output an overlay design warning. The software runs an index and match function for each design input. The functions find the index value corresponding to the selected design choice and record the selection index in a hidden column. For the selections that require an addition to the f_{150} value (see the last column in Table A.1), the software determines the maximum additional f_{150} (not a sum) and applies this only to the “Recommended Residual Strength” values (equation A-1), not the calculated “Effective Flexural Strength” value (equation A-2).

$$f_{150} = f_{150,base \text{ from Table A.2}} + f_{additional \text{ from Table A.1}}^D \quad (A-1)$$

$$f_{eff} = f_{1,input \text{ by user}} + f_{150,base \text{ minimum}}^D \quad (A-2)$$

To recommend an estimated FRC residual strength range, the software searches within the hidden column for the maximum index value. In Table A.1, the scenarios for a bus pad or parking lot are recommended to have a lower f_{150} regardless of the other input options, and as such they have been given a higher index value to ensure that they yield a unique f_{150} range. Table A.2 shows the base minimum and maximum f_{150} values corresponding to the maximum index value found from all of the design inputs.

Table A.2. Maximum and minimum f_{150} values in the FRC Residual Strength Estimator software

Maximum (Index Values) for the Input Combination:	Minimum $f_{150,base}$ (psi)	Maximum $f_{150,base}$ (psi)
0	0	75
20	100	150
35	125	200
50	175	250
100	125	200

The options under the “Desired Performance Enhancement” input only increase the recommended f_{150} range, not the flexural strength. If one of these options is selected, the material supplier should use a higher dosage of macrofibers to reach the recommended residual strength range. As a result, it is anticipated that the FRC pavement will have an additional benefit such as further reduction in crack widths, higher LTE across cracks, or further reduction in the rate of crack deterioration.

Various “Design Suggestions/Warnings” are displayed if certain specific index values are found for any of the design inputs. These warnings are listed in Table A.3.

Table A.3. Design suggestions and warnings in the FRC Residual Strength Estimator software

Index Value (max value)	Warning displayed
1	Consider unbonded design instead of bonded design
5	4 ft short slabs are not recommended for channelized traffic (ideally for parking lots only)
35	Do patching repair first
50	Consider a higher residual strength for your FRC mixture design
0	Fibers may not be have an added benefit for this combination of inputs

For certain potential combinations of inputs, such as if the remaining HMA is thick and in good condition, traffic levels are low, and joint spacing is short, adding fibers may produce limited benefits. In other cases, such as for asphalt in poor condition, thin asphalt, heavy truck traffic, or an expected concrete overlay thickness that is too thin, the software provides a warning to the user.

The user may change, for example, the “Desired Performance Enhancement” input to something besides “basic FRC design” in order to still see what the design software will compute the effective flexural strength to be for a particular overlay thickness.

National Concrete Pavement
Technology Center

